Welding Research

SPONSORED BY THE WELDING RESEARCH COUNCIL
OF THE ENGINEERING FOUNDATION

W. SPRARAGEN, DIRECTOR

SUPPLEMENT TO THE WELDING JOURNAL, MAY, 1956

NOTCH DUCTILITY OF WELD METAL

Interpretive report sponsored by the Welding Research Council explains the role played by weld notch ductility in determining the performance of weldments. It is an analysis of basic principles, aimed at providing guideposts in a complex and partially-explored technical area

BY WILLIAM S. PELLINI

SUMMARY. It is generally recognized that a steel which fractures in the conventional ductile manner under a given set of conditions may fail in a brittle manner under other conditions, particularly if a sharp notch or crack is present. Stresses slightly above yielding are required in the general area of the point of origin in order to initiate brittle fracture from a notch, no matter how sharp. This holds true for all temperatures below the temperature defined as the *nil ductility transition temperature.*

The conditions for propagation of a brittle fracture are not as severe as conditions for fracture initiation. Below a critical temperature, brittle fractures propagate if a certain minimum stress level is exceeded. With only moderate increase in temperature above this critical temperature the stress required for crack propagation rises rapidly to values approaching the yield strength. This sharp rise is designated the *fracture transition temperature for elastic loading.* Above this temperature range, some plastic deformation is associated with the fracture and a temperature soon is reached in which only ductile tearing is observed. This final transition represents a *fracture transition temperature for plastic loading.*

These three critical transition temperatures, i.e., nil ductility transition, transition for elastic loading and transition for plastic loading, can be determined by any one of several types of notch tests. Comparative values as determined by the Charpy V-notch test, the crack-starter explosion test and the drop-weight test are discussed.

In welded construction, the weld can and frequently does influence the fracture behavior of the structure. To properly evaluate the influence of the weld it is necessary to compare the fracture characteristics of the weld metal with those of the various base metals over a range of temperature and, also, to determine the transition temperature of the welded joint as there are four possible paths along which brittle fracture may propagate. These are the plate, the heat-affected zone, the fusion line and the weld metal. Propagation through any given path becomes possible only if the service temperature is below the critical fracture temperature for that zone.

The transition temperature of the weld metal can vary with the type of welding electrode. A lower transition temperature in the weld metal than in the plate metal is always desirable. If the transition temperature of the weld metal is appreciably lower than that of the adjoining base metal the weld can, under certain conditions, stop a brittle crack.

Transition temperatures determined by notch tests furnish valuable information for design, but as yet these data are qualitative because test data for only a few steels have been correlated with actual service performance.

Interpretive Reports Committee
Welding Research Council

William S. Pellini is Superintendent, Metallurgy Division, Naval Research Laboratory, Washington, D. C.

Introduction

It is fitting to introduce this report on the notch ductility of carbon and low-alloy steel weld metal with the remark that the time is "right" for a broad look at the subject. The catastrophic failure of large welded structures which were first observed during the late 1930's and the wartime failures of welded ships which followed, caused great consternation because the exact nature of the problem and methods of solution were not known. A great deal has been accomplished since that time, and today much of the mystery has been dispelled. Although arguments regarding details continue within the circle of specialists in this field, it should be recognized that practical methods of preventing brittle failures are known. To be practical from an engineering standpoint, these methods need not necessarily be perfect or ideal.

The basic role of welding in the problem of brittle fractures is now clear. In or near welds, crack-like flaws may be developed, for a variety of reasons. When the tips of such flaws (notches) extend into the base steel, the notch ductility of the steel becomes a governing factor. At this point, the engineer is no longer concerned with ductility of the steel as measured by conventional tensile tests, but with ductility that must be measured in the presence of notches. Temperature is a critical factor, inasmuch as notch ductility of ferritic steels decreases with temperature. The engineer wishes to know the temperature below which the notch ductility of the steel will be inadequate for the intended service, and the *possibility* of brittle fracture becomes an important consideration. This answer has been provided for the case of semi-killed and rimmed mild steels, as the result of extensive investigations of casualty material and of large scale tests of similar steels. The pattern of these

studies is now being extended to other types of steels, including fully killed steels, quenched and tempered alloy steels, cast steels, welds, etc. The ultimate aim is to catalogue the various materials with respect to temperatures below which brittle fractures may be developed under adverse conditions of service.

If the assumption is made that steels to be welded should be expected to operate in a notched fashion and that the notches are of the sharpest possible type (cleavage cracks), the base steel problem is simplified. Tests featuring cleavage crack notches may be made, and the critical temperature-ductility relationships established. Relatively large test specimens are desirable, however, a *practical* solution for the purposes of engineering design and specification must be found in terms of conventional notch tests, such as the Charpy V or keyhole types. That is to say, the significance of conventional notch-bar test data must be established by the development of empirical correlations with service failures and tests of large specimens.

While the problem of the brittle fracture of the base steel may justly be laid to the inherent notch ductility characteristics of the base steel, much remains to be understood concerning the role of weld metal notch ductility as a factor in the performance of weldments. Certainly, a sharp crack defect located in the base steel (resulting from an arc strike, rough flame cut, sheared edge, etc.) or a crack defect located in the heat-affected zone (HAZ), may result in the initiation of brittle fracture in the base steel irrespective of weld metal properties. However, flaws may exist in the weld itself, and fractures may run solely in weld metal. A weld metal of deficient notch ductility may develop cracks which are continued in the weld metal or are transmitted to the base steel. As will be described in detail, there are many aspects of weldment performance which must hinge on the notch ductility characteristics of weld metal.

The solutions obtained for the base steel problem point to similar approaches to questions of weld-metal notch ductility. First of all, it is necessary to consider the behavior of weld metal in the presence of notches, particularly as related to the effect of temperature on the initiation and propagation of brittle fracture. Only after adequate knowledge of the notch ductility-temperature relationships of various weld metals are established, will it be possible to consider the question of the interactions between weld metal and base metal.

The scope of this interpretive report is outlined by the following listing of subjects to be considered:

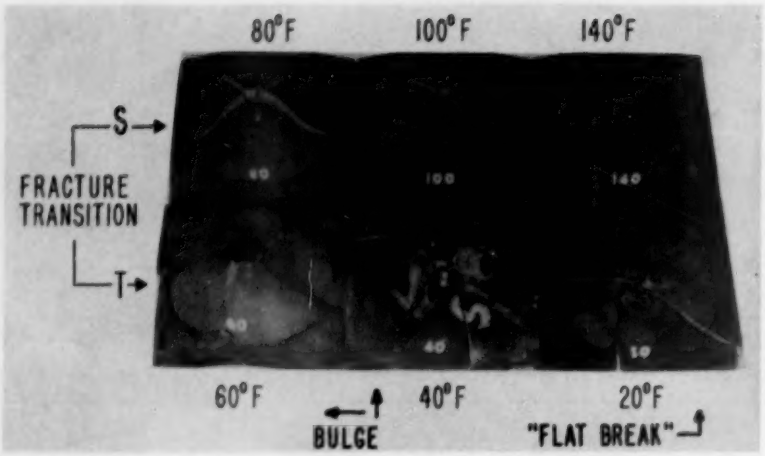

Fig. 1 Explosion loaded crack starter tests of 1-in. thick mild steel ship plate, illustrating the very great change in properties within a relatively narrow range of temperatures. The "T" to "S" fracture transition denotes a change from "through" to "stop" fractures

(1) The general significance of notch ductility, as related to the concepts of critical transition temperatures for the initiation and propagation of brittle fracture.

(2) The evaluation of the specific critical transition temperatures of various types of weld metal and comparison with the critical transition temperatures of various types of base metal.

(3) The conditions which determine the path of propagation of fractures in weldments.

(4) The conditions which determine the point of initiation of fractures in weldments.

This last item requires detailed consideration of the case involving the presence of notch-like flaws and of the case involving the absence of such flaws. Particular attention is directed in both cases to the role of weld metal notch ductility.

In the discussions to follow, it should be recognized that this report is concerned with the development of basic concepts related to the role of weld-metal notch ductility in the highly complex problem of weldment performance. The role of notch ductility of weld metal is but one of the fundamental questions involved in dissecting the factors which determine the performance of weldments. Therefore, a generalized picture of the importance of weld metal notch ductility may be obtained only by consideration of related aspects, including: (1) the properties of the steel and of the heat-affected zone; (2) the effects of the presence of notch-like flaws as contrasted to the case of their absence; and (3) questions related to design.

This report is not a manual on welding practices and was not intended as such—it is an analysis of basic principles, with the aim of providing guideposts in a complex and partially explored technical area. It is hoped that this interpretive summary of the role of weld metal notch ductility in determining the performance of weldments will serve to stimulate further research in this field.

Concepts of Critical Transition Temperatures

A general review of the mechanics of the development of brittle fractures is outside the scope of this report; however, it is essential to define the concepts upon which the interpretations are based. The questions to be resolved relate to the procedures by which notch ductility measurements may be used to specify whether a given steel (as base metal or weld) may be expected to initiate and propagate brittle fractures at specific service temperatures. From an engineering viewpoint, notch ductility values must ultimately be translated to signify safety or danger for specific temperatures and specific conditions of loading.

Item "one" in any discussion of the problem of brittle fracture is the fact that the temperature range of change in the properties of steels, from the completely ductile state to the highly notch sensitive state, is relatively narrow. Figure 1 vividly illustrates this fact for the case of explosion crack-starter tests*[1] of a conventional ship plate steel. At 20° F and lower temperatures, the steel shows no evidence of ductility, as illustrated by a "flat break" into

* A bead-on-plate weld of a brittle, hard surfacing electrode is deposited on the surface of a 14- x 14-in. plate. This plate is placed on a circular die and explosion loaded. The brittle weld provides a sharp crack which is the feature of the test. The contour of the supporting die may be seen on the surface of the plates shown in Fig. 1.

many pieces, immediately upon the development of the sharp, crack-like flaw (notch resulting from the cracking of the brittle weld). In the range of 20 to 60° F bulging precedes fracture, indicating that initiation was difficult and required "forcing"; however, complete fractures were obtained. In the range of 80 to 140° F, still greater amounts of bulging were required to "force" the start of fracture and the extent of propagation through the cold-worked (bulge portion) material diminished progressively to a point of no fracture. At temperatures above 140° F, this steel may be "blown" to a deep bulge prior to developing short, shear tears.

The pattern of change, in a range of approximately 100° F, from a highly frangible material (such as the 20° F example) to a completely ductile material (such as the 140° F example) has been found to hold for all types of steels tested in this manner. For some quenched and tempered steels, the range of complete change may be from −200 to −100° F and for some mild steels, the range may be from +100 to +200° F, i.e., each steel has its own characteristic range. The problem is to define the position of a given steel on the temperature scale and to understand the significance of certain, more subtle changes that occur within this range. With such extraordinary changes occurring within a relatively narrow temperature range, the problem of determining a significant transition temperature is not as difficult as is popularly considered.

The engineer is concerned with stresses and strains and naturally desires to fall back on concepts of brittle fracture based on these terms. This may be done, provided the additional parameter of temperature is considered. It is well established that stresses slightly above yielding are required in the general area of the point of origin in order to initiate brittle fracture from a notch, no matter how sharp. This statement holds for all temperatures below a certain critical temperature defined as the nil ductility transition (NDT). Above this temperature the amount of deformation required to "force" the initiation of fracture increases rapidly with increasing temperature, and the required initiation stress therefore must also increase rapidly with temperature. This is illustrated in Fig. 1 by the change from flat break at 20° F (nil ductility) to marked bulging (forced initiation) at 40° F. The NDT temperature may be established also by the drop-weight test[1] which results in fracture at and below the NDT temperature and a small amount of bending without fracture above this temperature. The importance of the NDT concept lies in the fact that stresses cannot be allowed to rise even slightly above the yield point (defined as the point of initial plastic flow) if sharp flaws are present and the temperature is below that of the critical transition. If sharp notches are present, the designer has the choice of ensuring that no point in the structure exceeds yielding or ensuring that the steel is of a quality such that the NDT temperature is below the lowest service temperature. Either approach satisfies the necessary conditions for the elimination of the possibility of fracture *initiation*.

The next question to be faced relates to the conditions necessary for continued propagation of a fracture which has started at a localized point of yielding, in a complex structure, and moves into areas of lower stresses. It should be recognized that the path of fracture in a large welded structure may entail the entry of the propagating crack into plates of steels that may have different notch-ductility properties from that of the initiation plate.

The classical work of Robertson[2] in England, and its extension in this country by Feeley and Northup[3] as the Standard Oil Development (SOD) tests, have provided a basis for understanding the combined effects of temperature and stress on the *propagation* of brittle fracture. These tests feature a plate specimen loaded to known nominal stresses and the initiation of fracture in a higher-stressed region (yield point exceeded) by means of a wedge or its equivalent. The localized region of higher stressing is necessary in these tests because brittle fracture may propagate at stresses below the yield point (item under study) but cannot initiate unless the yielding condition is met in the general area of the notch. The significance of the combined information developed by these tests is summarized schematically in Fig. 2. Below a critical temperature, brittle fractures propagate if a certain minimum stress level is exceeded. The level of this go-no go *propagation* shelf may be as low as 5000 psi. In a relatively narrow range of temperatures, the stress required for propagation rises rapidly to values in the plastic loading range. The sharp rise represents a *fracture transition for the case of elastic loading;* this transition will be defined in this text as the FTE temperature. Above this temperature range, plastic deformation loading is required for propagation; however, a temperature is soon reached above which only ductile tearing may be obtained. This final temperature represents a *fracture transition for the case of plastic loading* and will be defined as the FTP temperature.

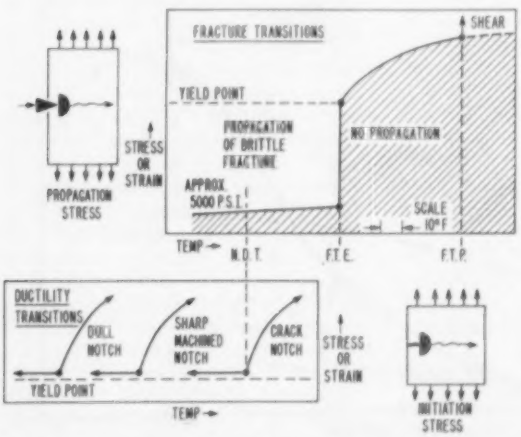

Fig. 2 Summary of the effects of stress level on the initiation and propagation of brittle fractures within the transition temperature range

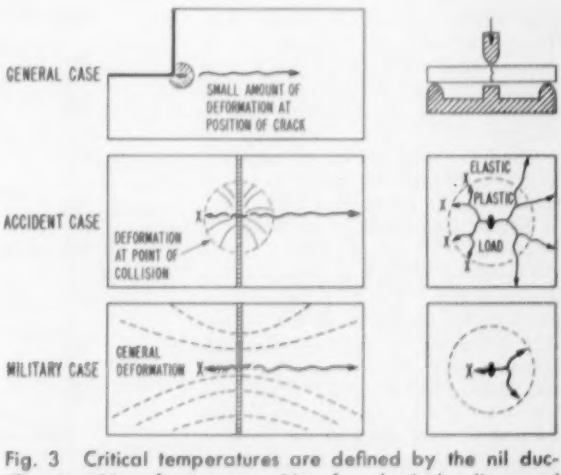

Fig. 3 Critical temperatures are defined by the nil ductility transition, fracture transition for elastic loading, and fracture transition for plastic loading for top, center and bottom service conditions illustrated. (See text for details)

The designer may find it difficult, if not impossible, to ensure the absence of points of yielding in a highly complex structure; however, there is no great problem in designing for the nominal stress condition of the major portion of the structure. Thus, if it were feasible to design to nominal stress levels in the order of 5000 psi or lower, the necessary conditions for the absolute prevention of *propagation* would be obtained. In most cases, this restriction is unacceptable, which means that the alternate condition of providing steel with FTE temperatures falling below the lowest temperature of service must be accepted if the possibility of the propagation of brittle fractures is to be eliminated.

It is axiomatic that brittle fractures will not propagate if there is no initiation. Therefore, the question of design based on initiation (NDT) and design based on propagation (FTE), or possible complete ductility (FTP), is raised for consideration. In order to enlarge on this question it is necessary to consider the relation of the three transition points. Since the Robertson and SOD tests do not provide information relative to the NDT temperature for initiation, comparisons were made between the results obtained by the Robertson test and by the Naval Research Laboratory (NRL) crack-starter tests, using the same steels of the ship plate type. Briefly, in these tests the Robertson transition corresponded closely to the highest temperature of complete fracture in the explosion test such as illustrated by the "T" point in the "through" to "stop," T to S, fracture transition illustrated in Fig. 1. Above this temperature, the Robertson test samples require plastic loading to support propagation and the explosion test samples fracture only in the plastically deformed center regions; i.e., not through the lightly loaded edge regions of the die-supported plate. Thus, the two test methods are in general agreement as to the highest temperature for propagation of brittle fracture under conditions of elastic loading.

The NDT temperature for initiation, as determined by "flat break" in the explosion test, or by the drop-weight test, is located approximately 30 to 50° F below the FTE temperature, taken as the midpoint of the T to S range in the explosion test. The FTP temperature for complete resistance to brittle fracture is located, by the explosion test, approximately 100° F above the NDT temperature for initiation. This simplification of the transition temperature features of mild steels in the presence of sharp cracks provides for a rationalization of the fracture problem in terms of stresses (or equivalent strains) and temperature. If the service stresses and service temperatures are defined, it may be deduced whether brittle fracture is possible or not, based on the three critical transition temperatures falling within a span of approximately 100° F.

The three critical transition temperatures: NDT, FTE, and FTP are significant to the service performance of welded structures in the sense indicated by the schematic illustrations of Fig. 3. The conditions of service are separated into three broad groupings: (1) the general case; (2) the accident case; and (3) the military or "special" case. The following comments are pertinent to each case.

The General Case. The structure is considered to operate under conditions of elastic loading, except that small amounts of plastic flow are possible at points of connection or discontinuity (corners, cutouts, etc.). For this condition, fracture initiation is possible only at temperatures below the NDT temperature because at higher temperatures gross deformation (stress greatly above the yield point) is required for initiation; while below this temperature initiation is possible immediately on exceeding the yield point. For this service, the NDT temperature determines the boundary of temperatures to be considered safe and temperatures to be considered dangerous.

The Accident Case. The structure is considered to operate under conditions of elastic loading except that, due to special circumstances (such as collision, etc.), gross deformation is developed in a local area of the structure which contains or generates a crack-like flaw. Under such conditions, fracture initiation will be "forced" at temperatures above the NDT point and the fracture will propagate in the cold worked deformation area. Continued propagation into the undeformed portions of the structure (elastic load regions) will be possible only if the temperature is below the FTE point. Thus, the development of a limited rupture or complete collapse of the structure may hinge on whether the steel is below the temperature of propagation under conditions of elastic loading or above this temperature. It is probable that the "accident case" applies also to conditions involving local cold-forming of weldments containing high-residual stresses.

The Military Case. The structure is expected to withstand conditions involving general deformation. This is a special case met principally in certain types of military service and in general cold forming of weldments. This is a case involving the prevention of brittle fracture despite the development of drastic deformation. This can be accomplished only if the steel is above the FTP temperature, i.e., at a temperature of complete resistance to brittle fracture.

Figure 3 illustrates results expected for temperatures above (left side of illustration) and below (right side of illustration) the applicable transition temperatures for each type of service. The corresponding behavior in crack starter tests is illustrated separately. The "X" marks denote fracture stoppage for conditions of temperature above the respective critical transitions.

It should be emphasized that design based on notch ductility results from a policy decision that the possibility of brittle fracture must be eliminated because of danger to life, property, etc. The selection of a suitable transition feature based on the anticipated service stresses may be important to costs as well as safety. Considering the presently available steel plates as an example, for the case of service to 0° F,

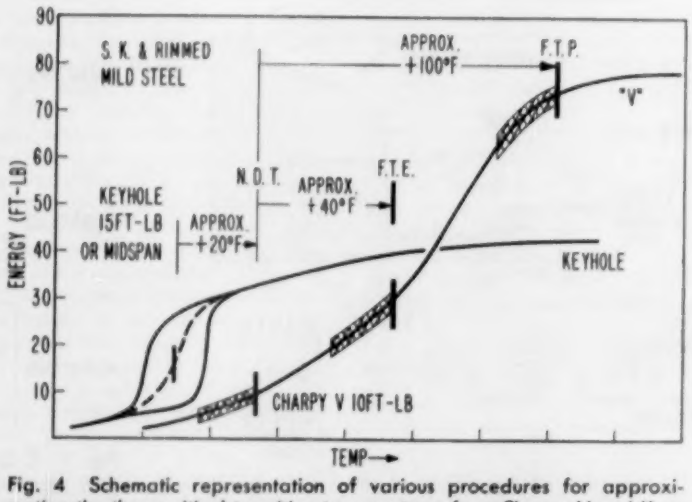

Fig. 4 Schematic representation of various procedures for approximating the three critical transition temperatures from Charpy V and Keyhole data of ship fracture steels

a selection based on NDT may permit the use of a suitable semikilled mild steel, a selection based on FTE may require a normalized fully killed mild steel, and a selection based on FTP will definitely require a quenched and tempered alloy steel. There is no implication in this discussion to urge the adoption of these procedures for any and all types of weldments and service. A decision to adopt notch ductility concepts in design must be based on a realistic consideration of the problem and of past experience.

Extensive investigations by the Naval Research Laboratory of a wide variety of steels* by means of explosion crack-starter tests and drop weight tests have established that the *temperature intervals* between the three critical transition temperatures are remarkedly similar. The following is a summary of the tests conducted on these various materials:

(1) NDT temperatures were determined by the drop weight method.

(2) Explosion test plates broke "flat" and fragmented at and below the NDT temperature.

(3) Propagation of fractures through the edge region of the explosion test plates stopped at temperatures of 40 to 60° F above the NDT temperature.

(4) At temperatures of 100 ± 20° F above the NDT temperature, all materials developed shear fractures only.

This information suggests that if a "fix" is obtained for the nil ductility transition temperature, a general Δt correction may be applied to establish the *approximate* critical transition temperatures for the cases of elastic and plastic loading. The NDT may be obtained directly by means of the drop weight test or indirectly by correlation with Charpy V or keyhole transition curves.

Figure 4 illustrates how Charpy V and keyhole transition curves may be used to establish the approximate values of the three critical temperatures. This approach has been exactingly evaluated for the case of semikilled and rimmed structural steels[4] involved in ship fractures. The critical reference point is the Charpy V 10 ft-lb temperature which marks the safe upper limit of the nil ductility transition. If the keyhole curve is used, this reference point may be approximated by a +20° F correction to the 15 ft-lb transition temperature (K_{15}) or the equivalent midspan transition (K_M).

Unfortunately, the reference point to the Charpy V curve and the Δt between the keyhole curve and Charpy V curves change with types of steel. Thus, the problem of using Charpy curves for "fixing" the critical NDT is one of finding correlation values applicable to the particular class of steel. Drop-weight tests indicate that for fully killed mild steels, the critical Charpy V energy point is approximately 20 ft-lb; for quenched and tempered alloy steel, it may be as high as 35 ft-lb.[1,4] The keyhole and Charpy V curves generally separate as the notch ductility of the steels increases. For quenched and tempered alloy steels the separation may exceed 100° F in some cases.

In the section to follow, the nil ductility transition characteristics of various common weld metals will be discussed and compared to known base steels. The correlation of weld metal NDT temperatures to Charpy V energy transition curves will be considered with the aim of indicating the significance of Charpy V and keyhole transition curves.

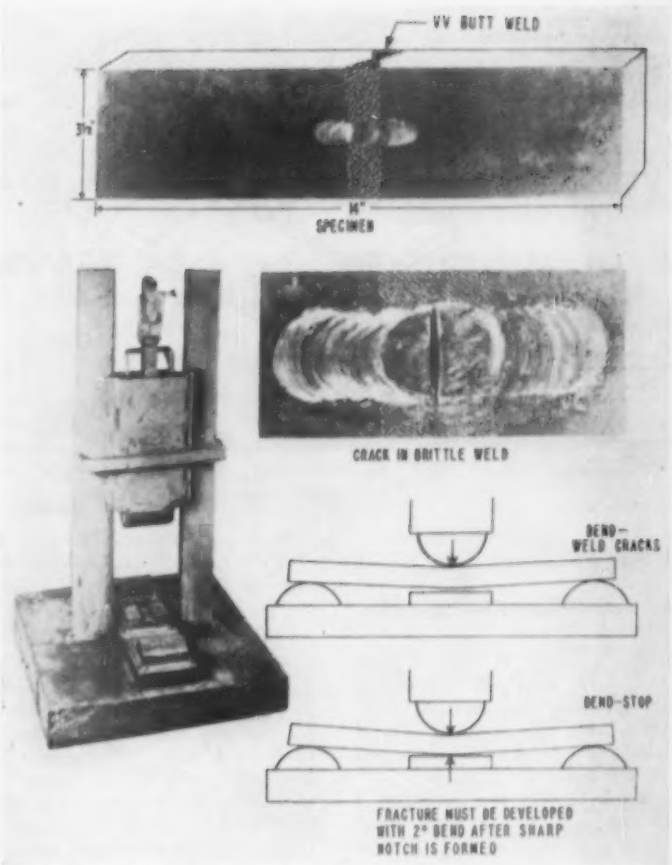

Fig. 5 Drop-weight test used to establish the nil ductility transition of weld metal

Transition Temperatures of Weld Metal

From a metallurgical point of view, the various types of ferritic weld metals are basically cast steels, usually of low-carbon content and alloyed to develop certain desired strength levels and microstructures. From a viewpoint of mechanics, weld metal should behave as steel and conform to the principles of transition temperatures. With these viewpoints, the same questions and problems arise concerning weld metal as arise for the case of steels.

First of all, it is necessary to obtain a general picture of the critical transition temperatures which are characteristic of specific types of weld metal. For example, it is desirable to ascertain if common types such as E6010, E7016, E10015 (Mn-Mo) and E12015 (G260) have transition temperatures at warm, freezing, or sub-zero levels. While such a picture is essential and provides rough guides, it is not fully sufficient for critical service requiring rigid specifications, because of variations from expected quality averages. Moreover, the present AWS Specifications do not include notch ductility requirements; therefore, it is essential to determine proper procedures for evaluating the critical transition temperatures of specific welds which are of interest for a given service application. Such procedures are necessary for purposes of specification and design. As in the case of steels, this means developing information as to the proper manner of

* Including mild steels, high-tensile steels, quenched and tempered steels, 12% Cr steels, cast steels, nodular iron and malleable iron.

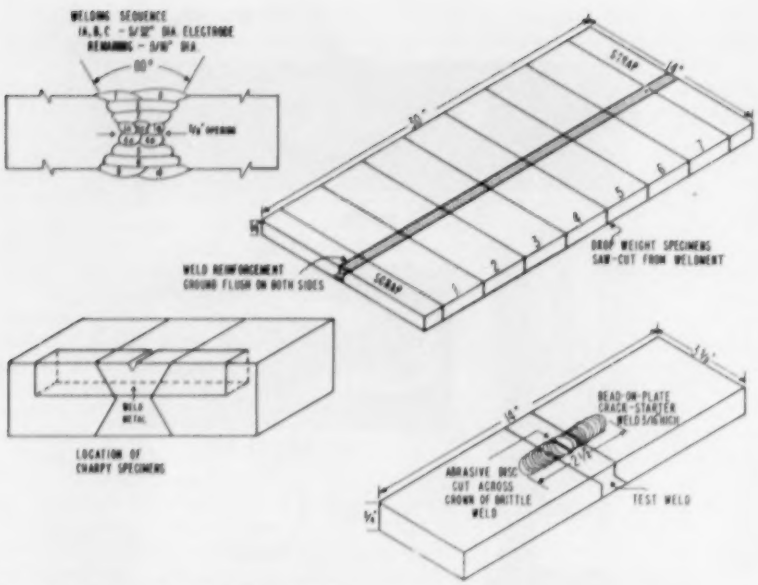

Fig. 6 Preparation of test specimens

comparing Charpy V and keyhole transition curve data and of deducing critical transition temperatures from such data. For this purpose, tests of large pieces of steel or of large samples of welds are out of the question.

The notch ductility characteristics of various common types of weld metal have been evaluated[5] with the aim of determining critical transition temperatures and correlations with Charpy data. The drop weight test, illustrated in Fig. 5, was utilized to establish the nil ductility transition for the ultra-sharp-crack case. As described in the previous reports by the author[1,4,5] the test defines the temperature at which a steel loses its ability to deform more than a very small amount, in the presence of a sharp crack. Figure 6 illustrates the welding procedures, the sectioning of the weld samples, and the method of application of the brittle weld which introduces the sharp crack into the test material. It should be noted that in this test, the initiation and propagation of the brittle fracture is restricted entirely to a conventional multipass butt weld; in this respect the prime plate enters the test only with respect to dilution effects.

Figure 7 illustrates the results of a typical test series, for the case of the E6010 weld. The nil ductility transition is indicated to occur at 0° F (highest temperature of fracture in the group noted as a standard test series). The relatively severe bending deformation which may be applied without fracture at 20, 30 and 40° F (nonstandard tests for purposes of illustration) indicates that fracture initiation is difficult above 0° F and corresponds to the sharp rise in the notch ductility curve illustrated schematically in Fig. 2 (*bottom*). The analyses of the base plate and of the weld deposits are presented in Table 1. A summary of the NDT temperatures of the various weld metals is presented in Fig. 8. This summary includes E6010 electrodes from various sources and illustrates the effect of peening the last pass of E6010 electrodes and the effect of stress relieving the high strength welds.

The following broad picture was developed by these tests:

(1) The NDT of E6010 types

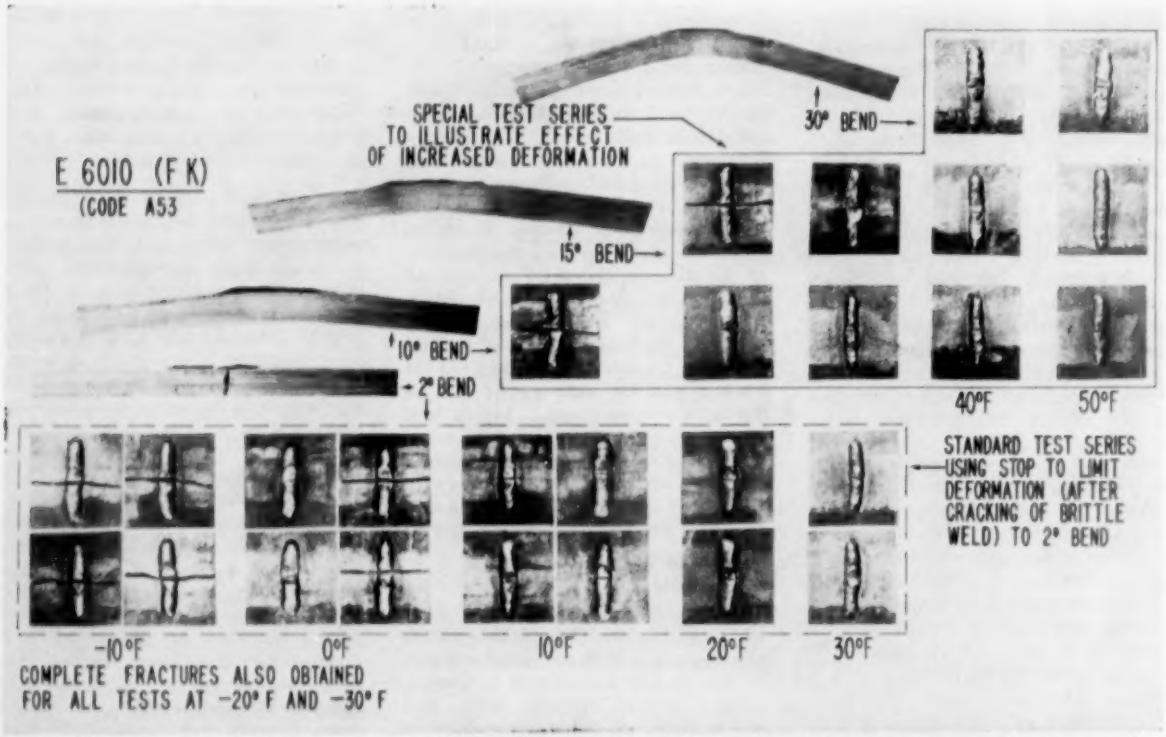

Fig. 7 Illustrating the critical effect of temperature on the ductility of E6010 weld metal in the presence of a sharp crack

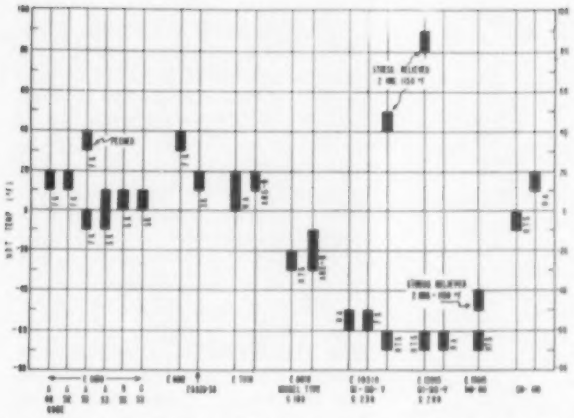

Fig. 8 Nil ductility transition temperatures of various weld metal types as established by drop-weight tests. Codes FK, SK, etc., denote steel types

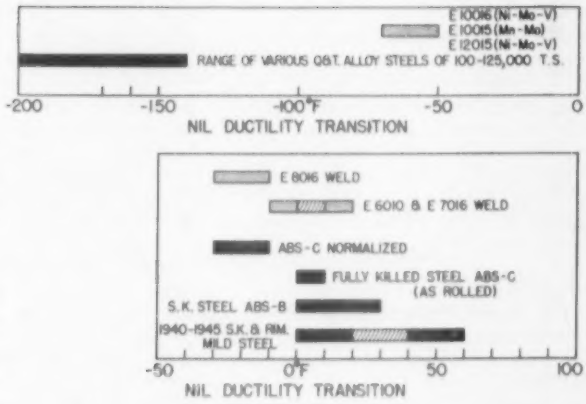

Fig. 9 Comparison of the nil ductility transition of various welds and steels, represented by $^3/_4$ to 1-in. plates. Dashed areas indicate "usual" values

consistently falls in the range of −10 to +20° F. The various heats of semikilled and fully killed steels which were used as base material did not affect the NDT significantly. Peening of the *last pass* was distinctly harmful and resulted in raising the NDT by 40° F.

(2) The E6012 type appears to be inferior to the E6010 type; the NDT occurs at 30 to 40° F. The E6020 and E7016 types are essentially equivalent to the E6010 group.

(3) The E8016 (Ni bearing G180) type develops NDT at −30 to −10° F and may be considered superior to the previously described types.

(4) The high-strength types E10015 (Mn-Mo), E10016 (Ni-Mo-V, G230), and E12015 (Ni-Mo-V, G260) develop NDT in the −70 to −50° F range. Stress relieving is indicated to be distinctly embrittling to the vanadium bearing G230 and G260 types; the NDT is raised to the +40 to +90° F range. Recent tests have indicated that it is possible to produce E10016 (Ni-Mo-V, G230) electrodes that retain −60° F NDT after stress relieving; however, no case of such achievement for the E12015 (G260) has been found to date.

(5) The Cr-Mo type appears to be essentially equivalent to the E6010 group; NDT occurs in the −10 to +20° F range.

This pattern provides a basic picture of what may be expected for the various types of electrodes, at least for the types available at the time of the tests (1953). Discussions with leading producers of electrodes at the time of writing this report (1955) disclosed the opinion that the relative rankings remained appropriate except for improvements in the E7016 class (considered in the present state of development to be superior to the E6010 class) and the development of special grades of notch ductile E6021

Table 1

Plate analyses

Type	*Code*	*C, %*	*Mn, %*	*Si, %*	*Ti, %*	*V, %*	*Ni, %*	*Cr, %*
Semikilled MS	SK	0.24	0.57	0.05	..	..	..	..
Fully killed MS	FK	0.16	0.67	0.21	..	..	..	..
Ship plate ABS-B Spec.	ABS-B	0.18	0.69	0.04	..	..	..	..
Navy high tensile	HTS	0.19	1.21	0.26	0.01	0.03	..	..
High alloy	HA	0.27	0.29	0.24	..	..	3.12	1.19

Weld Analyses

Electrode	*Plate*	*C, %*	*Mn, %*	*Si, %*	*S, %*	*P, %*	*Ni, %*	*Cr, %*	*Mo, %*	*V, %*
E6010										
(A46)*	FK	0.06	0.65	0.34	0.024	0.020	..	..	..	..
(A52)	FK	0.10	0.46	0.13	0.027	0.021	..	..	..	..
(A53)	FK	0.08	0.40	0.10	0.025	0.023	..	..	..	..
(A53)	SK	0.08	0.38	0.11	0.024	0.020	..	..	..	..
(B53)	SK	0.09	0.61	0.25	0.029	0.025	..	..	..	..
(C53)	SK	0.09	0.41	0.20	0.024	0.012	..	..	..	..
E6012	FK	0.07	0.29	0.20	0.031	0.022	..	..	..	..
E6020-30	SK	0.12	0.30	0.15	0.025	0.021	..	..	..	..
E7016	HA	0.10	0.45	0.43	0.027	0.023	0.40	0.18	..	..
	ABS-B	0.10	0.47	0.53	0.028	0.024	0.05	0.03	..	..
E8016-G180	HTS	0.07	0.57	0.58	0.024	0.020	0.88	0.14	..	..
	ABS-B	0.08	0.35	0.57	0.021	0.017	0.86	0.14	..	..
E10016-G230 (Ni-Mo-V)	HA	0.06	0.47	0.43	0.018	0.014	1.54	0.15	0.38	0.14
	FK	0.05	0.50	0.48	0.024	0.010	1.31	0.19	0.35	0.13
	HTS	0.06	0.52	0.48	0.020	0.016	1.47	0.24	0.41	0.13
E12015-G260 (Ni-Mo-V)	HTS	0.06	0.87	0.34	0.018	0.012	1.33	0.13	0.53	0.20
	HA	0.07	0.90	0.40	0.022	0.018	1.53	0.23	0.42	0.20
E10015 (Mn-Mo)	HTS	0.13	1.81	0.40	0.030	0.026	0.09	0.14	0.21	..
Cr-Mo	HA	0.08	0.54	0.31	0.024	0.010	0.38	1.77	0.53	..
	HTS	0.07	0.61	0.30	0.025	0.010	0.05	1.87	0.50	..

* A, B, C. Various brands. 46, 52, 53 = year of purchase; all other electrodes 1953 purchases.

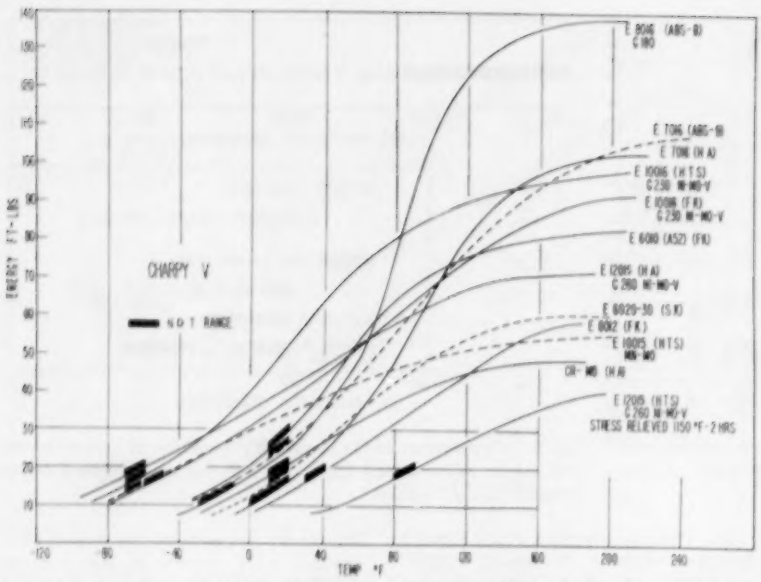

Fig. 10 General correlation of drop-weight test nil ductility transition to Charpy V transition curves. The bands indicate the nil ductility transition temperature of welds and corresponding Charpy V energies developed at these temperatures

In these tests, brittle fractures were noted to propagate extensively in the weld metal only if the temperature did not exceed the NDT by more than 20 to 40° F; similarly, the welds failed only by shear if the temperature was 80 to 100° F above the NDT. These limits were most apparent in the case of weldments of notch ductile base steels which completely resisted brittle fracture and thereby forced the development of failure into the weld areas, as will be discussed in sections to follow.

For the case of the base steel, a "fix" of the NDT, and consequently of the other two critical transition temperatures, may be approximated by correlation with Charpy V transition curves. For rimmed and semikilled structural steels of the type involved in the fracture of wartime ships, a "fix" is obtained in the range of Charpy V, 5 to 10 ft-lb transition temperatures. A safe "fix" is established by taking the 10 ft-lb transition temperature. For fully killed steels, a similar approximate "fix" is established by the Charpy V 20 ft-lb temperature; for quenched and tempered alloy steels of 125,000 psi T.S. class, a 25 to 30 ft-lb temperature is indicated.

considered to be equal to or possibly better than the E6010 type. It was stated also that high-volume electrodes of improved notch ductility, such as the E6012 type, are being demanded by users and that this has resulted in the production of special grades of improved E6012 electrodes. It is important to recognize that such changes are under way and that the picture presented in Fig. 8 is subject to rapid modification.

It is interesting to compare the NDT of the various welds with those of the steels (Fig. 9). It is apparent that the E6010 types are somewhat superior to the semikilled and rimmed structural steel plate of $^3/_4$ to 1 in. thickness and essentially equivalent to the fully killed structural steel plate in the as-rolled condition. The E8016 type is essentially equivalent to the normalized, fully killed steel plate. The need for high-strength, high-notch-ductility weld types to match the properties of quenched and tempered alloy steels in the as-deposited condition is obvious from the illustration.

As explained in the previous section, all of the steels investigated by explosion crack starter tests, resisted the propagation of fractures under conditions of elastic loading at temperatures of 40 to 60° F above the NDT, and fractures occurred only by shear at approximately 100° F above the NDT temperature. Welds appear to fall into this same pattern, as indicated by the results of many explosion bulge tests* conducted at the Naval Research Laboratory.

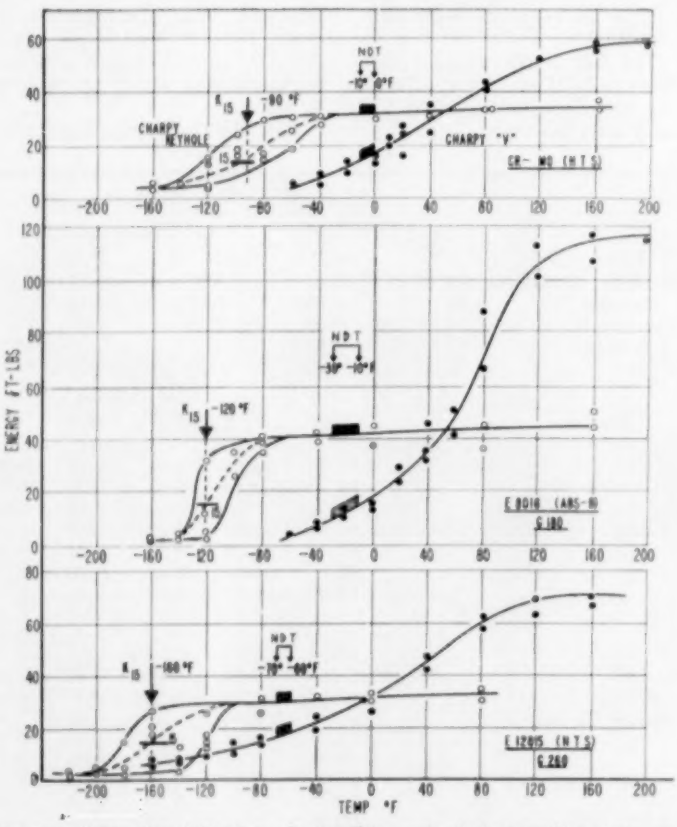

Fig. 11 Illustrating difficulties of using Charpy keyhole transition data and single temperature keyhole or Charpy V data. The nil ductility transition as determined by the drop-weight test is best established by correlation with the Charpy V 20 ft-lb temperature

* Explosion tests of 20- x 20-in. VV butt weldments of $^3/_4$- to 1-in. plates; weldments are bulged to failure.

Fig. 12 Stoppage of ship fracture at E6010 butt weld

Figure 10 illustrates the correlation found for the welds of Fig. 8. It appears that a general correlation is established in the range of 15 to 25 ft-lb and that the 20 ft-lb transition temperature may be taken as an average "fix" point. On this basis, the NDT of seven of the welds shown in Fig. 10 would be "fixed" to within 10° F, two would be "fixed" approximately 20° F low, and three would be "fixed" approximately 20° F high. It is possible that a statistical survey may disclose the need for establishing slightly different values of energy for the "fix" point of the various types; however, at this time, the best approximation of the NDT for the case of a sharp notch appears to be obtained by the Charpy V 20 ft-lb transition temperature.

It is important to recognize that the maximum energy developed at the upper shelf of the Charpy V transition curve is not significant to the notch ductility problem. The transition range of the Charpy test defines the notch ductility quality while the values at the upper shelf merely indicate relative energy absorption when fractures occur by shear. Failure by shear is not a problem of engineering concern, since such failures would occur only as the result of gross errors in calculations of allowable stresses.

As in the case of steels, correlations based on Charpy keyhole curves are difficult because the only significant portion of the keyhole curve (the scatterband portion) occurs at temperatures which are greatly below the critical transitions determined by large size test specimens. Figure 11 illustrates the difficulty of using keyhole data, including inconveniently low temperatures of testing and variable Δt between the keyhole transition and NDT or the Charpy V curve. The usual practice of conducting keyhole tests at fixed temperatures such as RT, 0 and −40° F is indicated to provide no discrimination for the three welds of Fig. 11, inasmuch as the scatterband occurs below −40° F in each case. In fact, higher values would be obtained for the E8016 weld (NDT −30 to −10° F) and equal values for the Cr-Mo (−10 to 0° F) and the E12015 weld (NDT −70 to −60° F). Unless the scatterband section of the keyhole transition curves are established, it is impossible to judge relative differences in critical transition temperatures. Even then, the addition of a suitable Δt correction to arrive at the actual NDT is, in the author's opinion based on many such attempts for welds and various steels, not a desirable operation because of the added uncertainty of the Δt correction. It is best to go directly to the use of Charpy V tests and thus avoid the use of an additional Δt correction to establish the NDT.

The use of Charpy V specimens requires the development of the lower portion of the transition curve; it is not necessary to develop the entire curve. The necessary "fix" may be obtained with curves ranging roughly from 10 ft-lb to 40 ft-lb in each case.

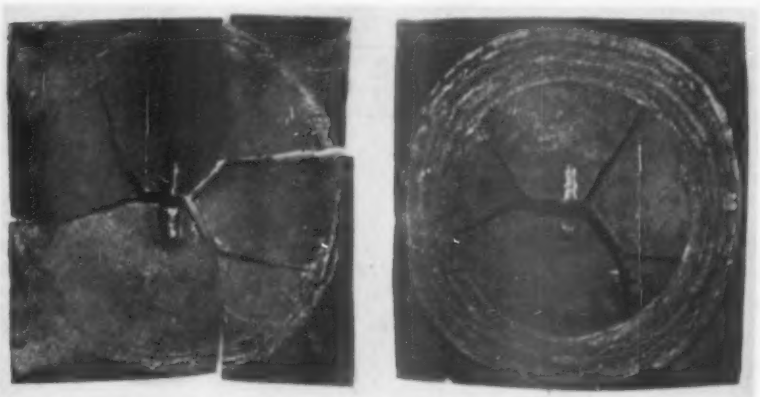

Fig. 13 Examples of ship plate fractures obtained in explosion crack starter tests at 20 to 40°F (*left*) and the effect of adding an overlay (both sides) of notch ductile E12015 (G260) weld metal (*right*). Overlay is one pass and approximately 3/16 in. thickness

The use of Charpy V curves for fixing the NDT may be criticized as yielding approximate information. It is agreed that this is the case; however, the alternative involves conducting large scale tests such as the drop weight. Moreover, it represents a great advancement over the previous state of knowledge in that a significant point of comparison is finally provided for the development and use of electrodes based on notch ductility.

It is interesting to note that Williams[6] reports, "in a number of cases, far out of proportion to the relative areas of weld and base metal, the (ship) fracture stopped at or near welds." Figure 12 illustrates an example, provided by Williams. It is possible that the lower NDT temperature and correspondingly lower FTE of the E6010 weld metal compared to the ship plate was responsible for some of the stoppages noted. In fact the illustration of Fig. 12 suggests that the stoppage is due to the weld rather than to the adjoining plate. A close inspection of the strain line pattern of the paint surface discloses that the focal point of the pattern is in the weld and not in the adjacent plate. Figure 13 illustrates that a circular weld pad of E12015 (G260) weld metal, which has an estimated FTP of approximately +40° F (NDT −60 to −70° F), successfully stops the propagation of fractures at 20 to 40° F in explosion crack starter tests of ship plate. A detailed study of the tip ends of the fractures disclosed that stoppage was due to the development of shear in the weld pad as the brittle fracture attempted to penetrate the weld region. Compressive stresses cannot supply an explanation of this behavior, since the weld region is deformed to the extent indicated by the opening of the crack tips in the illustration of Fig. 13.

Notch Ductility Data from Various Sources

A literature search was conducted with the purpose of summarizing all reported notch ductility transition data for weld metal. The search disclosed a limited number of complete transition curves. For the most part, the available curves were obtained with Charpy V tests. Charpy keyhole data featuring full transition curves were so few in number and the curves so poorly established that, after due consideration, it was decided that the keyhole information was not sufficient to warrant comment. Data relating to single temperature tests were not considered for reasons stated in the foregoing sections.

Requests for information from electrode manufacturers and various fabricators evolved relatively little further data of this type. For the most part, the only information which could be

obtained pertained to tests at one or two temperatures. There is no question of lack of cooperation; the desired information simply is not available. The writer is convinced that the status of notch ductility data for weld metal in 1955 is approximately the same as that for mild steel ship plate prior to 1945, i.e., very scanty.

A summary of the collected data is presented in Fig. 14, *A*, *B*, *C* and *D*, separated into three groups—the E60xx; the E70xx and E80xx; the high-strength E100xx and E120xx types; and various submerged-arc types. References are coded to the individual curves.

The orientation of the Charpy V notch used for the reference[5] tests was in the plate surface direction, see Fig. 6; all other references which provided this information used specimens with notches oriented in the plate thickness direction It is generally claimed that the last pass region of the weld involves unrefined as-cast structures and that the placing of the notch in this zone

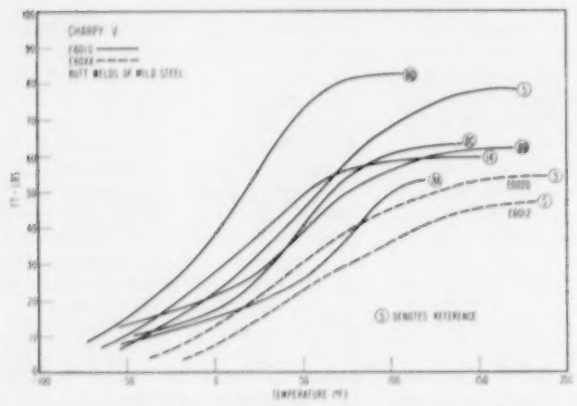

Fig. 14A Charpy V notch properties of various welds

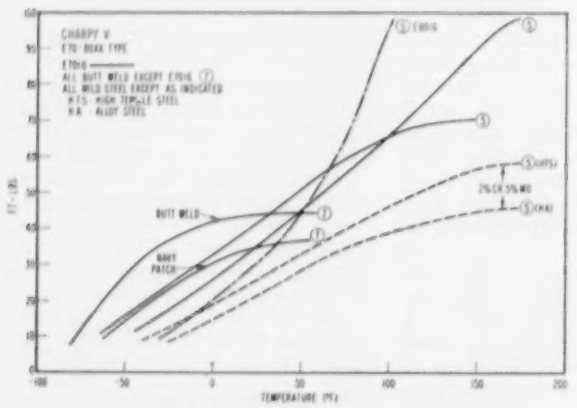

Fig. 14B Charpy V notch properties of various welds

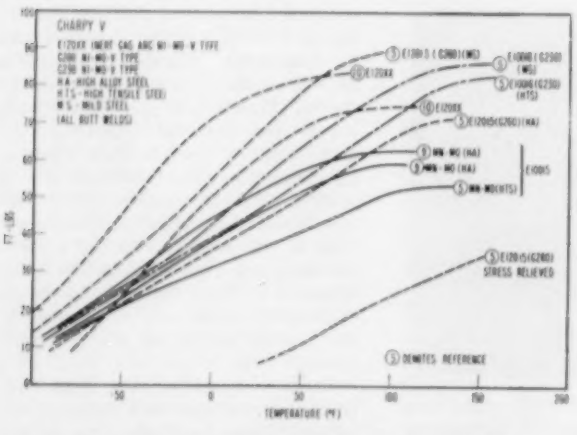

Fig. 14C Charpy V notch properties of various welds

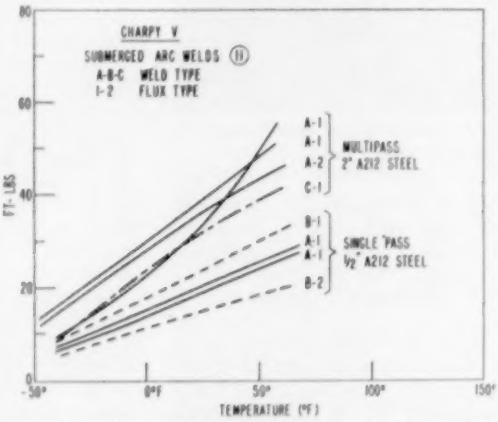

Fig. 14D Charpy V notch properties of various welds

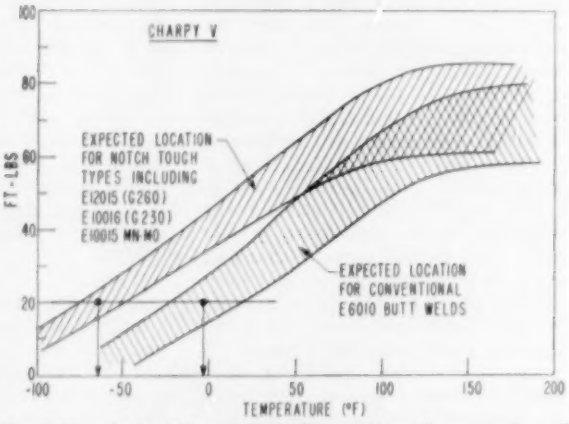
CHARPY V
EXPECTED LOCATION FOR NOTCH TOUCH TYPES INCLUDING E12015 (G260) E10016 (G230) E10015 MN-MO
EXPECTED LOCATION FOR CONVENTIONAL E6010 BUTT WELDS
FT-LBS
TEMPERATURE (°F)

Fig. 14E Typical "bands" of Charpy V notch properties of various welds

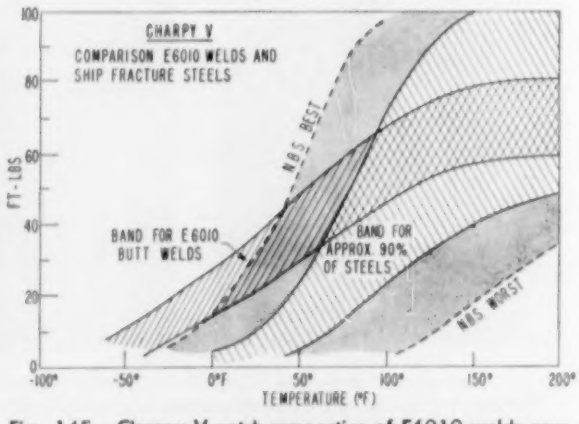

Fig. 14F Charpy V notch properties of E6010 welds compared to ship plate steels of World War II production

provides questionable data of the notch ductility of the body of the weld. In the case of the NRL tests (Reference 5), the crown of the weld was machined flush to the plate surface and the V notch was positioned in refined weld material. It is not possible to conjecture on the effect of notch orientation in weld tests, since the required comparison data are not available. The summary data of Fig. 14, *A* to *D*, indicate that the data in Reference 5 are in general agreement with the data of other references utilizing a different orientation of notch. This may result from the fact that in both cases the notch was placed in refined weld metal.

In order to compare Charpy V data of various welds, it would be useful to develop "typical" bands for one or two common types. This approach provides a means of ready reference, similar to the base line reference of steels represented by the ship fracture plates that have been studied in detail. Figure 14*E* presents bands indicating the expected location of E6010 butt welds commonly used for welding of mild steels and the notch-tough, high-strength welds developed for welding of notch ductile quenched and tempered alloy steels. These two groupings, while represented by a limited number of curves, still permit drawing of approximate reference bands. The two bands are separated by approximately 60° F in the 10 to 30 ft-lb transition range. The 20 ft-lb transition temperature, used as reference for a "fix" of the NDT temperatures, locates the NDT temperatures as indicated by the arrows in Fig. 14*E*. Drop weight tests of these two groups confirm the prediction of the two reference bands.

It is suggested that Fig. 14*E* be used to evaluate the relative position of other Charpy curves for weld metal. For example, the E120xx curves of Fig. 14*C* are noted to be somewhat superior to the band representing notch-tough grades in conventional use. The 2% Cr, 0.5% Mo welds of Fig. 14*B* are, by this reference comparison, approximately of equal notch ductility to the E6010 type. The E70xx and E80xx types of Fig. 14*B* in general fall between the two reference bands. The various E60xx type submerged-arc welds of Fig. 14*D* separate roughly into two groupings with the multipass types falling in the lower temperature region of the E6010 band, and the single-pass type falling in the high-temperature region of the subject band. Similar comparison may be made for other Charpy data obtained by the reader.

Another comparison of interest is the position of the E6010 band with bands determined for plate steels. Figure 14*F* presents such a comparison for the case of ship fracture steels.[4,6] It is readily apparent that the E6010 band falls at lower temperature than the average band for the steels, indicating superior notch ductility.

There are many other questions that could be considered but not answered because of the lack of requisite data. One such question relates to the effects of full heat treatment of welds. Another question relates to the effect of restraint during the cooling of the weld; in this respect, Reference 7, Fig. 14*B*, indicates that high restraint has an embrittling effect which may possibly be rationalized in terms of the development of weld microcracks such as investigated extensively by Flanigan.[12] These and other questions, such as that of the unrefined layer of the last pass, are important to the problem of weld notch ductility and require future investigation.

Notch Ductility of Weld Metal as a Factor Controlling the Performance of Weldments

There are four possible paths by which brittle fractures may propagate through a welded structure so as to develop catastrophic collapse (Fig. 15). These include: plate, heat-affected zone, fusion line, and weld paths. Propagation through any given path becomes possible only if the service temperature is below the critical fracture transition temperatures of that zone, as described in the previous sections.

Propagation by plate path has received almost exclusive attention in the literature because of the dramatic failures of wartime ships and of large welded structures by such a path, at temperatures commonly in the range of 30 to 60° F. In the case of the ships, there is a sharp cut-off in the extent of fracture such that complete fracture of the structure was frequently obtained below the 50 to 60° F range but not above this temperature range. At temperatures in the range of 60 to 80° F the fractures were restricted to single plates or to a few plates in line. This behavior results from the fact that the majority of the steels used in the fabrication were characterized by FTE transitions in the 50 to 70° F range. Above 60° F a large fraction of the steels were above the propagation temperature (limited fractures were obtained), while below 50° F almost all of the steels were below the propagation temperature (complete fractures of the ship were obtained).

An entirely different and special set of conditions exists for the case of weldments of certain quenched and tempered alloy steels, characterized by critical temperatures (FTE and FTP) below −100° F. At any atmospheric temperature (−60° F considered to be the lowest), such steels are completely

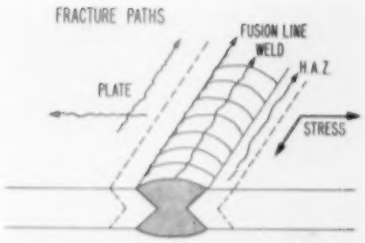

Fig. 15 Possible paths of brittle fracture in weldments

immune to the propagation of brittle fracture. If collapse by brittle fracture occurs, it must be by progagation of the fracture through the weld, heat-affected zone, or fusion line paths. In the discussions to follow, these two types of steels will be compared so as to illustrate extremes in the problem of weldment performance; i.e., the problem of weldments featuring plate fracture paths and the problem of weldments featuring the absence of a plate fracture path.

The existence of a brittle fracture path does not mean that such a path will necessarily become operative. Figure 15 illustrates that while propagation by plate path may occur in any direction dictated by the stress field, propagation by weld, heat-affected zone, and fusion line path is possible only when there is an adequate component of the applied stress acting in a direction perpendicular to these unidirectional paths. Studies of fracture paths have been made with the explosion bulge test [13–17] which features equal stressing in all directions and therefore provides a critical test for all crack paths by simultaneous loading in weld longitudinal and transverse directions. Figure 16 illustrates the performance which is typical of E6010 mild steel weldments of the type used in wartime ships. At 20 to 60° F, the fractures propagate only via a plate path, i.e., in the same

Fig. 16 Illustrating plate fracture paths developed in E6010 weldments of 1-in. mild steel; ship plate tested at 20 to 40°F

Fig. 17A Illustrating heat-affected zone fracture paths developed at subzero temperatures; E12015 weldments of quenched and tempered alloy steel

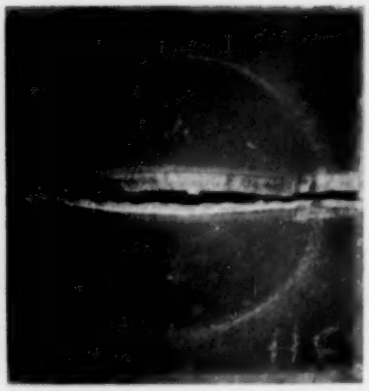

Fig. 17B Illustrating fusion line fracture path at 60°F for 25-20 weldment of quenched and tempered alloy steel

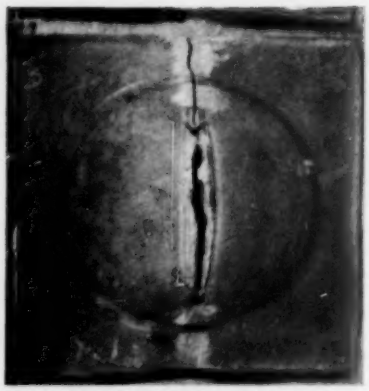

Fig. 17C Illustrating weld fracture path at 0°F for E12015 (embrittled by stress relieving) weldment of quenched and tempered alloy steel

fashion as observed in service failures. There is no tendency for propagation via weld, heat-affected zone, or fusion line paths. Fractures which cut across the weld in the 40 to 60° F tests show a distinct change in fracture appearance in the weld region, characterized by readily visible shear lips. This clearly indicates that the path of least resistance to brittle fracture is the plate material. As the temperature is lowered to the 0 to −20° F range, brittle fractures are propagated extensively also along the weld and the heat-affected zone. The point to be made is that each element of the weldment has its own characteristic temperature for the propagation of brittle fracture. In the case of the ships, the problem of brittle fracture in the 20 to 60° F range resulted from the fact that the plate fracture path was possible at the temperatures of winter operation but not at summer temperatures. In order to solve the problem of propagation by plate path it is necessary *to improve the notch ductility of the steel.*

Explosion bulge tests of various weldments of the quenched and tempered alloy steel described previously (FTP at or below −100° F) were made at temperatures as low as −100° F. Fractures by plate path were not developed in any case, even in the central portion of the bulge which was deformed severely. This should be expected because of the properties of the plate material. The fractures which did develop followed unidirectional paths along the heat-affected zone, weld, or fusion line depending on the particular type of weldment. Figure 17 (*A, B, C*) illustrates failures by heat-affected zone path, by fusion line path (25-20 weldments only), and by weld path.

Experience with explosion bulge tests of many varieties of weldments has shown that when the steel has a higher critical transition temperature (more brittle) than the weld, propagation by weld crack path is not developed until the test temperature used approaches the NDT of the weld metal, i.e., until the weld becomes highly brittle. When the base steel is of greatly lower critical transition temperature than the weld, complete fractures along weld paths may be obtained to about 40° F above the NDT of the weld. That is to say, when the steel is highly receptive to the propagation of brittle fractures, there is little tendency for a weld crack path to be taken unless the weld is at or below its NDT. When the steel is completely resistant to fracture propagation, the weld then accepts and propagates fractures to approximately +40° F above its NDT temperature. If the NDT of steel and weld are known, it is always possible to judge in advance if weld and/or plate fractures are possible in explosion bulge tests at specific temperatures.

It is clear from these tests that the lower the NDT temperature of the weld, the lower will be the temperature of *possible* fracture propagation by weld path. The problem is exactly the same as that of the steel; i.e., it is entirely a question of notch ductility as related to critical temperatures for propagation of brittle fractures. It is concluded that weld notch ductility is an important consideration for the prevention of brittle fractures in weld path directions. Problems of propagation of fractures along the weld in service must be approached and solved by improvements in the notch ductility properties *of the weld.*

Initiation Factors

It is axiomatic that brittle fractures will not be initiated in elements of the weld that are of nonpropagating type at the temperature in question. This is item "one" to be considered and recognized in any discussion of fracture initiation. The complexity of the initiation problem arises from the fact that a nonpropagating element may, under certain conditions, contribute to the process of fracture initiation in a propagating element. The contribution of the nonpropagating element is generally in the form of "developing the notch," which serves to test the propagating element. Figure 18 (*top*) illustrates the problem, in simple schematic terms, for the case of chance flaws. Chance flaws are defined as macroscopic flaws developed during fabrication or during the course of service. During fabrication the prime plate is subjected to the introduction of cracks resulting from arc strikes, rough flame cuts, etc; the heat-affected zone and fusion line may develop cracks as the result of thermal stresses, and the weld may contain gross defects of various types because of deviations from good practice. During the course of service the weld, fusion line, and heat-affected zones which are located in highly stressed regions, such as corners and other design notches, may undergo plastic deformation (plastic hinge points) resulting in the development of macroscopic, crack-like defects. The weld is

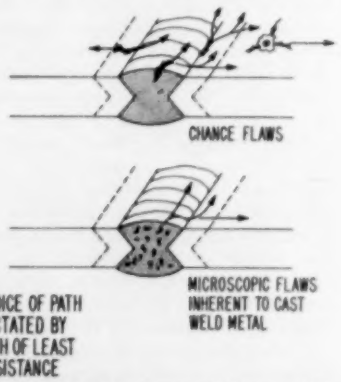

Fig. 18 Various types of flaws which provide notches required for the initiation of brittle fracture in weldments

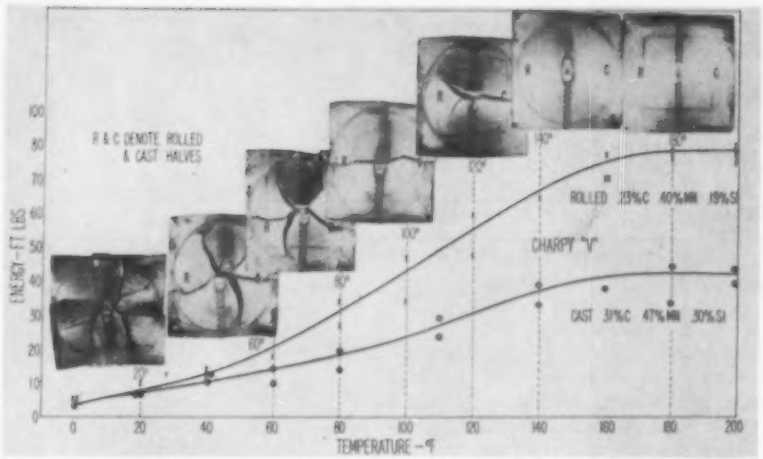

Fig. 19 Combined crack starter tests of rolled and cast steels of equivalent Charpy V transition features. Rolled and cast halves joined by welding

particularly susceptible to such action because of microscopic flaws, always present in cast metal, which tend to enlarge into macroscopic flaws, Fig. 18 bottom. These various defects, whatever the source, will tend to grow at positions of plastic flow; the growth will be slow, if the element which contains the flaw is nonpropagating, and will not affect the integrity of the structure until the tip of the defect (notch) "finds" an element which is susceptible to the initiation and propagation of cleavage fracture.

The role of the weld in such a process of flaw genesis and growth is of particular importance to this discussion. Data will be provided to support the following thesis:

(1) The weld, being a cast metal, always contains infixed, microscopic flaws, subject to a growth and "exploration for a fracture path" process.

(2) The notch ductility of the weld is an important aspect of this process—low-notch ductility will favor a crack-starting action, while high-notch ductility will act to suppress this process.

A series of tests were conducted on cast and rolled steels[16] with the aim of comparing the behavior of the two materials in a condition of the presence of a sharp notch and in the condition of "prime plate." The two steels were chosen on the basis of Charpy curves which developed transitions over the same temperature range. Figure 19 illustrates crack starter tests of composite plates (rolled and cast halves welded into single test plates); the crack starter weld was placed so as to introduce the sharp crack simultaneously into both halves. It is apparent from Fig. 19 that the two steels were exactly equal with respect to the initiation and propagation of brittle fracture in the presence of the sharp notch. The sharp crack acted as an equalizer in the sense that the natural flaws of the cast steel were not matched against the absence of equal flaws of the rolled steel. In this test, equal notch ductility means equal resistance to the initiation and propagation of brittle fracture at specific temperatures.

When these two steels were explosion bulge tested in prime condition,[16] a wide difference in performance was noted, Fig. 20. The rolled steel did not break flat (no measurable deformation) until temperatures of approximately 100° F below its NDT, while the cast steel could not develop consistently measurable deformation at about 40° F below its NDT. Obviously, the difference was the presence of inherent microscopic flaws in the cast steel and the absence of such flaws in the rolled steel. When the rolled steel was butt welded with E6010 weld (weld reinforcement removed), low deformation failures in the bulge test were developed at approximately 20° F below the NDT of the E6010 weld with the fractures starting in the E6010 weld. Welding of the cast steel with E6010 weld and E12015 (G260) weld did not change its performance; moreover, fractures always started in the cast steel plate. The schematic drawings at the bottom of Fig. 20 rationalize these events. Simply stated, adding the weld was equivalent to adding a band of cast metal containing inherent flaws. Since the cast steel had higher NDT than the two welds, there was no difference in performance because fractures always triggered in the *more brittle* of the two "notched" materials (weld and cast plate with microscopic natural flaws). For the rolled steel, a loss in performance resulted from the presence of inherent flaws in the E6010 weld cast band which served as notch sources.

Further studies[12-17] were made of the effect of introducing welds of different notch ductility (bands of cast steel of different notch ductility) in rolled mild steels. The intent was to determine if the notch ductility of the weld would show a controlling effect on the failure of the weldments. Comparison was also made with the effect of introducing sharp cracks in the prime plate. The tests were conducted by the explosion bulge method. Figure 21 (*top*) illustrates that temperatures in the order of 80 to 100° F below NDT of plate were required to develop low deformation failures for the case of the prime plate.

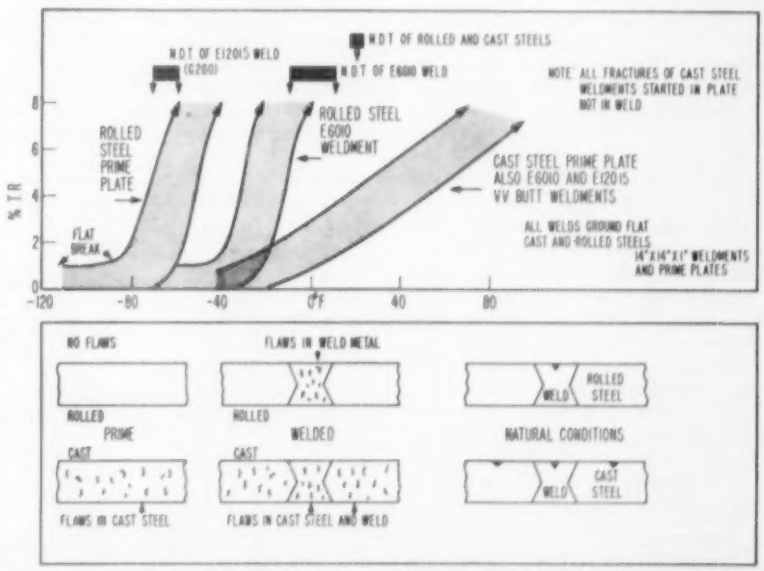

Fig. 20 Comparison of rolled and cast steels (of equivalent notch ductility) in explosion bulge tests; weldments and prime plates of 1 in. thickness. T.R. (%) represents thickness reduction of plate at fracture. (See Fig. 21)

In the *presence* of sharp cracks (crack-starter welds, arc strikes, etc.), nil deformation of the plate was attained at the NDT temperature of the steel. Weldments of E12015 (G260), Fig. 21 (*center*), develope l low deformation failures at approximately the NDT temperature (−70 to −60° F) of the E12015 weld metal. This signified that the inherent flaws of the weld metal became highly critical at temperatures equal to and below the NDT temperature of the weld metal. The brittle fractures which developed in the weld metal were transmitted also to the base plate with resulting fragmentation of the weldment (the steel at this temperature was far below its +20° F NDT temperature). Stress relieving of the E12015 welds raised the NDT of the weld to approximately +80° F; i.e., considerably above the +20° F NDT of the subject steel. Stress-relieved weldments of E12015 type, therefore, contain a band of cast metal which is more brittle than the steel plate. This is in contrast to the previous case in which the weld-metal notch ductility was greatly superior to that of the plate. In the case of the embrittled weld, brittle transverse* weld cracks were developed which acted exactly as the crack-starter bead on plate welds used for the fracture initiation studies. That is, the weldment fractured essentially flat at all temperatures below the NDT of the steel (+20° F). Above 20° F the progression of the cracks into the steel required "forcing" (since the steel was above its NDT) with consequent bulging prior to failure.

These data illustrate the principle that the performance of weldments of mild steel are controlled by the notch ductility of the weld metal. A close approach to the performance of the prime plate was obtained by the use of the highly notch ductile E12015 weld (NDT approximately −70° F); and a close approach to the performance of the plate in the presence of sharp cracks was obtained by the use of the brittle, stress relieved E12015 welds (NDT approximately +80° F). The inference is that high notch ductility suppresses the natural tendency of the weld to act as an "notching agent" to the plate, while low-notch ductility makes the weld act as an effective crack starter for the plate.

The data provided at the bottom of Fig. 21 illustrate that the optimum condition for a weld is that of a smooth-ground finish. It is noted that a shift in the bulge deformation transition to 40° F lower temperatures is obtained by removing the sharp weld ripples (notches)

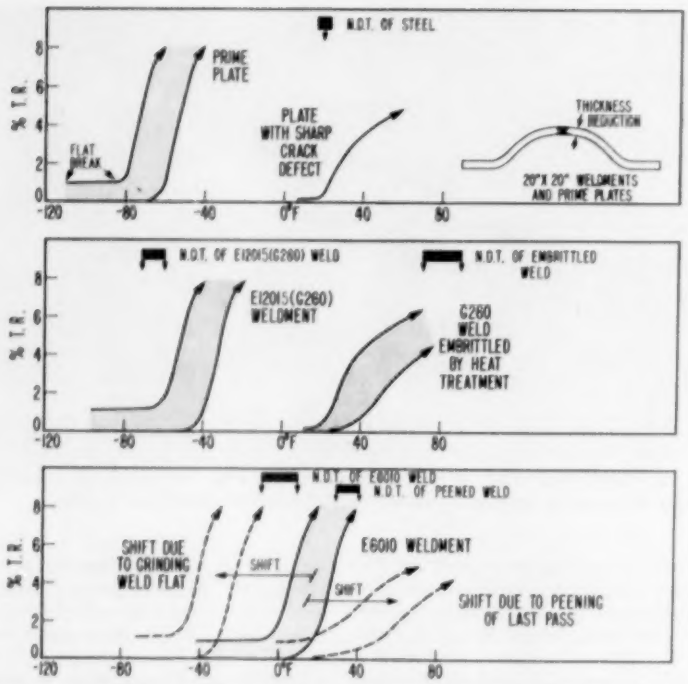

Fig. 21 Relative performance of weldments and prime plate in explosion bulge tests; mild steel ship plate of 3/4 in. thickness

associated with the weld crown. Also, it may be deduced that peening of the last pass tends to shift the performance curve to higher temperatures.[14] This is due to the embrittling effect of the cold working operation associated with peening (see Fig. 8). This conclusion does not apply to peening of passes other than the last pass.

It may be concluded that, in the absence of critical flaws in the plate itself or in the heat-affected zone, it is possible to shift the performance of weldments *at will* by control of weld metal notch ductility. However, when sharp crack flaws are located initially in or contiguous to the plate, weld notch ductility loses its significance and the performance of the weldment is completely controlled by the transition characteristics of the base steel. Weld notch ductility superior to that of the plate is always desired to counter the natural flaw condition of the cast weld metal. The use of welds having notch ductility inferior to that of the plate is catastrophic, for then the weldment behaves as if a profusion of cracks were present. In this sense, brittle welds act as crack-starters for steels capable of conducting brittle fracture. The special case of steels which do not permit fracture propagation is discussed in the following section.

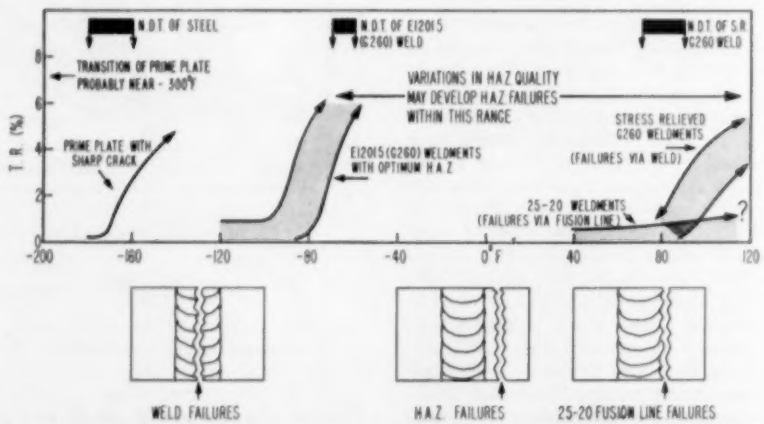

Fig. 22 Performance of quenched and tempered alloy steel (5/8 to 1-in. plate) as weldments and prime plate; summary of various tests

* In bulge tests of weldments featuring low-strength steels and high-strength welds, the weld always fractures transversely because the longitudinal direction is the direction of equivalent strain; see discussion related to Fig. 24. In this particular case a mild steel of 60,000 psi T.S. is joined by a weld of 120,000 psi T. S.

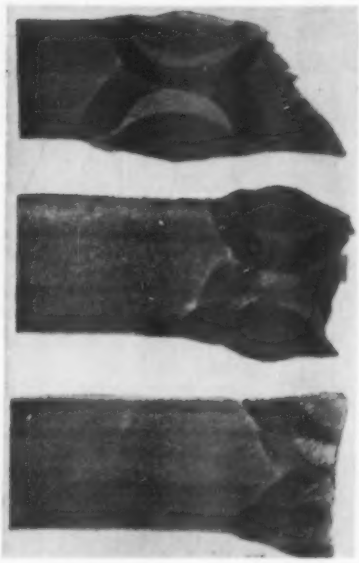

Fig. 23 Macrographs of fracture paths; 1-in. plate of quenched and tempered alloy steel welded with E12015 (G260) electrodes. (See text for details)

Steels of High Notch Ductility

In the case of steels which are completely resistant to brittle fracture to the lowest service temperatures, the plate fracture path is not available; therefore, if fracture is developed it must be as the result of propagation via the heat-affected zone, fusion line or weld paths. An example is provided by quenched and tempered alloy steels of high notch ductility. Figure 22 presents a summary of explosion bulge tests for such a steel; the NDT temperature was established by drop-weight tests as being in the range of -180 to $-160°$ F. Explosion crack-starter tests demonstrated that the steel developed shear fracture at all temperatures down to approximately $-100°$ F. Explosion bulge tests of the *prime* plate demonstrated that full bulges (complete hemispheres with 15% or more reduction of thickness) could be developed consistently at $-100°$ F. Actually, such a steel would be expected to behave in this manner to much lower temperatures.

When welded with E12015 (G260) electrodes, utilizing procedures designed to develop a heat-affected zone of optimum ductility, extensive bulge deformation could be obtained to temperatures in the order of the NDT (-70 to $-60°$ F) of the weld metal. At temperatures of 20 or 40° F below the NDT of the weld metal, brittle cracks initiated and propagated extensively in the weld, thus limiting the ductility of the weldment to a low order. This is in sharp contrast to the high ductility demonstrated by the prime plate at these same temperatures. Since the failures did not follow the heat-affected zone, it must be concluded that the notch ductility of the weld limited the performance of the weldment as a whole. A more spectacular example of the controlling effect of weld-metal notch ductility was apparent in the case of stress-relieved E12015 (G260) weldments which, when tested at room temperature, generally failed with little deformation and by brittle fracture located entirely in the weld. In this case, the weld metal NDT was in the order of +90° F.

By variations in welding procedures, it was possible to develop a heat-affected zone of poor quality such that failures entirely along the heat-affected zone were developed at room temperature. In the case of 25-20 welds, a poor quality zone (composed of mixed stainless and ferritic steel) was developed which caused the failure of weldments, with almost flat breaks, at room temperature. In this case, the sole fracture path was the fusion line.

These tests demonstrated that the performance of weldments comprising steels of high notch ductility may be controlled by the weld, heat-affected zone, or fusion line. Since none of these zones may act to promote the initiation of brittle fracture in the notch-ductile steel, the controlling zone tends to act also as the propagating element. In cases where there was no evidence of propagation in the heat-affected zone or the fusion line, the performance of the weldments was controlled by the notch ductility of the weld. When poor quality heat-affected zones or fusion line zones were present, a high order of notch ductility in the weld was of no avail, since low ductility failures of the weldment were dictated by the heat-affected zone or by the fusion line, and failures progressed along these paths.

It is evident from Fig. 22 that weld notch ductility exercises its usual control in the case of alloy steels of high notch ductility. For service in cold climates, the problem of these steels is not so much the weld (if not stress relieved, the E12015 (G260) weld protects the weldment to the lowest ambient temperature) but of the heat-affected zone, because of the high hardenability of the steel, or of the fusion line if austenitic electrodes are used.

Figure 23 illustrates various types of fracture obtained in explosion bulge tests of the subject quenched and tempered alloy steel, butt welded with E12015 (G260) weld metal. Figure 23 (*top*) illustrates ductile fractures consisting of short tears. Figure 23 (*center*) illustrates fractures due to a brittle heat-affected zone; such fractures may be obtained at room temperatures depending on heat-affected zone quality. Figure 23 (*bottom*) illustrates weld path fractures obtained at -60 to $-100°$ F; i.e., at or below the NDT of the as-deposited weld metal. Such fractures are obtained also at room temperature if the G260 weld is stress relieved (NDT raised to approximately +90° F).

Weld Strength Factors

The relative flow strengths of the weld and the base metal may be considered as factors of importance to the performance of weldments. Depending on the orientation of the applied load,

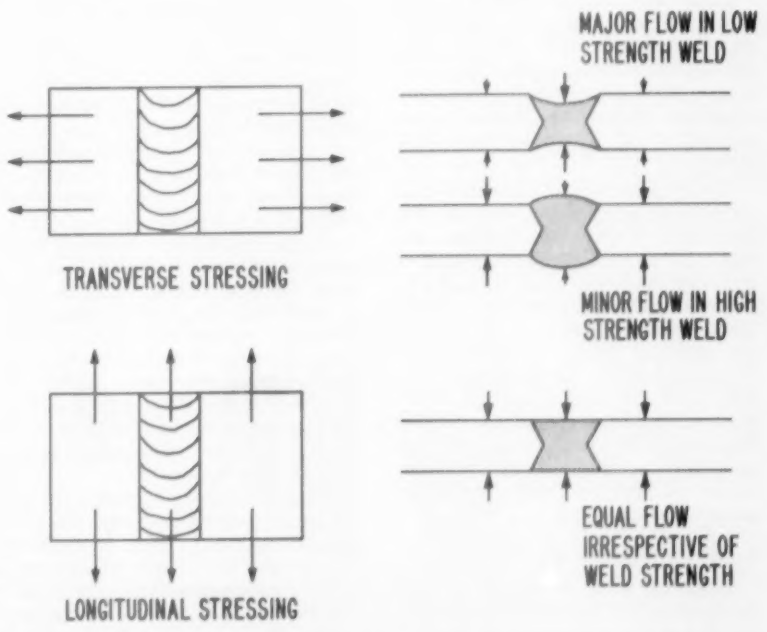
MAJOR FLOW IN LOW STRENGTH WELD
TRANSVERSE STRESSING
MINOR FLOW IN HIGH STRENGTH WELD
LONGITUDINAL STRESSING
EQUAL FLOW IRRESPECTIVE OF WELD STRENGTH

Fig. 24 Effect of loading direction on the plastic flow characteristics of welds

and for conditions of marginal weld notch ductility, weld strength factors may be the deciding factor in the development of failure; however, a brittle crack path must be available. The role of weld strength factors must be considered as "tipping the balance" for a potentially catastrophic system.

The overwhelming credit given to weld strength factors in the earlier days of development of welding electrodes stems from the almost exclusive evaluation by transverse bend tests of butt welds and the relatively "warm" temperatures of testing. Both of these factors reduced the importance of notch ductility and provided for misleading conclusions which have since been rectified in electrode development procedures. The following analysis is aimed at clarifying the contributions of weld strength as factors in the performance of weldments. The discussion is based on strain measurements, by photogrid techniques.[19]

For purposes of simplifying the discussion, simple butt welds machined to the same thickness as the plate will be considered, Fig. 24. On *transverse* loading into the plastic range, the relative flow strength of the weld as compared to the plate will determine if strain is concentrated or deconcentrated in the weld region. Welds of high flow strength transfer deformation to the plate material which ultimately may be made to fail by a necking process. If the flow strength of the weld greatly exceeds that of the plate, the deformation developed in the weld may be of low order; accordingly, weld ductility may not undergo test.

Longitudinal loading does not provide for strain deconcentration by high strength welds. To the contrary, weld and plate must strain equally. For such loading, weld notch ductility is always important irrespective of the relative strength of the weld compared to the plate.

The inadequacy of high strength in the absence of high notch ductility was illustrated[18] by the case of the stress-relieved E12015 (G260) weldments of mild and alloy steels (Figs. 21 and 22). Stress relieving of this weld causes vanadium carbide precipitation which has a strengthening effect as well as an embrittlement effect. In the biaxial stress system of the bulge test, the high strength could not compensate (in the longitudinal direction) for the decrease in notch ductility, and the biaxially loaded weldments suffered a drastic decrease in performance.

Testing of Weldments

There has been an element of confusion regarding the significance of the notch ductility of weld metal, resulting from the fact that Kinzel- and Lehigh-type weldability tests have been reported to reflect no effect of weld-metal notch ductility for the case of mild steels.[20] That is, tests of E6010 and E12015 (G260) welds yielded essentially the same results. This is in contradiction to the findings of the explosion bulge tests which indicate control by weld-metal notch ductility, as detailed in the foregoing sections. Actually, there is no contradiction if the mechanics of the two tests are analyzed critically, particularly with respect to the factors which determine the site of initial separation in the process of the development of fractures.

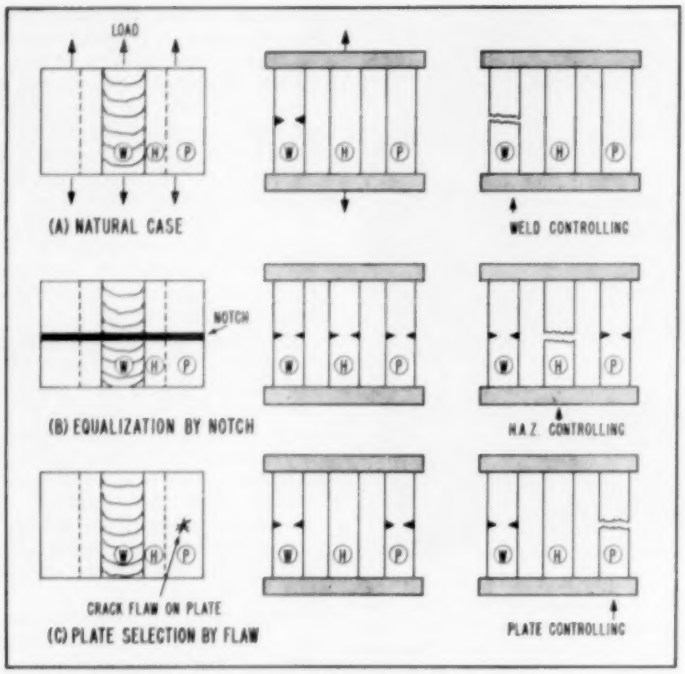

Fig. 25 Schematic illustration of factors which determine the site of initial separation in the development of fractures

Figure 25 (*top*) illustrates schematically the *natural* case for a weldment which does not contain macroscopic chance flaws; however, inherent microscopic flaws must be considered to be present in the cast weld metal. To the right it is illustrated schematically that on straining, the weld behaves as a notched tensile specimen, while the heat-affected zone and plate behave as unnotched tensile specimens. In this case it is obvious that the notch ductility of the notched (weld) element must be the controlling factor; that is what the explosion bulge tests show.

Figure 25 (*center*) illustrates the case of the weldability specimens which are notched across the weld, heat-affected zone, and plate. Now the schematic tensile specimens must be illustrated as notched in each case. The machined notch acts in the direction of being an equalizer in the same sense that the notch introduced into the cast and rolled steel (Fig. 19) was an equalizer. In this test there is a search for the most notch sensitive element, indicated in the quoted studies[20] to be the heat-affected zone, inasmuch as changes in weld notch ductility had no effect on the results. It is not surprising that weld notch ductility plays no part in these tests, for the test conditions are set against the development of the true role of weld metal in a conventional weldment, such as is illustrated as the natural condition (Case (A) of Fig. 25). In the natural case, there is no notching of all elements and almost complete removal of the weld metal, such as is the condition of the weldability tests. Equalization by notch, with a suppression of the role of weld metal, is an excellent way to evaluate changes in quality of the heat-affected zone; in essence, that is exactly what the tests were aimed at—to evaluate the response of the steels to the thermal cycles of welding. The difficulty appears to be that the primary purpose of the weldability tests have been lost sight of, and there is a tendency to eva'uate the results in much too sweeping a manner.

The case of the chance flaw on the plate, Fig. 25 (*bottom*) may be illustrated schematically by a notched weld (with inherent microscopic flaws), an unnotched heat-affected zone, and a notched plate. The competition here is between the plate and weld flaws; again, the superior notch ductility of the weld is made evident by plate control of

failure, as discussed for the case of arc strikes.

It is impossible, in the face of all existing evidence, to rationalize the results of weldability tests as indicating that there is no need for notch ductility in welds. Weldability, as measured by the established weldability tests, is only one of the many complex factors to be considered in analyzing the mechanics of weldment performance.

Conclusions

From a metallurgical viewpoint, the various types of ferritic weld metals are basically cast steels, usually of low-carbon content and alloyed so as to develop certain desired strength levels and microstructures. From a viewpoint of mechanics, ferritic weld metal should behave as a ferritic steel and conform to the established principles of transition temperatures as related to the problem of fracture initiation and propagation.

During the past decade, the basic factors which determine the fracture behavior of steels have been determined and engineering procedures for design based on notch ductility have been established. These procedures are based on the following concepts:

(*a*) It is assumed that sharp cracks (notches) will be present in the structure and that the steel will perform in a ductile or brittle manner depending on its notch ductility.

(*b*) Below a critical temperature, termed nil ductility transition (NDT), the steel demonstrates inability to deform more than a very slight amount in the presence of a sharp crack, while above this temperature ductility rises rapidly with increasing temperature.

(*c*) The NDT temperature of a given steel may be approximated by Charpy V tests, following the development of correlations of Charpy tests with large scale tests and service performance.

(*d*) Specifications, such as Charpy V 10 ft-lb minimum at the lowest service temperature, have been evolved to ensure that certain semikilled and rimmed steels will resist fracture initiation to the lowest service temperature. There is considerable evidence that the subject specification values differ somewhat with type of steel.

(*e*) If it is assumed that a local region of the structure may be deformed severely by accident, fracture initiation may be "forced." For such cases, it is essential to design on fracture transition; i.e., to ensure that fracture propagation in regions outside the overloaded spot will not be possible. The fracture transition falls approximately at 30 to 50° F above the NDT. This means that the specification temperature based on initiation (NDT) must be set 30 to 50° F below the lowest service temperature for such cases.

Specification of notch ductile steels are aimed at ruling out fracture by "plate path." The development of cracks in the weld or the heat-affected zone cannot endanger the notch ductile "plate" portion of the structure. If the weld or heat-affected zone are of deficient notch ductility, fracture propagation may occur via these two remaining possible paths. In a case of failure by weld metal path, the notch ductility of weld metal must be sufficiently improved to preclude either initiation or propagation, depending on the service conditions involved. In brief, this means that the more notch-ductile prime steels should be welded with welds of, at least, equivalent notch ductility if low temperatures permissible for the steels in question are to be likewise permissible for the weld metal portion of the structure.

Another, and more general case, must be considered—the use of steels of inadequate notch ductility which, somehow, must be protected from fracture. In essence, this means eliminating notches which would be dangerous for these steels. Notches may be developed by virtue of "on the plate defects," such as arc strikes, by cracks in the heat-affected zone, and cracks which may be present or developed in welds. Weld notch ductility contributes to the safety of such structures by virtue of eliminating one major factor from concern. Insofar as the other factors are involved, other remedial procedures should be used, such as preventing or removing arc strikes. Welds of inadequate notch ductility or dangerous in this case inasmuch as such welds would act as "crack starters."

In order to use notch ductility concepts in welded design, it is necessary to establish the critical transition temperatures of the steels involved—both the prime steel and the weld. This report provides general guides as to the expected transition temperatures of various steels and weld metals. The subject information indicates the general positions on the temperatures scale that are occupied by the materials in question. Because of quality variations from heat to heat of steel and from weld to weld, the positions in question may be described as temperature ranges. For example, E6010 welds are categorized by NDT in the range of −10 to +20° F and E12015 and E10015 welds by NDT in the range of −70 to −50° F. Obviously, the use of a −60° F NDT weld metal with +40° F NDT steel is not justified on economic grounds, while the opposite case would be highly undesirable on engineering grounds. These data provide a means of matching the notch ductility of these two components of the weldment.

Evaluation of the approximate position on the temperature scale of the critical transition temperatures of welds and base steel may be made by the use of conventional Charpy V tests. The point on the Charpy V curve which correlates with the NDT temperature varies somewhat with materials but falls generally within the range of Charpy V 10 and 30 ft-lb; weld metal appears to correlate well based on the Charpy V 20 ft-lb temperature as the significant point.

The role of weld strength factors is analyzed and indicated to involve "tipping the scale" for potentially dangerous systems. That is to say, in the absence of "fracture paths," weld-strength factors cannot lead to *brittle* fracture.

This report, by virtue of its purpose, has dealt most specifically with the effects of weld notch ductility. It should be stated that this is a most important factor, but only *one* of many factors which determine the performance of weldments.

References

1. W. S. Pellini, "Evaluation of the Significance of Charpy Tests," Symposium on the Effect of Temperature on the Brittle Behavior of Metals, ASTM Special Publication No. 158, 1954.

2. T. S. Robertson, "Propagation of Brittle Fracture in Steel," *The Journal of the Iron and Steel Institute*, Vol. 175, Dec. 1953. Discussion also covers additional studies by this author.

3. F. J. Feeley, D. Hrtko, S. R. Kleppe, and M. S. Northup, "Report on Brittle Fracture Studies," THE WELDING JOURNAL, **33** (2), Research Suppl., 99-s, 1954. Discussion also covers additional studies by these authors.

4. P. P. Puzak, M. E. Schuster, and W. S. Pellini, "Applicability of Charpy Test Data," *Ibid.*, **33** (9), Research Suppl., 433-s, 1954.

5. W. S. Pellini, and E. W. Eschbacher, "Ductility Transition of Weld Metal," *Ibid.*, **33** (1), Research Suppl., 16-s, 1954.

6. M. Williams, "Analysis of Brittle Behavior of Ship Plates," Symposium on the Effect of Temperature on the Brittle Behavior of Metals, ASTM Special Publication No. 158, 1954.

7. Private communication, Naval Shipyard.

8. (*A*) D. Swan, A. Lytle, and C. McKinsey, "Stress Relieving and Fracture Strength," THE WELDING JOURNAL, **30** (3), Research Suppl., 138-s, 1951. (*B*) J. Heuschkel, "Effects of Temperature on Weld Metal Properties," *Ibid.*, **33** (8), Research Suppl., 388-s, 1954. (*C*) F. Daniels, F. Gardner, and R. Reed, "The Comparative Behavior of Mild Steel Welds," *Ibid.*, **27** (9), Research Suppl., 439-s, 1948. (*D*) W. H. Bruckner, and W. E. Ellis, "Strain Aging in Welding Low-Carbon Structural Steel," *Ibid.*, **27** (9), Research Suppl., 446-s, 1948.

9. H. C. Campbell, "Transformation in Mn-Mo Deposited Weld Metal," *Ibid.*, **30** (5), Research Suppl., 253-s, 1951.

10. Private communication, electrode manufacturer *A*.

11. Private communication, electrode manufacturer *B*.

12. A. E. Flanigan, and M. Kaufman, "Microcracks and Low-Temperature Cooling Rate Embrittlement of Welds," THE WELDING JOURNAL, **30** (12), 613, 1951.

13. C. E. Harthower, and W. S. Pellini, "Investigation of Factors Which Determine the Performance of Weldments," *Ibid.*, **30** (10), Research Suppl., 499-s, 1951.

14. W. S. Pellini and E. Eschbacher, "Effects of Peening Last Pass of Welds," *Ibid.*, **33** (2), Research Suppl., 71-s, 1954.

15. P. P. Puzak and W. S. Pellini, "Embrittlement of High Strength Ferritic Welds," *Ibid.*, **31** (11), Research Suppl., 521-s, 1952.

16. W. S. Pellini, and E. Eschbacher, "Investigation of the Performance of Weldments and Prime Plate of ABS-B Steel," *Ibid.*, **33** (10), Research Suppl., 524-s, 1954.

17. NRL Memorandum Reports covering the performance of weldments of quenched and tempered alloy steels.

18. W. S. Pellini, E. Layne, and F. Brandt, "Performance of Cast and Rolled Steels in Relation to the Problem of Brittle Fracture," *A.F.S. Trans.*, 1953.

19. C. E. Harthower, and W. S. Pellini, "Explosion Bulge Tests of the Deformation of Weldments," THE WELDING JOURNAL, **30** (6), Research Suppl., 307-s, 1951.

20. W. J. Murphy, and R. D. Stout, "Effect of Electrode Type in the Notch Slow-Bend Test," *Ibid.*, **33** (7), Research Suppl., 305-s, 1954.

Welded Continuous Frames and Their Components
Progress Report No. 17

BEHAVIOR OF WELDED SINGLE-SPAN FRAMES UNDER COMBINED LOADING

Results of tests carried out on full-size portal frames indicate the applicability of plastic analysis to structural design

BY C. G. SCHILLING, F. W. SCHUTZ, JR., AND L. S. BEEDLE

SYNOPSIS. The results of tests carried out on two full-size portal frames are presented. These frames were of welded construction and had spans of 30 ft and column heights of 10 ft. The column bases were pin-ended in one case and fixed in the other. The frames, which were fabricated from 12WF36 shapes, were subjected to simultaneous application of vertical and horizontal loads.

The behavior of the component parts of the frames (beams, columns, welded connections) as indicated by various measuring techniques are compared with computed values based on simple plastic theory. Attention was given to the problem of plastic instability.

The lateral forces required to restrain the frames to their original plane were measured and analyzed. These forces are of significance in both elastic and plastic design of such structures.

Information with regard to the action of fixed base frames under very high horizontal loads is presented.

Introduction

1. Object and Scope of Investigation

The tests reported herein are the third and fourth frame tests to be carried out at Lehigh University as part of the broad investigation titled "Welded Continuous Frames and Their Components." The frames were simple rectangular portals, one with pinned column bases and the other with fixed column bases. Both were fabricated from a 12WF36 steel section with a beam span of 30 ft and column heights of 10 ft. The previous two frames tested in this program[1] were also rectangular portals with beam spans of 14 ft and had columns 7 ft high with pinned bases. The variable in the earlier frames was the size of section used; one was made from 8B13 shapes while the second was from 8WF40 shapes.

In contrast to the first and second test frames, which were subjected to vertical loads only, Test Frames 3 and 4 were subjected to a combination of horizontal and vertical loads.

In recent years an extensive study into the plastic behavior of steel structures has also been carried out at Cambridge University in England and tests of frames loaded under both vertical and horizontal loads have been reported.[2] The tests reported in these studies have been made on somewhat smaller frames fabricated from steel shapes rolled in England.

The main objective of the tests was to determine if the ultimate load-carrying capacity of such frames under combined loading could be predicted by simple plastic theory. In addition, valuable information regarding the lateral support required for such frames was ascertained as were the final modes of failure.

The frame with fixed column bases (Frame 4) demonstrated the large reserve strength such column fixity gives the frame to horizontal loads.

Description of Frames and Test Apparatus

2. Test Specimens

The test specimens used are detailed in Fig. 1. Both were single bay rectangular rigid frames with beam spans of 30 ft and column heights of 10 ft. The knees were of all-welded construction and were Type 8B described in Reference 3. Both frames were fabricated in the laboratory by welders and fitters whose regular jobs involve similar operations at the plant of a steel fabricator.

If these frames were assumed to be selected from an imaginary building with an assumed vertical working load of 60 psf and design wind load of 20 psf, the resulting total vertical load would be nine times the total horizontal load. Such reasoning as this leads to the loading ratio which was maintained constant throughout Test 3 and during the first phase of Test 4. Loads were applied at the third points of both the beam and windward column. (The windward column herein refers to the column to which the horizontal loads were applied.)

The two frames differed only in the condition at the column bases. Frame 3 was pin-ended; that is, both column bases were mounted on knife edges. During the test the distance between knife edges was kept constant by means of tie rods. To simulate a fixed-ended condition, the column bases of Frame 4 were welded directly to a stiff base beam. Since the base beam was not infinitely stiff the columns' bases were not completely fixed. This lack of complete fixity had no effect on the theoretical ultimate load of the frame, although the frame's behavior in the elastic range was affected.

Both frames were fabricated from 12WF36 "as-rolled" steel sections. The cross-sectional dimensions were acquired with the aid of a micrometer and the actual properties of the section differed considerably from those given in the AISC Steel Construction Manual.[4] A comparison of the actual and handbook properties is given in Table 1. Both the actual section modulus, S_x, and plastic modulus, Z_x* were approximately 5% lower than the handbook values due largely to the discrepancy in flange thickness.

The mechanical properties of the steel

C. G. Schilling, F. W. Schutz, Jr., and L. S. Beedle are associated with Fritz Engineering Laboratory, Department of Civil Engineering and Mechanics, Lehigh University, Bethlehem, Pa.

Presented at AWS 1954 Fall Meeting in Chicago, Ill., November 1-5.

This work has been carried out as part of an investigation sponsored jointly by the Welding Research Council of the Engineering Foundation and the Navy Department with funds furnished by the following: American Institute of Steel Construction, American Iron and Steel Institute, Office of Naval Research (Contract No. 39303), Bureau of Ships, and Bureau of Yards and Docks.

* Z_x (plastic modulus) for symmetrical sections is 2 times the first moment of one-half of the section about the neutral axis.

Table 1—Section Dimensions and Properties

	Weight per ft, lb.	Area, $in.^2$	Depth, in.	Flange: Width, in.	Flange: Thickness, in.	Web thickness, in.	I_x, $in.^4$	S_x, $in.^3$	Z_x, $in.^3$
Handbook[4]	36	10.59	12.24	6.565	0.540	0.305	280.8	45.9	51.4
Actual	34.8	10.21	12.17	6.59	0.510	0.307	266.2	43.7	49.1
Variation*	−3.3%	−3.6%	−0.6%	+0.4%	−5.6%	+0.7%	−5.2%	−4.8%	−4.5%

* % based on handbook value. Values in table computed for T4 assumed applicable to both T3 and T4.

Table 2—Physical Properties

X-section location	Coupon for frame no.	Yield stress level, σ_y (ksi)	Ultimate strength, ksi	Modulus of elasticity, E ($\times 10^3$ ksi)	Strain-hardening, ϵ_{st} (in./in.)
1	3	39.23	62.00	30.6	0.015
	4	39.08	62.23		0.017
	3	−38.06*		29.7	0.014
	4	−40.47			0.011
2	3	45.10	67.80	29.8	0.024
	4	44.66	66.56		0.018
	3	−45.15		29.7	0.014
	4	−47.20			0.013
3	3	39.70	62.20	29.8	0.018
	4	39.45	62.74		0.023
	3	−38.09		30.3	0.015
	4	−39.81			0.018
4	3	41.20	66.20	30.8	0.014
	4	38.66	62.85		0.019
	3	−38.49		30.9	0.013
	4	−38.35			0.009

Section properties used
σ_y = 39.2 ksi
M_y = 1713 k"
M_p = 1925 k"
E = 30.2 × 10^3 ksi
EI = 80.39 × 10^6 k-in^2

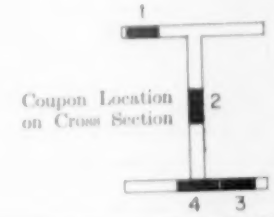

* −, indicates compression test.

used were determined by standard coupon tests (both tension and compression) conducted at a slow laboratory rate on coupons taken from four locations in the cross section. A set of coupons was taken from the beam section used in fabricating each frame. The steel was ordered to meet the requirements of ASTM Designation A7-50T.

The laboratory coupon tests are summarized in Table 2. In using these results to determine the yield moment (M_y = 1713 kip-in.) and the plastic moment (M_p = 1925 kip-in.) of the section the yield-stress level of those coupons (tension and compression) located in the flanges were averaged and used as the yield stress. This average yield-stress level was 39.2 ksi, which is lower than the upper yield strength of 42.53 ksi given in the mill report (Table 3). The latter value was determined from a coupon selected from the web and tested at the usual (faster) loading rate permitted by the acceptance specifications.

If the plastic moment were computed on the basis of a weighted yield stress (both flange and web coupons being used) its value becomes 1943 kip in. This weighted value being 0.9% larger than the plastic moment used in this report.

3. Lateral Support System

Past experience in testing of rigid frames into the plastic range had shown that adequate lateral support was essential if the theoretical ultimate load were to be attained. Therefore, the present test frames were provided with a lateral support system which might be equivalent to that used in actual building construction. In Test 3 this support was provided by 18 struts which held the frame in a plane about 10 ft from the wall of the laboratory building (see Fig. 2*a*). Four of these struts, which were located in elastic regions, carried very small forces in Frame 3 and, therefore, were not used in Test 4 which had a similar moment condition in the beam. The locations of lateral support struts are indicated by the small circles drawn on the flanges of the beam in Fig. 1.

In order to insure free vertical movement of the frame beam in its plane, the lateral support struts were fitted with flex bars at both ends. The lateral support at a typical beam section is shown in Fig. 3. Provisions were made to adjust the struts for large vertical deflections and the tests were planned so that no horizontal adjustment was necessary. Electrical strain gages were attached to one of the flex bars of each lateral support strut so that the force in the individual struts could be ascertained at any time.

The lateral support system can be seen in the photograph of the general test arrangement shown in Fig. 2*a*.

4. Loading System

In both frames the loads were applied by a self-contained system made up of the frame, a base beam and hydraulic jacks. Each jack was attached in series to an aluminum tube dynamometer for measuring the load applied. All loads were applied to the frame through horizontal pins located at the centroid

Table 3—Mill Report on 12WF36

Chemical composition, %		Mechanical properties	
C	= 0.18	Yield strength (upper yield)	= 42,530 psi
Mn	= 0.65	Ultimate strength	= 67,420 psi
P	= 0.014	Elongation in 8 in.	= 25.2%
S	= 0.038	Reduction in area	= 50.0%

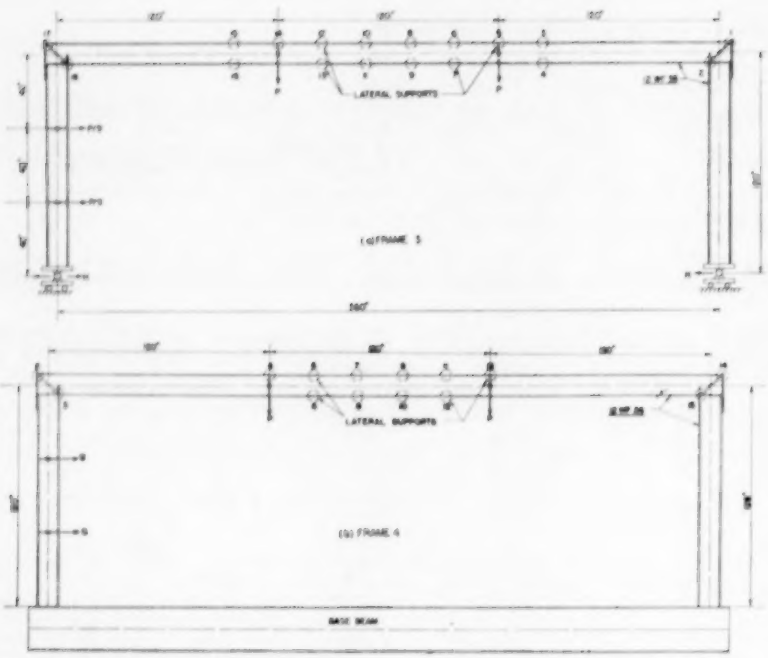

Fig. 1 Frame dimensions and details

of the beam and provided with transverse stiffener plates to help distribute the load to the section. The loading systems are shown in schematic form in Fig. 4.

In Frame 3 (see Fig. 4*a*) one jack was used for each of the two vertical loads, one for the horizontal loads, and one for the horizontal reaction at the column bases. This system of opposing horizontal jacks was used to adjust the longitudinal position of the frame so that the beam of the frame had no horizontal movement thereby simplifying the lateral support system. Each jack was connected directly to a hand-operated pump.

A slightly different loading system as shown schematically in Fig. 4*b* was used in Test 4. One jack was used for each load but the two vertical jacks were connected to a common pump. Similarly, the two horizontal jacks were connected to a second pump. This system expedited the test in the plastic range by automatically maintaining the loads applied by the two jacks approximately equal. The maximum difference in these loads was 2.1% which occurred after ultimate load in Phase II. Reactions for the horizontal jacks were transferred to the base beam at points under the column bases. Reactions for the vertical jacks were also taken by the base beam so that the loading system was completely self-contained within the rectangular ring formed by the frame and the base beam. The tops of the columns of Frame 4 were fixed in space by a horizontal support rod and the sidesway that occurred caused the base beam to move on rollers provided under it.

It should be pointed out that the loading systems used in these tests give the worst possible effect from the side loads since they require the beam to carry a maximum axial compression load. If, for instance, the horizontal load were applied in parts to both columns the beam would be subject to less axial compression load.

5. Determination of Experimental Moments

Both frames were statically indeterminate, Frame 3 to the first degree, and Frame 4 to the third degree. It was, therefore, necessary to measure redundants in order to determine the experimental moments throughout the frames.

In Frame 3 it was sufficient to measure the horizontal force which existed in the column base tie rods. This was accomplished by means of SR-4 electrical strain gages mounted on aluminum links in the tie rods.

Six pairs of SR-4 electrical strain gages were attached to webs of the columns of Frame 4 in order to measure unit rotation at three points in each column. From the unit rotations, the moments were computed since the gages were mounted in regions expected to remain elastic. In the latter part of the test, the columns yielded at two of these points (one in each column) so that the moment could no longer be ascertained with certainty at those points. The four pairs of gages remaining, however, were more than enough to determine the moments throughout the frame. During the early part of the test when all gages could be used, the moments at the tops and bottoms of both columns were determined by using various combinations of gages. The maximum variation in the moments

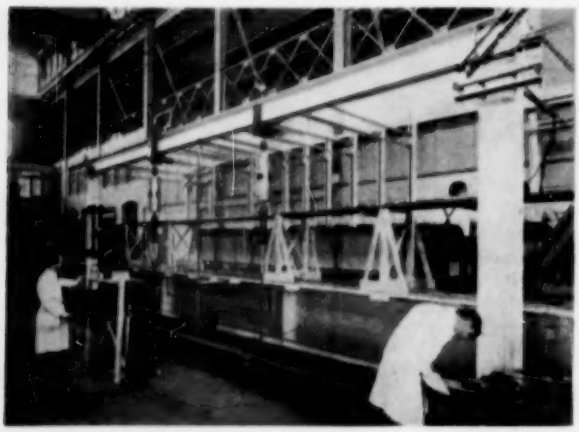

(a) Frame 3 before test

(b) Frame 4 after test

Fig. 2 General views of frames

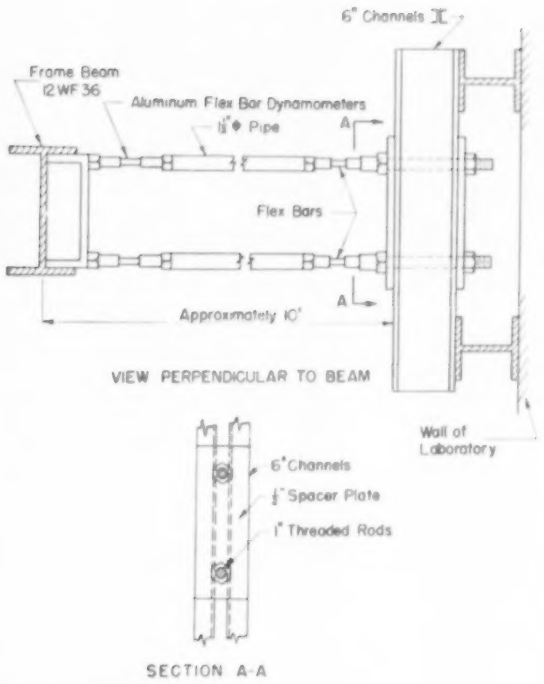

Fig. 3 Lateral support struts

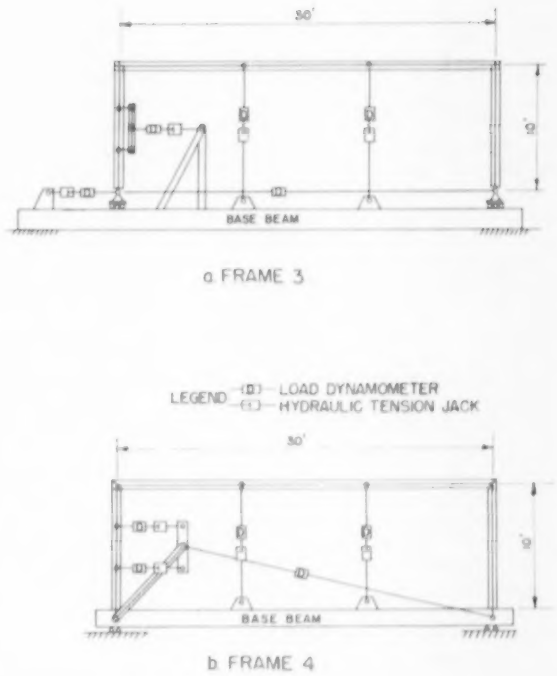

Fig. 4 Schematic of loading systems

thus obtained was about 10%. This method of determining moments is discussed at some length in Reference 1.

Once the redundants were determined the experimental moments throughout the frames were obtained by statics. These moments were corrected for frame distortions by using the measured frame deflections.

6. Rotation Measurement

Measurements to determine the rotation occurring along a unit length of beam and across the knees of the frames were made by use of the rotation indicators described in Reference 1. Such rotation indicators, four on Frame 3 and eleven on Frame 4, were located at points where plastic hinges formed. In order to get some indication of the extent of the plastic zone near the lee knee of Frame 4, a total of five indicators were located adjacent to the knee in the column and beam.

7. Deflection Measurement

Ordinary surveying instruments were used to determine the deflected shape of both frames to within $^1/_{50}$ of an inch. This precision was adequate in view of the fact that deflections in the order of 3 in. were experienced at ultimate load.

A transit (one for each column) was used to establish a fixed vertical plane from which the horizontal deflections of the column were measured. Similarly, an engineer's level was used to establish a fixed horizontal plane just above the frame from which the vertical deflections of the beam were measured. A single mechanical dial gage was used to measure the deflection at beam center as a check on the surveying instruments and for control during the test.

8. Buckling Instrumentation

Several types of instruments were used to detect lateral and local buckling. Mechanical dial gages were used to measure local movement of both the web and compression flange at critical locations. In Frame 3 further indication of local flange buckling was given by pairs of SR-4 electrical strain gages mounted on opposite sides of the compression flange at critical points.

An indication of lateral buckling was obtained by measuring the lateral twist, or rotation, of the beam. In Frame 3 this was accomplished by transverse level bars (described in Reference 1) mounted at three critical sections on the beam. This method was much more precise than necessary so a movable twist indicator was devised to measure the lateral twist at critical sections on the beam in Test 4.

9. Test Procedure

Both tests consisted of two parts: (1) check test of the frame in the elastic range and (2) main test carried out continuously through the elastic and plastic ranges to failure. The check tests were used to ascertain the behavior of both the testing apparatus and the frames.

Frame 3 was check-tested as a determinate structure by removing the tie rods connecting the column bases. In this condition the frame was loaded in three different ways: by vertical beam loads only, by horizontal column loads

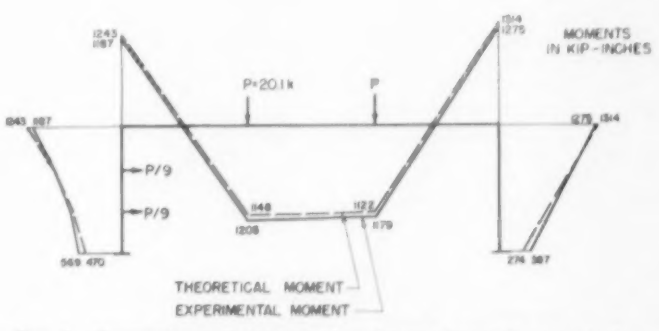

Fig. 5 Comparison of theoretical and experimental moments for Frame 4 in elastic state

only, and by tie rod forces on the column bases. The resulting deflections at the beam center and column bases were measured. The maximum deviation of these deflections from the theoretical values was 6.5% indicating that the testing apparatus and frame were functioning satisfactorily. Frame 3 was also check-tested as an indeterminate structure. The force in the tie rods was measured and found to agree within 2% with the theoretical value.

For Frame 4 such an elaborate check test was not possible since the specimen could not be reduced to a determinate structure. The beam center deflection, however, was measured and found to agree within 7% of the theoretical value when the load was 12 kips in the vertical jacks. A further indication of the action of the frame is given by a comparison of the actual and theoretical moment diagrams in the elastic range shown in Fig. 5. Except at the column bases, these moments differed by approximately 5%.

The main tests were carried out continuously until the lateral plastic buckling near the lee knee became excessively large causing rapid reductions in load-carrying capacity. The time required for the continuous tests was about 60 hr.

During the early stages of the tests, readings were taken on all measuring devices at frequent load intervals. No data were taken at a given load increment until the beam center deflection had stabilized; that is, with the loads on the frame held constant the increase in deflection with time became negligible.

As the applied loads approached the theoretical plastic ultimate load the time required for the deflection to stabilize increased rapidly. To reduce this stabilizing time a "deformation-increment" criterion was adopted for the later part of the tests. Under this criterion a predetermined deformation increment was applied by means of the jacks. This deformation was then held constant while the loads decreased with time. Eventually, these loads remained practically constant and a set of data was taken.

For Frame 3 the horizontal loads were $^1/_9$ of the vertical loads throughout the test. Test 4, however, consisted of two distinct phases. In the first phase, the frame was loaded with vertical and horizontal loads in a nine-to-one proportion until 97% of the theoretical plastic ultimate load for this load condition was reached. In the second phase, the vertical loads were held constant at a value slightly less than the theoretical ultimate load and the horizontal loads were increased from zero to their ultimate value. Actually near the end of the test it was found impossible to keep the vertical loads constant without greatly increasing the vertical beam deflections. At this stage the vertical loads were allowed to decrease slightly.

In effect, Test 4 was two tests—one in which the vertical loads had a dominant effect, the other in which the horizontal loads were more significant. The first case, wherein the vertical loads were maintained at values 9 times the horizontal load, is referred to as Test 4-Phase I or Test 4(I); in that part of the test in which the vertical load was held constant as the horizontal load was increased is referred to as Test 4-Phase II or Test 4(II).

Theoretical Analysis

10. Theoretical Loads and Moments

The results of the theoretical analysis of the frames are summarized in Figs. 6 and 7. In the elastic range the structures were analyzed by ordinary elastic methods for indeterminate structures. Since the base beam in Frame 4 was not infinitely rigid, its actual rigidity was taken into account in the elastic analysis. The structure was analyzed as a closed ring composed of the frame itself and the base beam. It must be emphasized, however, that this base beam flexibility had no effect on the theoretical ultimate load found by simple plastic analysis so long as the base beam remained elastic. Methods of simple plastic analysis by which the ultimate loads of frames such as these may be predicted have been described.[5–7]

Table 4 gives the applied loads at the theoretical first yield (P_y and Q_y) and at the theoretical ultimate load condition (P_p and Q_p). They are based on the actual physical properties of the section, M_y = 1713 kip-in. and M_p = 1925 kip-in. A study of this table reveals that the theoretical ultimate strength given by plastic analysis is 1.26 times as great as the conventionally accepted maximum strength (load at first yield) for Frame 3 and 1.22 times as great for Frame 4(I). Another point of interest is the capacity of Frame 4

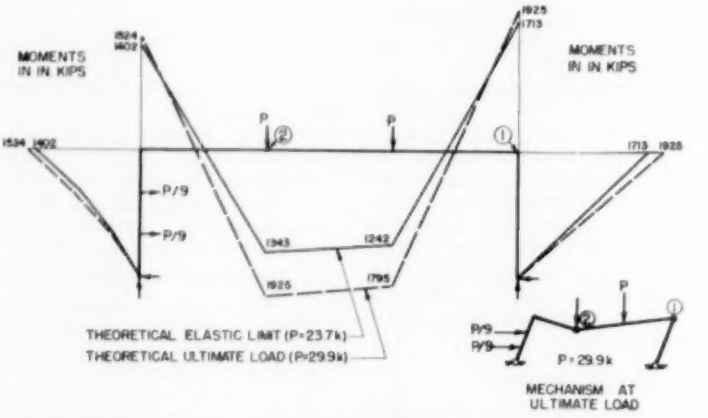

Fig. 6 Theoretical moment diagrams for Frame 3

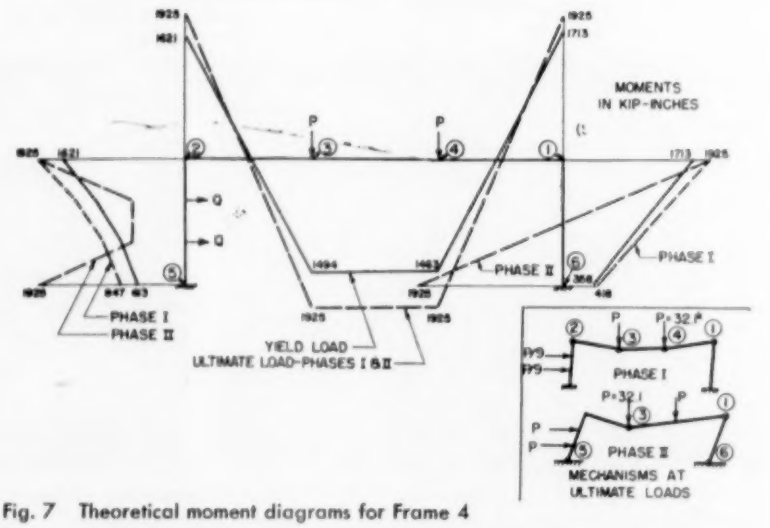

Fig. 7 Theoretical moment diagrams for Frame 4

Table 4—Critical Loads from Theoretical Analysis

Load	Frame 3, kips	Frame 4—Phase I, kips	Frame 4—Phase II, kips
P (yield)*	23.7	26.2	18.7
Q (yield)*	2.63	2.91	18.7
P (ultimate)	29.9	32.1	32.1
Q (ultimate)	3.32	3.57	32.1

* Load at which bending stresses alone are equal to yield stress of material (39.2 ksi). If axial stress were added loads P_y and Q_y would be lower.

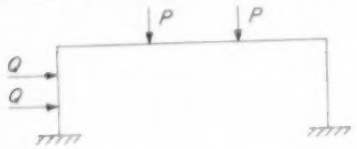

to withstand very high horizontal loads. In Phase II of the test the horizontal ultimate loads are as large as the vertical ultimate loads. The plastic analysis ultimate load for the condition of equal horizontal and vertical load (Frame 4(II)) is 1.72 times as great as for the first yield ultimate concept. It should be pointed out that the first yield loads listed in Table 4 are based on stresses caused by bending moments alone. If axial forces were also considered (as they generally are in elastic analysis) the first yield loads would be somewhat lower.

The ultimate loads were obtained by using simple plastic theory. The sequence of the formation of plastic hinges is given by the circled numbers in Figs. 6 and 7. The first four hinges shown for Frame 4 in Fig. 7 were required in order that the theoretical ultimate load in Phase I could be reached. Hinges 1 and 3 remained hinges in Phase II. In addition to these hinges, two others (5 and 6) were necessary in order that an ultimate load could be reached in Phase II. In Phase II, hinges 2 and 4 behaved elastically because the moment at these hinges produced by the horizontal loads was opposite to the plastic moments produced by the vertical loads in Phase I.

The base beam used in Test 4 was not infinitely stiff, and therefore the true values of E and I were used in the theoretical computations whose results are summarized above. It is of interest to note that while this lack of complete fixity at the base of the columns in Frame 4 does affect the moment distribution in the frame in Phase I it does not affect the total load-carrying capacity of the frame. The ultimate load (P = 32.1 kips) moment diagram shown in Fig. 7 (and repeated in Fig. 8) for Frame 4(I) takes into account the base beam flexibility. If the base beam were infinitely stiff or rigid the theoretical ultimate load (P = 32.1 kips) moment diagram would be altered. A comparison of the two conditions is given in Fig. 8.

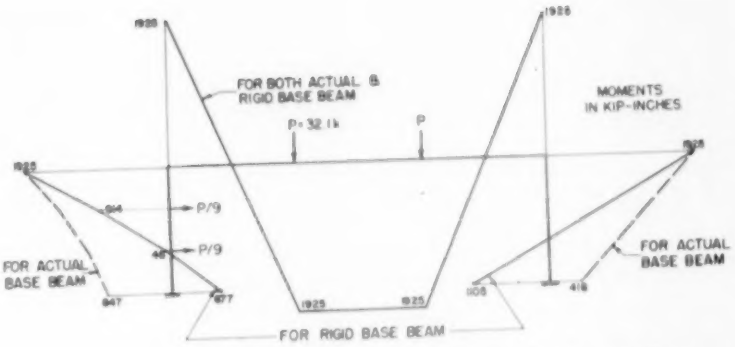

Fig. 8 Base beam rigidity effect on ultimate load moments—Frame 4(I)

II. Theoretical Deformations

In order to check the actual behavior of the frames against the theoretical behavior, some measureable quantity other than applied forces should be predicted by theoretical means. One such quantity chosen for the present tests is the deflection of the center of the beam.

While the frame is in the elastic range the beam centerline deflection may be determined by ordinary elastic analysis. However, such analysis assumes the frame to be formed from members having lengths given by the centerline dimensions of the frame. This assumption leads to an answer which is approximately correct but it can be improved upon by taking into account the fact that the particular knees of the frame rotate more than the equivalent length of plain beam. A rational method of predicting such difference in rotation is given in Reference 3. In the case of Frame 3, this procedure led to a beam center deflection of 1.79 in. at yield load instead of 1.74 in. This increase is so small that the effect was ignored in the computations for Frame 4.

Approximate values for deflections of the frames may be determined just as the ultimate load is reached by a very simple method described by Symonds and Neal[8] and Yang, *et al.*[9] This method assumes that yielding is concentrated at the plastic hinges and that these hinges are free to rotate under the constant moment, M_p, other parts of the frame remaining elastic. Just as the last plastic hinge is formed, the slope at either side of the hinge must be equal. Using these assumptions and the slope-deflection equations, one may find the deflected shape of the structure. For Frame 3 this gives an estimated beam

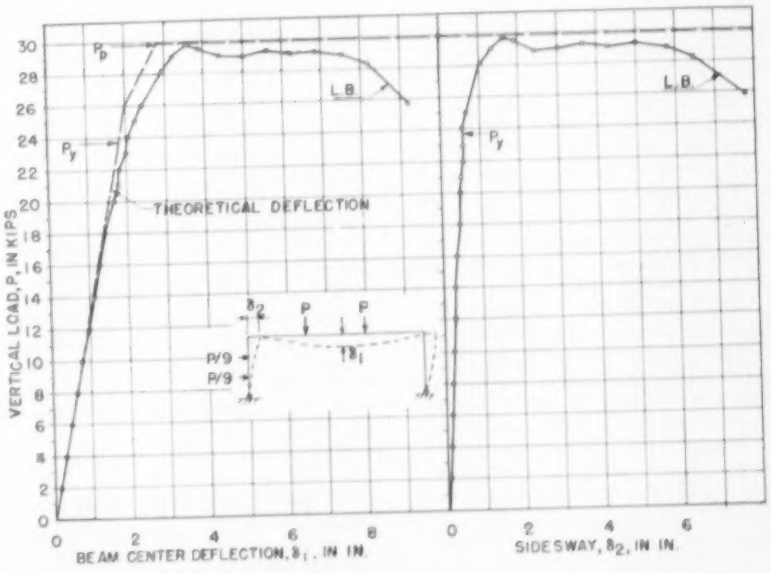

Fig. 9 Load-deflection curves—Frame 3

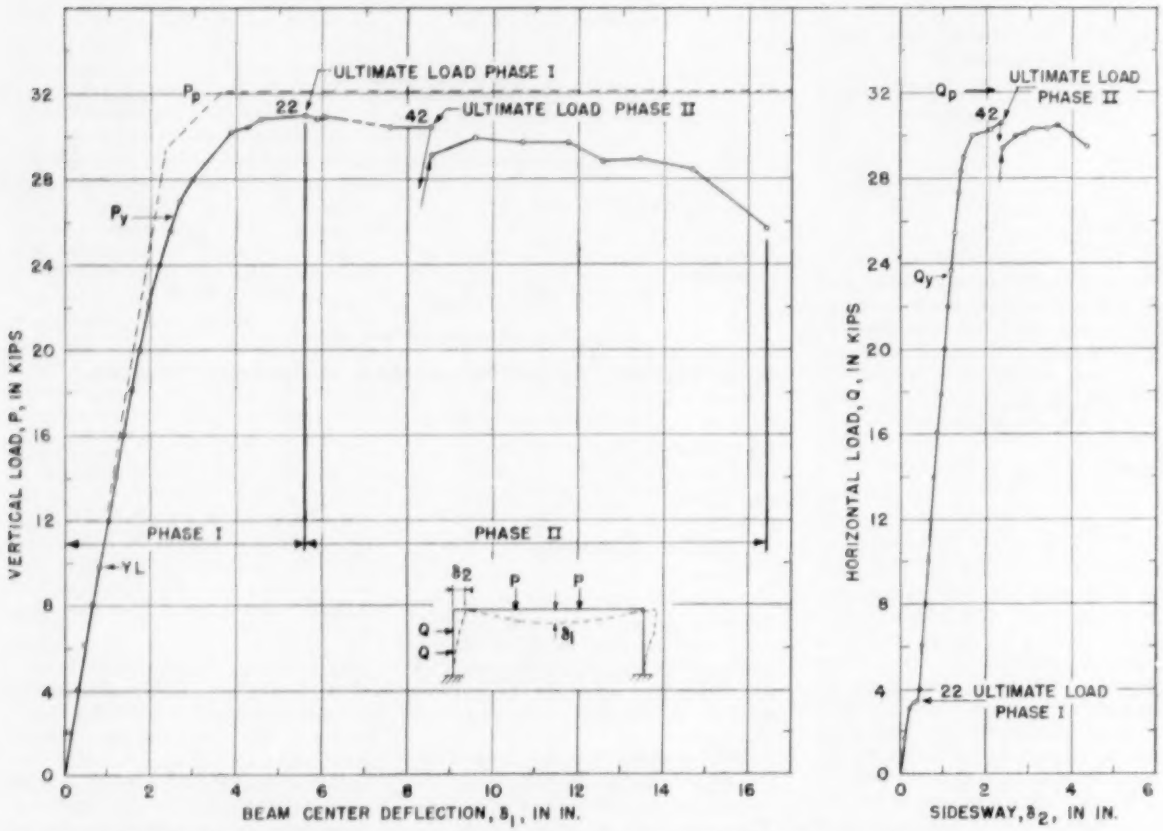

Fig. 10 Load-deflection curves—Frame 4; (numbers on test curves designate loading numbers)

center deflection of 2.82 in. at ultimate load. It seems reasonable that the actual deflection should be larger than 2.82 in. since yielding is spread out over lengths of the beam and not concentrated at the hinges as assumed in the analysis. This would be particularly true in the present case since the entire center third of the beam is withstanding a moment greater than M_y when the ultimate load is reached.

The deflection computations discussed above for Frame 3 allow one to draw the theoretical load-deflection curve shown on Fig. 9. Similar computations result in the theoretical load deflection curve shown in Fig. 10 for Frame 4 where the beam center deflection at ultimate load was computed to be 3.64 in. Again it should be pointed out that for Frame 4 as well as for Frame 3 the actual moment diagram violates the assumption, "plastic hinges are concentrated at points" made in the deflection computation. Figure 7 shows that the entire middle third of the beam in Frame 4 is under the theoretical plastic hinge moment at the ultimate load condition. This condition assures one that the actual deflection will be considerably larger than the computed value. In the case of structures having moments that continuously vary, there should be much closer agreement between theoretical and experimental deflection values.

In any case, the fact that the actual deflections at maximum load are somewhat larger than the theoretical values is not critical since at plastic design working loads the agreement between theory and experiment is excellent.

Results of Tests

12. *General Behavior*

The present test frames and test apparatus behaved as well as was expected in all respects. It is believed that the results indicate the performance that might be expected from an actual building frame where the proper consideration is given the lateral support system. At the same time, a lateral support system capable of providing the support given the test frames might not be impractical; in fact, even better support (such as floor slabs, etc.) is often given the frames of elastically-designed structures.

The frames carried the predicted yield loads and approached the theoretical ultimate load very closely. In addition, both frames showed an ability to carry loads very near the predicted ultimate load even when the deflections were *double* those at the time the ultimate load was first reached. This characteristic, which is clearly seen in Figs. 9 and 10, demonstrates the large energy absorbing capacity of structural steel rigid frames when loaded into the plastic state.

Final failure for Frame 3 was eventually brought about when the lee column buckled laterally just below the beam-column connection after the frame had been deflected twice as much as at ultimate load. This buckling occurred in a region that was fully plastic and was a clear case of plastic instability. Other cases of plastic local crippling and lateral deformation occurred but did not progress to such an extent as to be the cause of the frame failure. The ability of the frame to survive these earlier cases of plastic instability was undoubtedly due to the effective lateral support system.

Plastic instability also brought about the final failure of Frame 4, but not until the frame had been deformed considerably from its shape at ultimate load. For this frame the lateral buckle occurred in the beam in a region immediately adjacent to the connection of the lee column.

13. *Experimental Loads and Moments*

(a) *Test Frame 3.* The results of

Test 3 with regards to load-carrying capacity are shown in one form in Fig. 9 where the beam center deflection and the sidesway are plotted against the vertical load. The experimental load for this frame was 29.7 kips which is 99.3% of the theoretically computed load of 29.9 kips. Table 5 shows the ratios of certain test loads to the theoretically computed equivalents for Frame 3 and for the other portal frames tested in the program. For Frame 3 the first observed yield (aside from very minute local yield) was observed at 15.9 kips of vertical load as compared to computed yield load of 23.7 kips. (This computation for yield load neglected the effect of axial load.) The tendency of a real frame to yield at low loads is discernible in Fig. 9, in which inelastic action commenced at a vertical load of about 10 kips.

It is of interest to note what the allowable load for Frame 3 would be under present AISC specifications[4] when Section 12 (Combined Stresses) is applied. If only the vertical loads were placed on the frame, the AISC allowable load would be 12.2 kips. The case of vertical and horizontal (wind) loads would not control since, when this case is considered, the allowable stress is increased 33% and the allowable load becomes 14.8 kips for Frame 3. Thus the real elastic design safety factor against the actual ultimate load was 2.44 for Frame 3 (29.7 ÷ 12.2). This value compares with a value of 1.96 which would be obtained by dividing the actual yield stress by the allowable stress (39.2 ÷ 20).

During the loading sequence of Frame 3 a complete set of data was taken when the vertical loads reached 12.0 kips each. The resulting moment diagram for this load condition is shown in Fig. 11. The maximum stress due to bending at this load was 19.44 ksi at the lee knee of the frame. The moments shown in this diagram (the solid line in Fig. 11) are close to those which would occur in this frame if it were designed elastically by AISC specifications.[4]

When the elastic design moment diagram discussed above is compared with the two ultimate load moment diagrams in Figure 11, the reserve strength of the frame is further illustrated. The ultimate load moment diagram (Fig. 11) computed by use of simple plastic theory shows extremely close agreement with the one derived from measured reactions and statics in the actual frame.

(b) *Test Frame 4-Phase I.* As has been described before (Articles 9 and 10), Frame 4 was subjected to two separate loading conditions. Under each condition the frame was loaded to its ultimate capacity. During Phase I of Test 4 the loading condition was identical with Frame 3 (the vertical loads being 9 times larger than the horizontal loads). The plastic mechanism which formed, however, was confined to the beam, and sidesway was held to a minimum as can be seen from Fig. 10. The sidesway at the ultimate load (Load 22) was only about 0.4 in. compared to a value of 1.6 in. for Frame 3 at its ultimate load.

Table 5 and Fig. 10 give comparisons of the experimental and theoretical behavior of Frame 4(I). The ultimate load reached in the test was 31.0 kips which is 97% of the ultimate load of 32.1 kips computed by plastic theory. It should be pointed out, however, that this phase of the test was discontinued arbitrarily at this point in order that

Table 5—Strength Comparison

Frame no.		Yield strength: First yield line, kips	Yield strength: General yield, kips	Maximum strength: Elastic analysis comparison, kips	Maximum strength: Plastic analysis comparison, kips
1	Observed	22.0	40.4	52.4	52.4
	Computed	39.4	39.4	39.4	47.7
(8WF40)	Ratio	0.56	1.05	1.33	1.10
2	Observed	5.5		18.0	18.0
	Computed	13.1		13.1	18.1
(8B13)	Ratio	0.42		1.37	0.99
3	Observed	15.9	25.3	29.7	29.7
	Computed	23.7	23.7	23.7	29.9
(12WF36)	Ratio	0.68	0.68	1.26	0.99
4	Observed	19.0	26.0	31.0	31.0
Phase I	Computed	26.2	26.2	26.2	32.1
(12WF36)	Ratio	0.34	0.99	1.18	0.97
4	Observed		26.7	30.5	30.5
Phase II	Computed	18.7	18.7	18.7	32.1
(12WF36)	Ratio		1.43	1.63	0.95

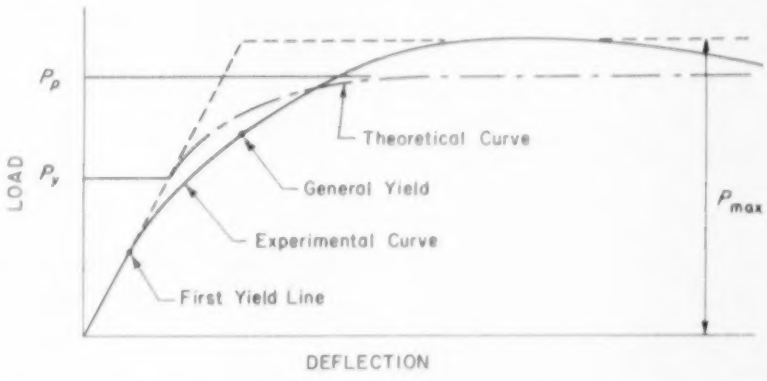

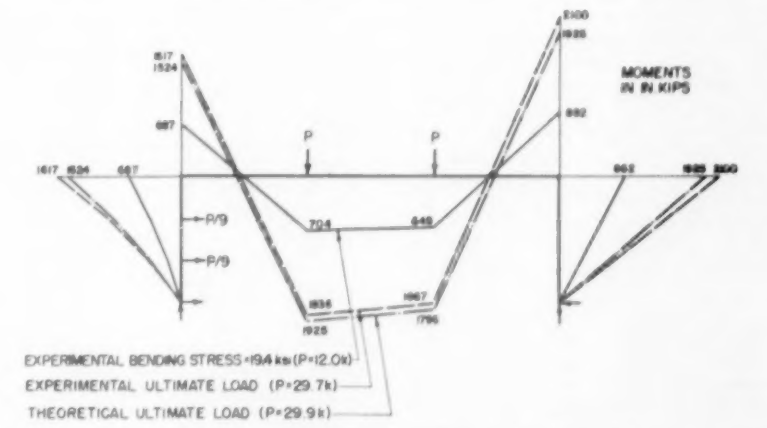

Fig. 11 Theoretical and experimental moment diagrams for Frame 3

Phase II could be undertaken before the frame became too seriously deformed. The subsequent behavior of certain critical parts of the frame in Phase II indicates that the ultimate load had not been reached at Load 22 (vertical load = 31.0 kips) and had the test been continued under the Phase I loading ratio, it would have carried vertical loads as high as about 33.4 kips which would have been 104% of the theoretical ultimate load.

The first significant yielding occurred in Frame 4 during Phase I at a load of 9.0 kips or at only 34% of the computed yield load (yield load being computed neglecting the effect of axial loads). The elastic design load for Frame 4(I) when the AISC interaction formula is used would be 12.6 kips for vertical loads only and 16.3 kips for vertical loads and horizontal wind loads. Thus the vertical loads would control an elastic design. Therefore, the demonstrated safety factor for the frame was 2.46 during the first phase (31.0 ÷ 12.6) and might have been higher if the test had been continued. The difference between the safety factors of 2.46 and 1.96 (yield stress, 39.2, divided by allowable stress, 20.0) is due to the equalization of the moment diagram as plastic hinges are formed and to the shape factor (full plastic moment divided by yield moment). For the particular WF section (12WF36) used in these tests the shape factor is 1.12 (1925 ÷ 1713).

Figure 12 shows moment diagrams for Frame 4(I). The experimental moments observed at a load (P = 12.0 kips) near the elastic design load is shown. The other two diagrams give a comparison of the experimental and computed moments at the ultimate load condition. There appears to be a large discrepancy between these two diagrams. (In spite of this, the experimental and theoretical ultimate loads are in close agreement.) The explanation for the discrepancy in moment diagrams is that in attaching the frame column bases to the base beam, the column bases were forced apart in order to meet the required dimensions, thereby introducing a state of "locked-up" moments approximately equal to those shown in Fig. 13*a*. The exact horizontal force exerted at the bases of the columns when the frame was attached is not known, but by taking the average of the errors in experimental moments at the knees at ultimate load in Fig. 12 the force of 1.72 kips shown in Fig 13*a* was obtained. Such a value is well within reason.

The electrical strain gages used for moment determination in Frame 4 were mounted after these "locked-up" moments had been induced. Therefore the moments indicated by these gages were always in error by an amount equal to the "locked-up" moments. When the "locked-up" moments shown in Fig. 13*a* are added to the experimental ultimate load moments shown in Fig. 12 the more nearly correct experimental moment diagram shown in Fig. 13*b* is obtained.

It should be emphasized that the "locked-up" moments discussed above have no effect on the ultimate load carrying capacity when plastic action is relied on. In a like manner the true ultimate load carrying capacities of rigid steel frames are not affected by such things as foundation settlement and rotation, small fabrication errors in dimensions of parts, or temperature changes. According to conventional (elastic) concepts, such factors are of significant influence. However, more often than coping with them, they are ignored in present design procedures; knowingly or not, plastic action is depended upon to assure the successful operation of the structure.

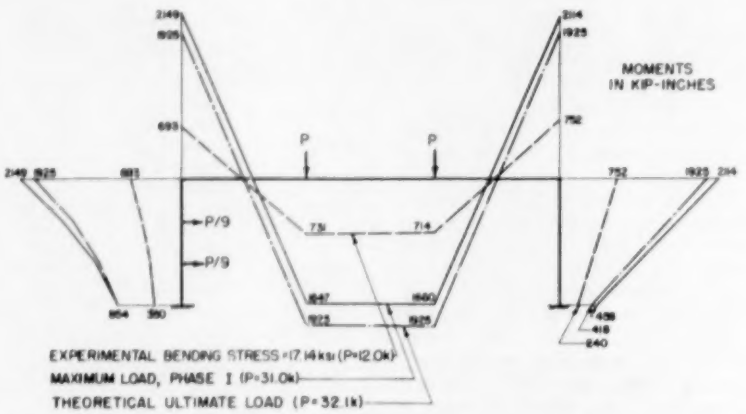

Fig. 12 Theoretical and experimental moment diagrams for Frame 4. Phase I

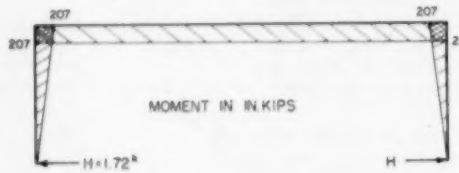

(a) "LOCKED-UP" MOMENTS CAUSED BY SPREADING OF COLUMN BASES PRIOR TO WELDING

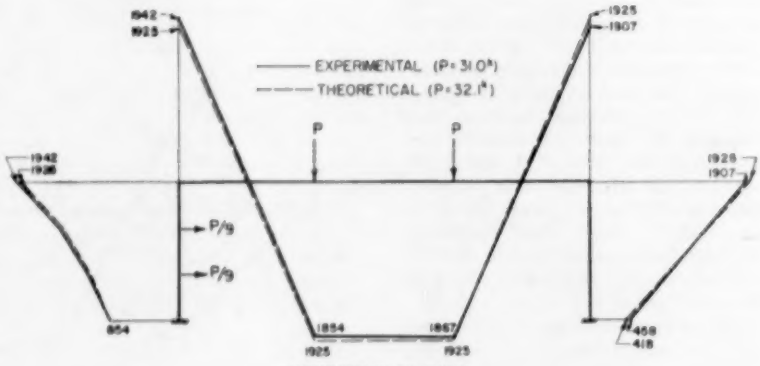

(b) CORRECTED EXPERIMENTAL MOMENT DIAGRAM AT ULTIMATE LOAD

Fig. 13 Effect of "locked-up" moments in Frame 4. Phase I

(c) *Test Frame 4-Phase II.* During Phase II of Test 4 the vertical loads were held as nearly constant at 31.0 kips as possible while the horizontal loads were increased. This increase in horizontal load was possible since the plastic mechanism developed in Phase I was local—that is, confined to the beam. The columns were still stable structural elements since no plastic hinges had formed at their bases. In reviewing the behavior of the frame during Phase II, it should be remembered that the beam had already become a mechanism at the end of Phase I with a deflection at the center of the beam of 5.8 in. The frame undoubtedly would have withstood a larger ultimate load had the vertical and horizontal loads been equal from the outset in the test of an undeformed frame.

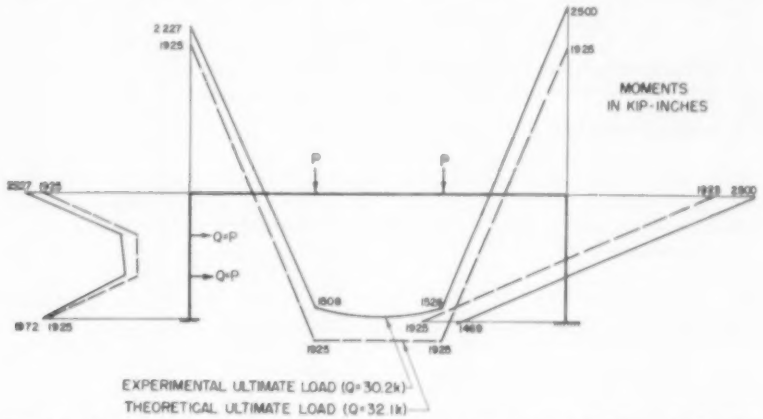

Fig. 14 Theoretical and experimental moments at ultimate load—Frame 4, Phase II

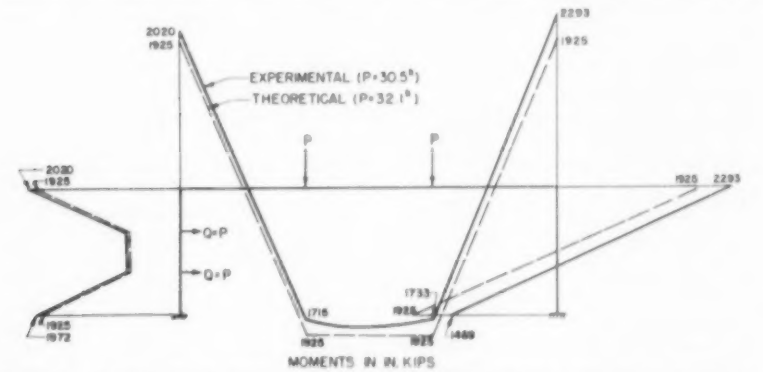

Fig. 15 Experimental moments corrected for "locked-up" moments—Frame 4, Phase II

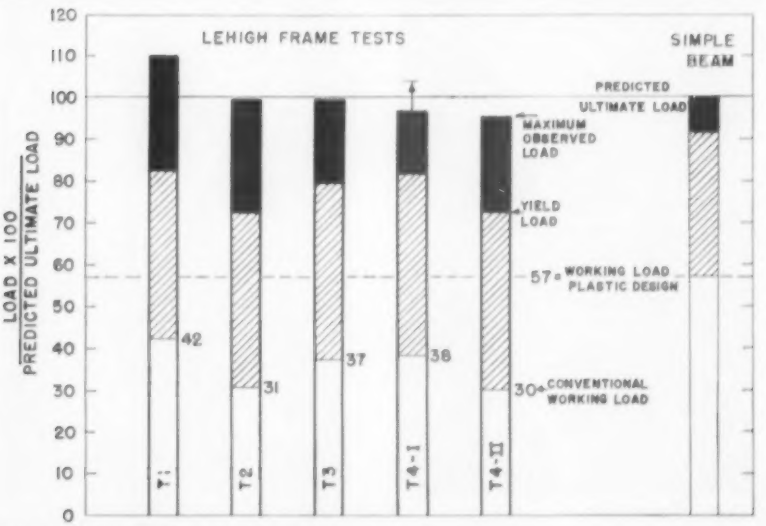

Fig. 16 Bar chart of frame strengths

Despite the severe deformation of the frame at the start of Phase II, Frame 4 was able to withstand horizontal loads of 30.5 kips which is 95% of the theoretical plastic analysis load of 32.1 kips (see Table 5 and Fig. 10). This load was reached at about the same time the available stroke on the tension loading jacks was used up. As is indicated on Fig. 10, the frame had to be unloaded at this point (Load 42) in order to shorten the loading rods. Once this was done the frame was never able to carry again its previous high load.

The advantage of fixed-based columns for certain loading conditions is clearly illustrated by the fact that Frame 4 in Phase II withstood horizontal loads 9.24 times as great as that supported by Frame 3 with a resulting sidesway of 2.4 in. compared to a value of 1.6 in. in Frame 3.

If one were to assume the horizontal loads applied to Frame 4 in Phase II were not wind loads (such a high ratio of wind load to vertical load is unlikely) the elastic design load would be 9.65 kips. Thus the present frame despite its adverse strain history was able to demonstrate a safety factor of 3.16. The factor would have been somewhat higher, perhaps as much as 3.4, if the frame had been loaded in its virgin condition with equal vertical and horizontal loads.

A comparison is made in Fig. 14 between the experimentally and theoretically determined moments at ultimate load in Frame 4(II). The experimental moments here plotted are subject to the same errors brought on by the "locked-up" moments described for Phase I. The experimental moments at ultimate, Phase II, corrected for the "locked-up" moments given in Fig. 13*a* are shown in Fig. 15. Discrepancies between the experimental moments and the theoretical values in Fig. 15 are partly due to the adverse strain history of the frame in Phase II and the fact that both corner connections are capable of carrying moments higher than the plastic hinge moment of a plain beam section. Another factor to be discussed later was the fact that part of the middle third of the beam had buckled laterally during Phase II, thereby reducing the moment-carrying capacity of that beam section and forcing the corner connections to carrying increased moments.

(d) *Plastic Design Working Loads.* The preceding sections discussing the load-carrying capacities of Frames 3 and 4 have pointed out the large reserve in strength these frames have demon-

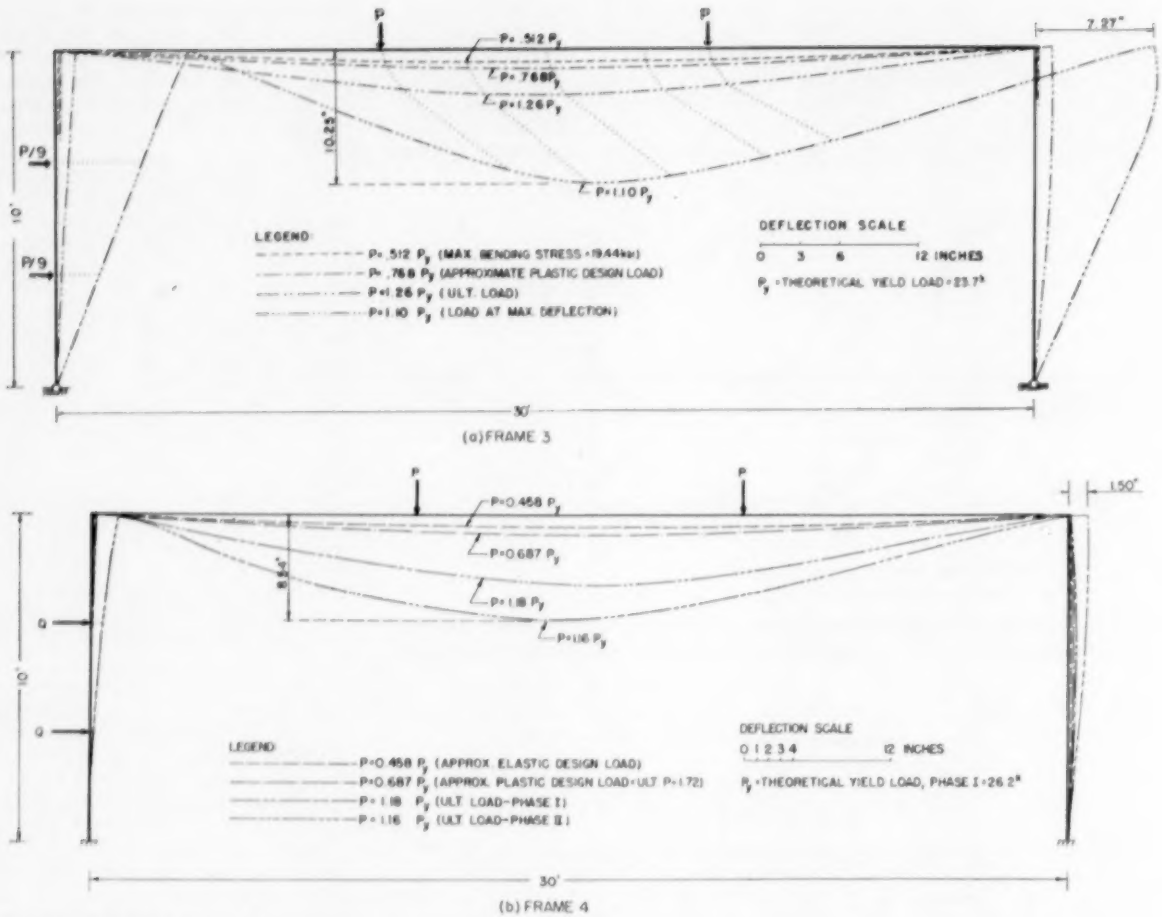

Fig. 17 Deflected frame shapes

strated over and above the commonly accepted elastic design loads. This characteristic is due to the continuity existing in the frame brought about by welding such that the full plastic strength was developed. A new concept of design in structural steel, called "plastic design," makes use of this reserve strength which has herein been demonstrated. Much progress has been made in Great Britain in this area where actual structures have been built which were designed by use of plastic analysis.[9] One advantage of plastic design is the fact that all structures so designed will have a uniform and rational factor of safety regardless of the degree to which the structure is indeterminate in the elastic state.

Figure 16 illustrates how the five tests carried out at Lehigh University under the present program would have a uniform factor of safety under the plastic design concept. For purposes of discussion a load factor of safety of 1.75 against the theoretical ultimate load has been chosen. Thus the plastic design working load would be 57% of the theoretical ultimate load for all frames and for the typical simple beam as well. The bar chart (Fig. 16) shows that the conventional elastic design procedures would use varying amounts of the ultimate load capacities (from 30 to 57%). It will be noted that elastic design and plastic design would permit the same

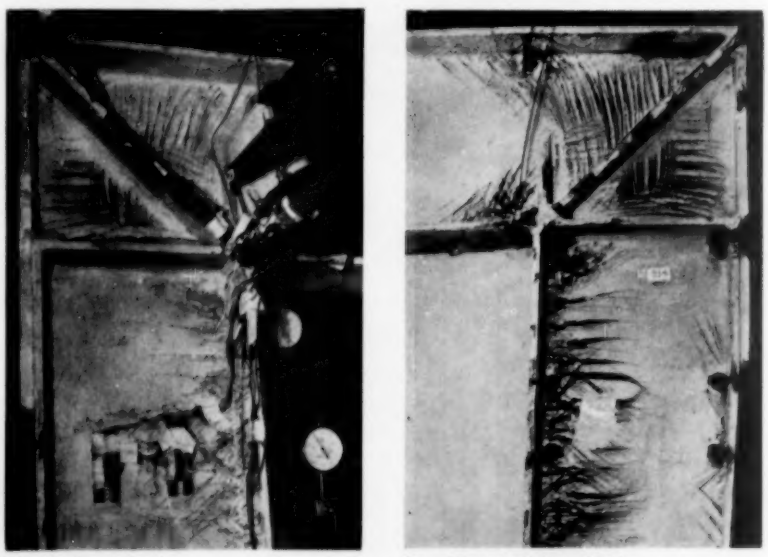

(a) At ultimate load (b) After completion of test

Fig. 18 Lee knee—Frame 3

working load for the case of a simple beam. Therefore, the rigid frame proportioned by plastic design would enjoy the same real safety factor as do present elastically designed simple beams.

Further, Fig. 16 shows that no part of the frames tested would have reached a condition of general yielding at the plastic design working load. Indeed, only the most unusual frame would be called upon to withstand general yielding at working loads as determined by plastic design using a reasonable load factor of safety.

The bar indicating the behavior of Frame 4(I) in Fig. 16 is topped by an arrow showing the ratio of test load to theoretical that would be expected had the loading Phase I been continued. This expected load was based on subsequent behavior of parts of the frame in Phase II. It should also be remembered that Phase II of Test 4 was started after the frame had undergone large deformations which undoubtedly adversely affected its ultimate load-carrying capacity.

14. Experimental Deflections

The deflection characteristics of Frames 3 and 4 are shown in Figs. 9 and 10, where the deflections at the center of the beam span and the sidesway of the tops of the columns are plotted versus the loads applied. In general, the deflections measured were as predicted by theory. Both frames showed beam deflections which deviated from the theoretical curves well before the theoretical yield load was reached. However, this deviation did not start to increase at a large rate until after the theoretical yield load, P_y, had been exceeded. Thereafter, it was "controlled" until the observed maximum load was reached.

Another presentation of the manner in which the structures deformed is given in Fig 17, where the deflected shapes of the frames at several load conditions are shown. The first deflection curve drawn in Fig. 17*a* shows the shape of Frame 3 when the vertical load in each jack was 12 kips. This load produced a moment of 852 in-kips at the lee knee and a unit stress of 19,440 psi due to bending stress. It is approximately equal, then, to a normal design load by conventional elastic methods if direct stress is neglected.

The second deflected shape of Fig. 17*a* is drawn for a vertical load of 18 kips. This load is near the allowable load that might be used in a plastic design using a load factor of safety of 1.75. At this load the frame is still well within the elastic limit. The maximum deflection at this load was 1.47 times the maximum deflection at the conventional elastic design load.

The shape of the frame at ultimate load, 29.7 kips, is given by the third curve on Fig. 17*a*. The curve showing the largest deflection is for the last load put on the structure and is therefore the greatest deformation that occurred. The load at this time was 26.5 kips. The lee column had already buckled laterally at this stage of the test. Despite the column failure and the large distortions, the frame was still carrying 89% of the ultimate, 221% of the normal elastic design load, and 151% of a "possible" plastic design load which uses a safety factor of 1.75 against the ultimate load.

The two curves showing the smaller deflections in Fig. 17*b* were drawn for vertical loads of 12 and 18 kips on Frame 4(I). These loads correspond roughly to working loads that would be allowed on the frame by elastic design and plastic design, respectively.

The third deflected shape shows the condition of Frame 4 at its ultimate load (P = 31.0 kips) at the end of Phase I. The fourth, and last, curve is drawn for the ultimate load (Q = 30.5 kips) condition in Phase II.

The deflections shown in both parts of Fig. 17 are exaggerated for clarity. The scale for plotting deflections is 4.8 times larger than the scale to which the frame center line is drawn.

15. Moment-Rotation Relationships

(a) *Beam to Column Connections.*

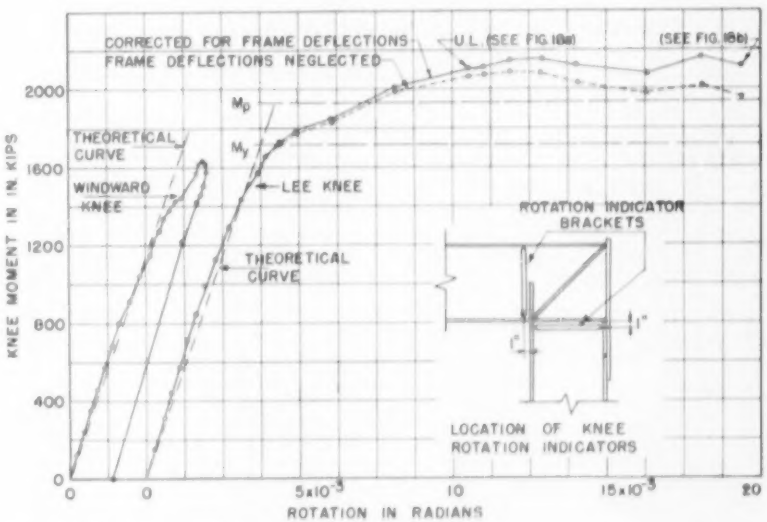

Fig. 19 Moment-rotation curves for knees—Frame 3

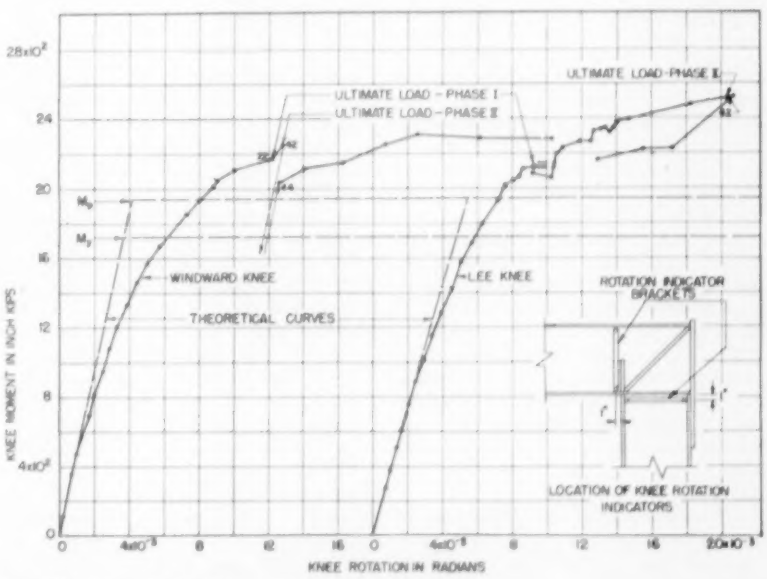

Fig. 20 Moment-rotation curves for Frame 4 knees

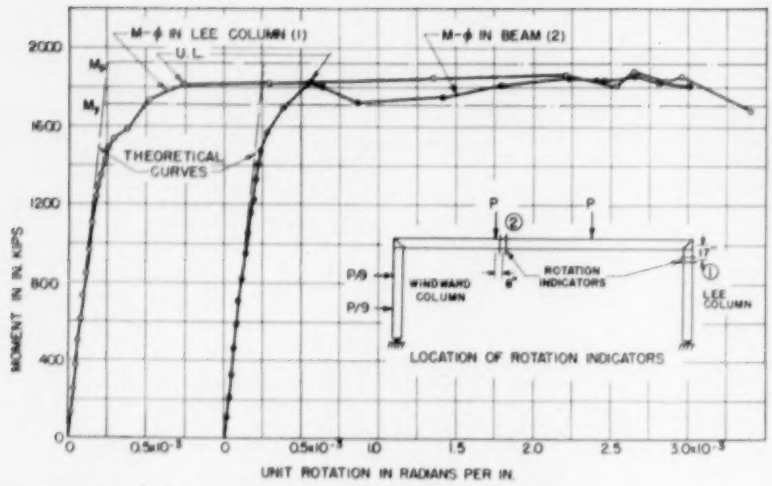

Fig. 21 Moment-unit rotation curves for sections in Frame 3

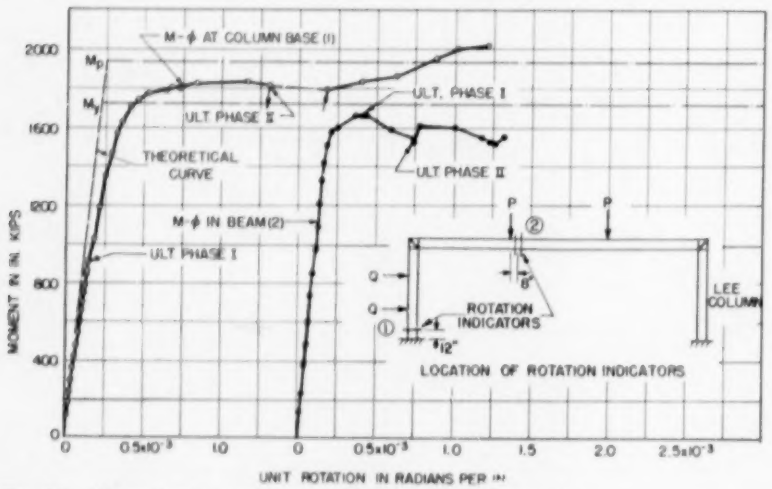

Fig. 22 Moment-unit rotation curves for sections in Frame 4

Since one of the basic requirements of a material and a section to be used in a structure designed by plastic analysis is the ability to form plastic hinges, it is of interest to study moment-rotation relationships of certain critical parts of the present frames.

One such critical part is the beam to column connection or the knee of the portal frame. The knee should be able to withstand the full plastic moment of the beam section through large rotations. The connections used were chosen for the present frames because previous tests[3] at Lehigh University assured their good performance. The connections used in the present frames were designated as Type "8B" in Reference 3.

At no time during the tests did any knee show signs that it had a smaller moment capacity than the beam section. There was no local crippling of any parts even though yielding of the material was widespread in some of the knees.

The photographs in Fig. 18 are close-up views of the lee knee of Frame 3. This knee was subject to large rotations and high moments. The photograph in Fig. 18*a* was taken just after the frame had reached its ultimate load. It will be noted that at this load yielding (indicated by the dark bands in the white wash coating) had extended beyond the connection proper into both the beam and column. The condition of the same connection at the end of the test is shown in Fig. 18*b*. In this photograph the shift of the neutral axis in the column due to the axial load is clearly illustrated by the yield bands. On the other hand, the yielded zones in the beam just outside the connection are nearly symmetrical. The fact that the zone of yielded material extends further into the column than the beam can be attributed to two conditions. First, the high axial load stresses in the column are additive to the bending stresses. Secondly, the moment gradient is much steeper in the beam than in the column (see Fig. 6, ultimate load moment diagram). The rotations of the connections at which the photographs in Fig. 18 were taken are indicated on Fig. 19.

The moment-rotation curves for both knees of Frame 3 are shown in Fig. 19. At no time during the test did the knees show signs that they had smaller moment capacity than the beam section. There was no local crippling of any part even though yielding of the material was widespread in the knee at the lee column. The knee showed the capacity to carry the full plastic moment of the beam section through large rotations. The moments at the intersection of beam and column center lines based on measured reactions and measured frame deflections are used in the plotting of one set of curves (drawn with solid lines) shown in Fig. 19. The second curve for the lee knee (dashed line) was plotted with moments found when the deflection of the frame was neglected. The difference in the curves becomes significant only at very large rotations, well after the ultimate load had been reached.

The knee at the windward column was never called upon to carry a moment equal to the theoretical yield moment; nevertheless, the moment-rotation curve for this knee is not a straight line, and when the frame was unloaded the knee had taken on a small amount of permanent set, indicating inelastic action. As can be seen in Fig. 19 the two knees of Frame 3 behaved in almost identical fashion at equal moment levels.

The moment rotation curves for Frame 4 shown in Fig. 20 are plotted on the basis of experimental moments corrected for the frame deformations. These moments, however, have not been corrected for the suspected "locked-up" moments discussed in connection with Fig. 13. These curves are in very close agreement with those of Fig. 19, if the error in moment due to the initial "locked-up" moments is taken into account. One point worthy of note is the fact that the windward knee had virtually no increase in rotation during the interval between ultimate load-Phase I (Load 22) and ultimate load-Phase II (Load 42) while the rotation in the lee knee more than doubled. This behavior is in complete agreement with the plastic theory for Phase II where the horizontal loads were increased while the vertical loads were held constant.

Another point of interest in Fig. 20 is the unloading of the lee knee that occurred after the ultimate load had been reached in Phase II. This unload-

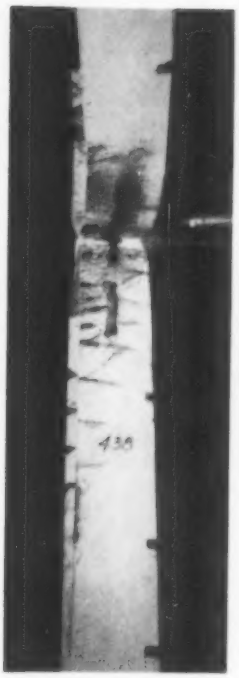

Fig. 23 Lateral buckle in lee column—Frame 3

ing occurred as the connection and the adjacent beam began to buckle laterally. Despite this unloading of the buckled lee knee the loads on the frame did not reduce at the same rate, in fact the vertical loads remained about constant while the horizontal loads were increased (see Fig. 10). This action was possible because of the ability of the windward knee to withstand increased moment and rotation as shown by the later part of its moment-rotation curve.

(b) *Beam Sections.* The moment-unit rotation relationships for two locations in Frame 3 are shown in Fig. 21. The theoretical curves shown in this figure are simplified by showing only the two straight-line portions of the true theoretical moment-vs.-unit rotation curve. The values of the moments plotted here were determined from measured reactions and were corrected for frame deformations. The curve for Location 1 in the lee column shows that the full plastic moment was never reached at this point in the frame; nevertheless, what appears to be plastic hinge action was started at the ultimate load condition when the moment at the section was 94% of the theoretical plastic moment. As the rotation increased rapidly after the ultimate load had been reached, the moment increased slightly to 97% of the M_p value but only after the rotation was about 5 times greater than it was at the ultimate load. This reduced plastic moment can be attributed in part to the axial load in the column.

It should be pointed out that the moment-carrying capacity at Location 1, Fig. 21, was not appreciably decreased until the column buckled laterally. The rotation when column buckling occurred was about 5.3 times as large as the rotation when the ultimate load was reached.

The second curve in Fig. 21 shows the moment-vs.-unit rotation relationship found by the rotation indicator mounted on the frame near the theoretical location of the second plastic hinge (Location 2). This curve is very similar to the first curve except for the drop in the moment which occurs just after the ultimate load was reached. This reduction can be explained by the fact that the beam tried to buckle laterally in this region soon after the maximum load was attained. This buckle could be observed by eye shortly after the ultimate was reached but its effect was undoubtedly indicated much sooner by the drop in moment at this section and by the drop in applied load seen on Fig. 9. The detrimental effect of this lateral buckling action was finally overcome as the lateral supports in the region were sufficient to prevent increased lateral movement. After this sudden drop, the moment at the section increased again and exceeded the peak value which occurred at the ultimate load condition.

Moment-unit rotation curves for two beam sections in Frame 4 are shown in Fig. 22. As in Fig. 21, the theoretical curve is "idealized" by two straight lines. In the first curve, the moment 6 in. from the base of the windward column is plotted versus the average unit rotation of the lower 12 in. of the column. This area of the frame was still elastic at the ultimate load condition for Phase I, but became plastic as the horizontal loads were increased in Phase II. The experimentally determined moments at the base of the windward column are approximately correct since the "locked-up" moments shown in Fig. 13*a* are zero there. Evidence of strain hardening is shown by the last portion of the curve.

The second curve in Fig. 22 shows the moment-unit rotation relationship for a section of the beam 8 in. from the windward vertical load in Frame 4. The rotation indicator was mounted in an area where the last plastic hinge formed in Phase I (see Fig. 7) since the third and fourth hinges formed simultaneous-

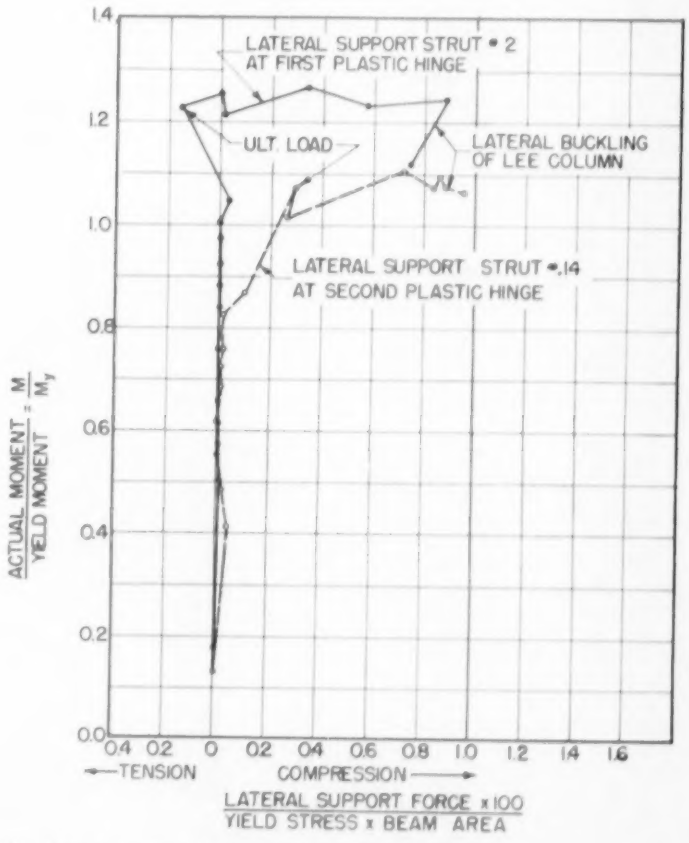

Fig. 24 Lateral support forces at plastic hinges in Frame 3

ly in Phase I. This explains the small rotation experienced by the beam at the ultimate load, Phase I. This curve is characterized by a sudden drop in moment just after ultimate load, Phase I, much like that shown in the corresponding curve in Fig. 21. Again, lateral buckling of the beam in the center third is the explanation.

The moments used in plotting the second curve in Fig. 22 were those computed from experimental data with corrections made for frame deflection. However, they were not corrected for the probable "locked-up" moments described in Fig. 13. If this correction had been made, the maximum moment carried at this point of the frame would have been 96.5% of its theoretical plastic moment, M_p. This percentage compared very favorably with a value of 97% shown by the corresponding beam section in Frame 3.

16. Plastic Buckling and Lateral Support

(a) *General.* The present frames illustrated clearly the fact that the final failure of continuous rigid frames is usually brought about by instability of some parts or parts of the frame. The proportions of most frames and rolled sections are such that this instability does not develop in the elastic range. Once the steel member has yielded, however, the possibility of this phenomenon occurring is increased many times. Current investigations at Lehigh University are making extensive studies into the field of plastic instability of rolled steel sections with the aim that adequate protection against premature buckling can be assured.

One way to prevent instability failure is to support the frame transversely. The location and strength of the lateral support system for a frame is of primary importance. At the same time the width-to-thickness ratio of the elements of the sections is also very important, since such elements may suffer from local buckling or crippling and thus bring about premature failure of the frame.

The proportions of the 12WF36 section used in the present tests are such that local buckling prior to strain hardening would not occur (see Reference 10). Indeed, this characteristic was one reason for choosing the section for the tests. Studies now under way at Lehigh University indicate that if a section does not buckle locally before it reaches strain hardening it will have adequate rotation capacity for plastic design purposes provided it does not suffer from lateral (torsional) buckling.

(b) *Frame 3.* Frame 3 sufferesl from buckling in three regions. All three zones affected were in a plastic state when the buckling occurred. The first evidence of instability was observed by eye after the ultimate load had been reached and took the form of a lateral displacement of the compression flange of the beam near the second plastic hinge. The effect of this lateral buckle has already been discussed with regard to the drop in moment capacity of the beam in the region where the buckle occurred (see Fig. 21). This buckle took the form of a wave about 3 ft long, but further displacement was controlled by the lateral supports which were attached to the beam at the intersection of web and flange. (The locations of these supports along the beam are indicated by the circles in Fig. 1*a*.)

At the same time that the lateral

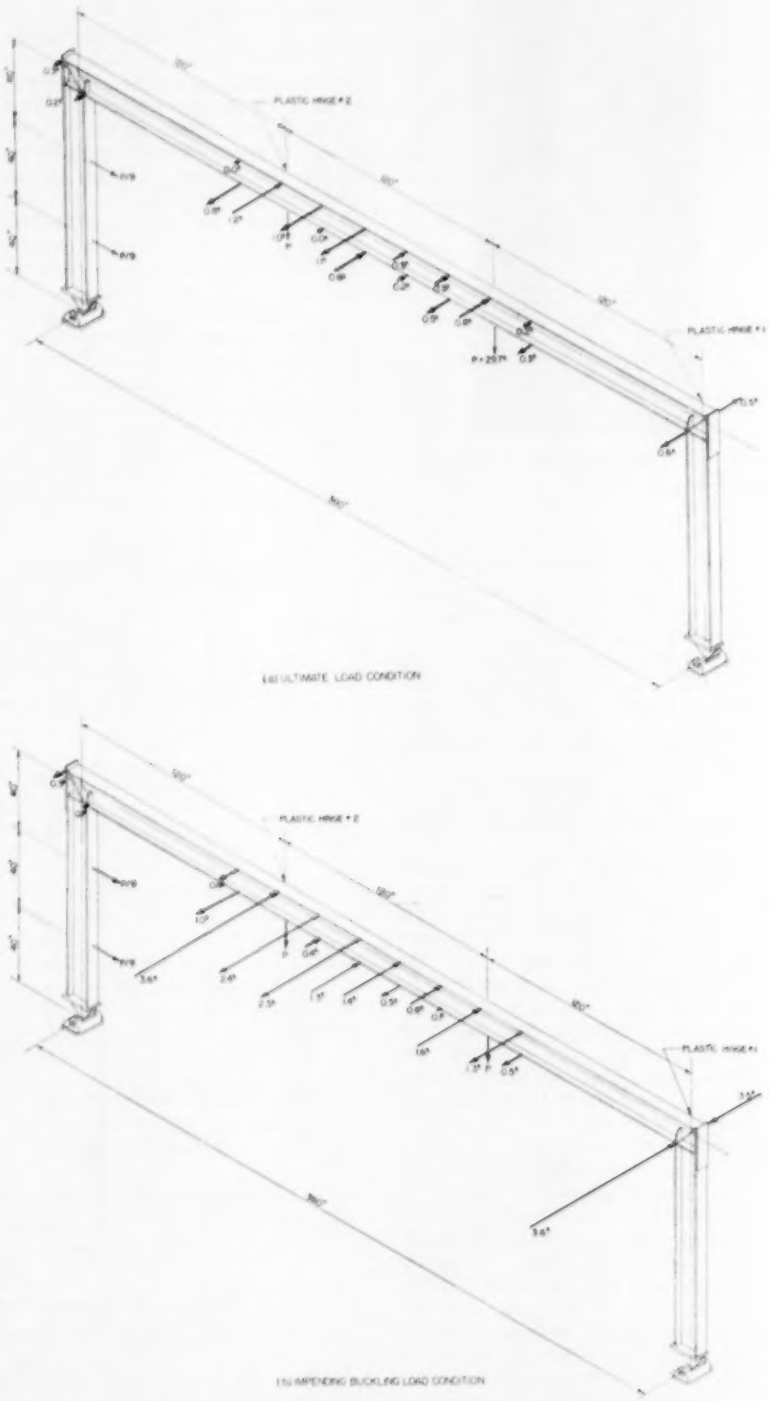

Fig. 25 Lateral support forces in Frame 3

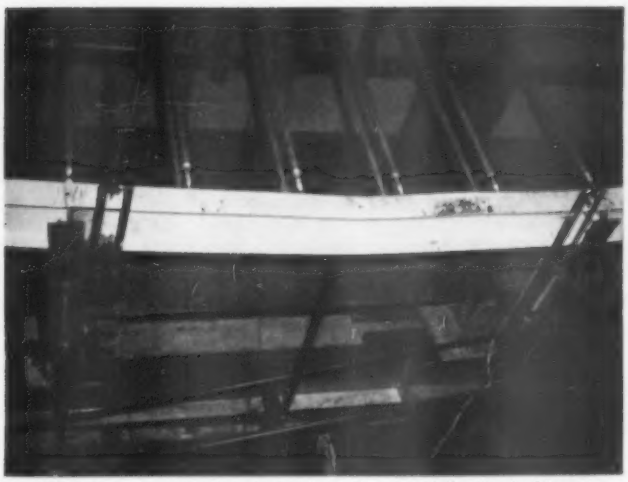

Fig. 26 Top view showing lateral buckle in middle third of beam—Frame 4

Fig. 27 Lee knee after test—Frame 4

buckle was observed in the beam, another type of instability was observed in the bottom flange of the beam at the lee knee in the form of flange crippling. The buckle occurred only in one-half of the flange with a wave length of about 3 or 4 in. The center of the wave was about 4 in. from the intersection of beam and column. The yielded zone in which this buckle occurred can be seen in Fig. 18*a*. The buckle could be seen on the beam at the time the photograph was taken, but it is not easily discernible in the photograph. Though this buckle was observed soon after ultimate load had been reached, it did not appear to hinder the performance of the frame in any way. Certainly it did not have the weakening effect of the lateral buckle which occurred in the middle third of the beam.

In this second case of instability, as in the first, good lateral support was near at hand and may have prevented damage that might have developed had it not been there.

The third case of instability came when the unsupported compression flange of the lee column buckled laterally and the frame finally collapsed (see "*LB*" in Fig. 9). This buckle showed some early signs of developing in the form of an unequal yield pattern on the flange but apparently was held in check for some time by the lateral support attached to the compression flange at the intersection of beam and column. However, when the deflection at the center of the beam had reached a value of about 2.3 times its value at ultimate load, there was a distinct and rapid increase in the size of the buckle wave and a corresponding sudden drop in load. Despite this buckling, the frame supported 87.2% of its ultimate load but further straining produced rapidly decreasing load capacity. Just before the lee column buckled the load was 95.3% of the ultimate load.

The buckle in the lee column is shown after completion of the test in Fig. 23. The photograph, which was taken from the inside of the frame looking out, shows clearly the lateral-torsional buckling type of failure characterized by the lateral displacement of the compression flange.

It has already been pointed out that earlier failure of the frame was undoubtedly prevented by the effective lateral support furnished for the test frame. A study of the forces that were measured in the lateral supports showed that the frame required negligible lateral support in the elastic range, but as zones of yielding in the frame formed, the lateral support system was called upon to carry larger and larger loads. Those lateral support struts located at the theoretical plastic hinges were called upon to carry the larger part of the lateral loads. When the frame was at the verge of collapse, there was a total of 12,700 lb tension and 12,700 lb compression in the lateral support struts; at the same time the single forces required at the first and second hinges were 3600 lb each. Thus the lateral forces at the plastic hinges made up 57% of the total lateral force.

Fig. 28 View looking up at lateral buckle in beam at lee knee—Frame 4

To obtain a dimensionless plot of the relationship between experimental frame moments and lateral support forces, the experimental moment at the section supported was divided by the theoretical yield moment, and the lateral support force was expressed as a percentage of the axial force that would be required to cause yielding of the beam section if used as a very short column.

Such dimensionless plots for the lateral forces at the two plastic hinges in Frame 3 are shown in Fig. 24. The curve for lateral support strut no. 2, located at the inside corner of the lee knee, shows lateral force of only 0.15% of the axial yield load at ultimate load, whereas the support force at the windward vertical load point (plastic hinge no. 2) was about 0.3% of the base value. The maximum value of any lateral support force measured during Test 3 was less than 1.0% of the axial yield load of the beam section.

In order that the distributions of the forces in the various lateral support struts might be seen for two critical load conditions, the isometric views of Frame 3 are given in Fig. 25. The lateral forces are represented by the vectors which show the sense and the magnitude of the force. In addition, the magnitude of the force in kips is shown directly adjacent to the vector.

The forces induced in the lateral bracing system by Frame 3 at ultimate load ($P = 29.7$ kips) is shown in part "a" of Fig. 25, while the condition when the frame had been deformed about two and one-half times as much as at ultimate load is shown in part "b."

Several facts illustrated by Figs. 24 and 25 should be pointed out. The maximum values of the lateral forces occurred at the plastic hinges. The larger lateral forces occur at the compression flange of the beam. The presence of the lateral buckle in the top flange in the middle third of the beam is evident from the large values of lateral load in the two lateral support struts to the right of the windward vertical load point. Virtually no force was required to constrain the windward knee which was never subjected to a moment as large as the yield moment for the beam section. The forces at the top and bottom of the beam at any one section were always of opposite sense indicating that a twisting tendency always existed when the plastic condition had been reached. This tendency suggests that lateral bracing should be stiff enough to prevent torsional rotation of the members at the hinge points.

(c) *Frame 4.* The behavior of Frame 4 with respect to buckling was very similar to that of Frame 3 discussed above. All instability was confined to regions which had yielded.

The first observed case of instability in Frame 4 occurred in the middle third of the beam just after the ultimate load in Phase I had been reached. The buckle of the compression flange here took the form of an "S" shape curve. The node points of the waves exactly coincided with lateral support points 5, 7 and 9 (see Fig. 1*b*). These support points are 2 ft apart. The lateral buckling of the beam may be seen in Fig. 26. This photograph was taken looking down on the middle third of the beam of Frame 4. Even though this buckle developed immediately following the ultimate load in Phase I, it did not prevent the frame from carrying increased horizontal loads in Phase II.

The second case of buckling in Frame 4, which finally brought about its collapse in Phase II, was a lateral buckle in the beam adjacent to the lee knee. A side view of this knee after the test is shown in Fig. 27. The photograph in Fig. 28 was taken looking up from the inside of the frame toward the lee knee and shows the lateral displacement of the compression flange of the beam.

The forces measured in the strut attached to the inside corner of the lee knee are plotted in Fig. 29 versus the moment at the knee. In addition, the relationship between the angle of twist developed in the beam at the connection of beam to lee column and the knee moment is shown. The lateral forces and angles of twist measured at ultimate loads, Phase I and II, are indicated on the graphs. The maximum of the lateral support forces in Frame 4 occurred in the strut (no. 15) used for plotting Fig. 29. At ultimate load, Phase I, the maximum lateral support force was about 0.4% of the axial yield load. Despite the fact that Phase II was undertaken with a severely deformed frame the maximum lateral force measured at ultimate was only 1.3% of the axial yield load of the beam section.

The distribution of forces in the lateral support system for Frame 4 are shown in Fig. 30. The ultimate load conditions for Phase I and Phase II are shown in parts *a* and *b*, respectively. In general the lateral forces measured in Frame 4 were larger than those measured for Frame 3.

Summary

The apparatus and procedures used in testing two fullsized all-welded portal frames have been described very briefly so that the test results could be interpreted. The details of the frame and test apparatus are shown in Figs. 1 and 2. The test set-up as used was satisfactory in all respects. The loading system was especially simple and allowed the testing of the frames to continue at a slow rate well after ultimate load so that much additional information was obtained.

The results of elastic and simple plastic analysis of the frames are given so that their behavior during test could be evaluated.

In this report, the major emphasis has been on the results of the tests. The following statements sum up the results.

1. The elastic behavior of the frames was for all practical purposes identical to the theoretically predicted behavior when the increased flexibility of the knees was taken into account. Methods are available by which such elastic analysis of the knee may be made (see Reference 3).

2. The analysis of data showed that the component parts of the frame behaved in a manner that was similar to separate isolated tests of connections, beams and columns.

3. The ultimate loads by test were 99, 97 and 95%, respectively, of the ultimate loads predicted by simple plastic theory for Frame 3, Frame 4(I) and Frame 4(II) (see Fig. 16).

4. The frames were able to carry

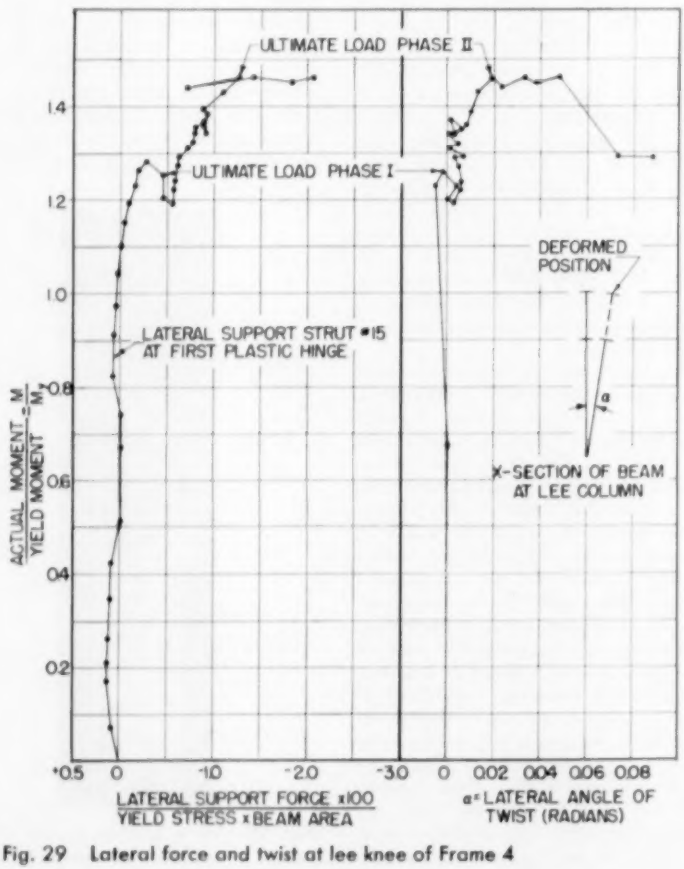

Fig. 29 Lateral force and twist at lee knee of Frame 4

loads very near the predicted ultimate load through deflections twice as great as those which existed when the maximum experimental load was first reached (see Figs. 9 and 10).

5. The frames showed the ability to absorb relatively large amounts of energy. Frame 3 finally absorbed about 9 times as much energy as it had when the theoretical elastic limit had been reached and about 3 times as much as when the ultimate load had been reached (see Fig. 9).

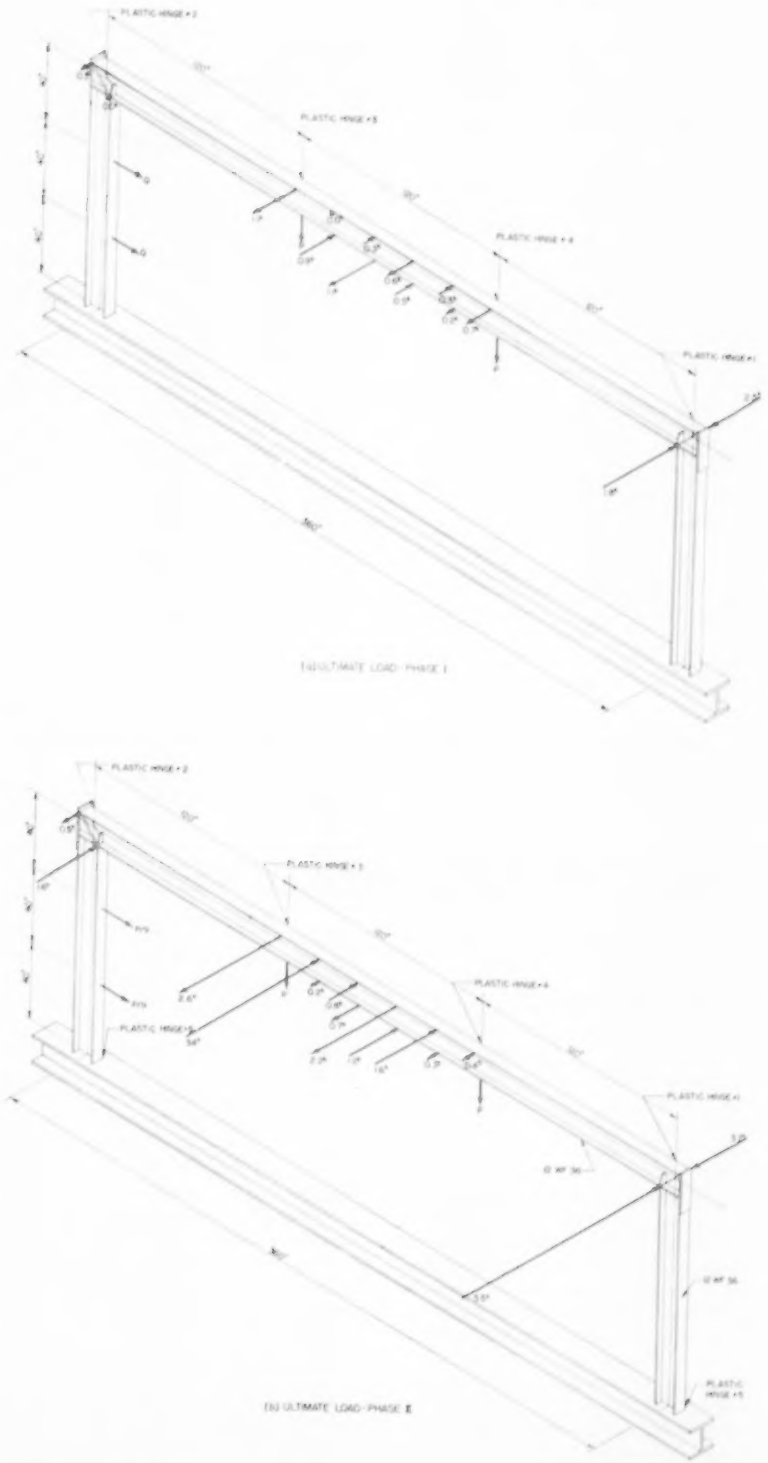

Fig. 30 Lateral support forces in Frame 4

6. The knees used in the frames were capable of carrying more than the plastic moment for the beam section without showing any signs of failure. These high moments were carried even though the rotation of the knee finally became in one case about 5 times as great as the rotation at yield moment and 2.7 times as great as the rotation when the plastic moment of the beam section was first reached (see Fig. 19).

7. The 12WF36 section used in the frames showed an ability to withstand large rotations at moments which were close to the theoretical plastic moment. The beam underwent unit rotations in the order of 16 times the theoretical unit rotation at the predicted yield moment (Fig. 21). This rotation took place without flange or web crippling.

8. The magnitude of the lateral support forces required to insure the good plastic action of the frame was relatively small. The largest force measured at a single support point was about 2% of the theoretical axial yield load of the beam section. The maximum lateral support force measured at an ultimate load condition was 1.3% of the axial yield load which was measured at the plastic hinge formed at the lee knee of Frame 4(II) (see Figs. 24 and 29).

9. The largest lateral forces measured in either frame were at the plastic hinge locations (see Figs. 25 and 30).

10. The frames were subject to lateral buckling when large regions of the beam sections became plastic. The adverse effects of this buckling were minimized by the lateral support system. All signs of plastic instability occurred after the ultimate loads had been reached (see Figs. 24 and 29).

11. Final failure of Frame 3 was brought about by lateral buckling of the lee column after the frame had supported virtually its ultimate load through deflections 230% of those when ultimate load was first reached (see Fig. 9). The column had no lateral support except at its intersection with the beam and at its base (see Fig. 23).

During Phase I of Test 4 no evidence of collapse by buckling was observed. This was to be expected since the frame had not shown positive proof that it had reached its true ultimate load when this phase of the test was discontinued.

Frame 4 finally failed in Phase II of the test when the beam adjacent to the lee knee buckled laterally. This buckling occurred when the beam center deflection was 2.6 times as large as it was at the ultimate load-Phase I (see Fig. 10).

12. The 12WF36 shape was intentionally chosen to minimize the effect of local flange buckling. One

small wave of flange buckling was detected in each frame soon after the ultimate load had been reached, but neither developed to any degree.

In general, the results furnish encouraging evidence of the applicability of plastic analysis in structural design. At the same time, they confirm the need for adequate lateral support or other provisions for protection against lateral buckling. The lateral bracing furnished in these two tests was proved to be adequate.

Aknowledgments

The tests and analysis described in this report are part of an investigation carried on as a result of a cooperative agreement between the Welding Research Council of the Engineering Foundation, the Navy Department, and the Institute of Research of Lehigh University. Funds are supplied by the American Institute of Steel Construction, American Iron and Steel Institute, Office of Naval Research, Bureau of Ships, and the Bureau of Yards and Docks. The investigation is being supervised by the Lehigh Project Subcommittee (T. R. Higgins, chairman) of the Structural Steel Committee, Welding Research Council. The suggestions and guidance of this committee are gratefully acknowledged.

The tests reported herein were carried out through the efforts of several persons in addition to the authors. Much of the early planning was done by K. E. Knudsen, former research assistant professor, J. P. Verschuren, former research assistant, designed parts of the test apparatus for Frame 3. In addition, the competent work of the laboratory machinists and technicians under the direction of K. R. Harpel, foreman, helped bring the tests to successful conclusion.

References

1. Ruzek, J. M., Knudsen, K. E., Johnston, E. R., and Beedle, L. S., Progress Report No. 7, "Welded Portal Frames Tested to Collapse," *SESA Proc.*, XI, (1) 1953. Reprinted, THE WELDING JOURNAL, **33** (9), 467-s, 1954.

2. Baker, J. F., and Roderick, J. W., "Tests on Full-Scale Portal Frames," *Proc. Inst. of C. E.*, London, January, 1952.

3. Beedle, L. S., Topractsoglou, A. A., and Johnston, B. G., Progress Report No. 4 "Connections for Welded Continuous Portal Frames," Part I—"Test Results and Requirements for Connections," THE WELDING JOURNAL **30** (7), Research Suppl., 359-s, 1951. Part II—"Theoretical Analysis of Straight Knees," *Ibid.*, **30** (8), Research Suppl., 397-s, 1951. Part III—"Discussion of Test Results and Conclusions," *Ibid.*, **31** (11), Research Suppl., 543-s, 1952.

4. American Institute of Steel Construction, "Steel Construction Manual," 1947.

5. Symonds, P. S., and Neal, B. G., "Recent Progress in Plastic Methods of Structural Analysis," *Journal of the Franklin Institute*, **252** (5 and 6), Nov., Dec., 1951.

6. Baker, J. F., and Horne, M. R., "New Methods in the Analysis and Design of Structures in the Plastic Range," *British Welding Journal*, **1** (7), 307, 1954.

7. British Constructional Steelwork Association, "The Collapse Method of Design," B.C.S.A. Publication No. 5, 1952.

8. Yang, C. H., Beedle, L. S., and Johnston, B. G., Progress Report No. 3, "Plastic Design and the Deformation of Structures," THE WELDING JOURNAL, **30** (7), Research Suppl., 348-s, 1951.

9. Lewis, E. M., "Construction of the B.W.-R.A. Testing Laboratory," *British Welding Journal*, **1** (12), 1954.

10. Hanjer, G., and Thürlimann, B., "Local Buckling of Wide-Flange Shapes," Fritz Laboratory Report 205E.5., December, 1954.

Nomenclature

E	=	Young's modulus of elasticity
H	=	Horizontal reaction
I_x	=	Moment of inertia
LB	=	Point at which lateral buckling occurred (in figures)
M	=	Moment
M_p	=	Full plastic moment
M_y	=	Moment at which yield point is reached in flexure
P	=	Concentrated vertical load
P_p	=	Theoretical ultimate concentrated vertical load
P_y	=	Theoretical first yield concentrated vertical load
Q	=	Concentrated horizontal load
Q_p	=	Theoretical ultimate concentrated horizontal load
Q_y	=	Theoretical first yield concentrated horizontal load
S_x	=	Section modulus, I/c
UL	=	Ultimate load (in figures)
YL	=	First observed yield line (in figures)
Z_x	=	Plastic modulus, $Z_x = (M_p/\sigma_y)$
α	=	Lateral angle of twist
δ	=	Deflection
ϵ_{st}	=	Strain at strain-hardening
σ_y	=	Yield stress level
ϕ	=	Rotation per unit length, or average unit rotation; curvature

THERMAL EFFICIENCY IN ARC WELDING

The different energies which play a role during arc welding determined separately by the use of a special calorimeter

BY J. TER BERG AND A. LARIGALDIE

Introduction

The estimation of the amount of energy absorbed in the fusion of metal, compared to the total energy supplied during the same time, makes it apparent that the thermal efficiency of the operation is quite small. This fact leads to research on the manner in which the electrical energy fed to the arc by the current source is utilized.

J. ter Berg and **A. Larigaldie** are associated with S. A. Philips, France.

The study of this problem began with the work of Doan,[1] Compton and Van Voorhis[2] and Myer,[3] who referred more specially to metallic arcs under atmospheric pressure. According to results published at that time, we see, for example, that out of a total of 645 calories, 330 were utilized in the fusion of the metal, the efficiency hardly exceeding 50%.

The progress represented by the production of coated electrodes has not, generally, contributed to the improvement of thermal efficiency. A certain fraction of the energy available is, in fact, absorbed in the fusion of the coating as indicated by Naka and Nakajima.[4]

A higher efficiency is, however, obtained with the recent "contact"[5] electrodes, in which part of the metal deposited comes from the fusion of the iron powder incorporated in the coating.

The study of thermal efficiency is presented also in a different form, in the case of infusible electrode arcs, protected by an atmosphere of inert gas. This subject has been treated by Lancaster.[6]

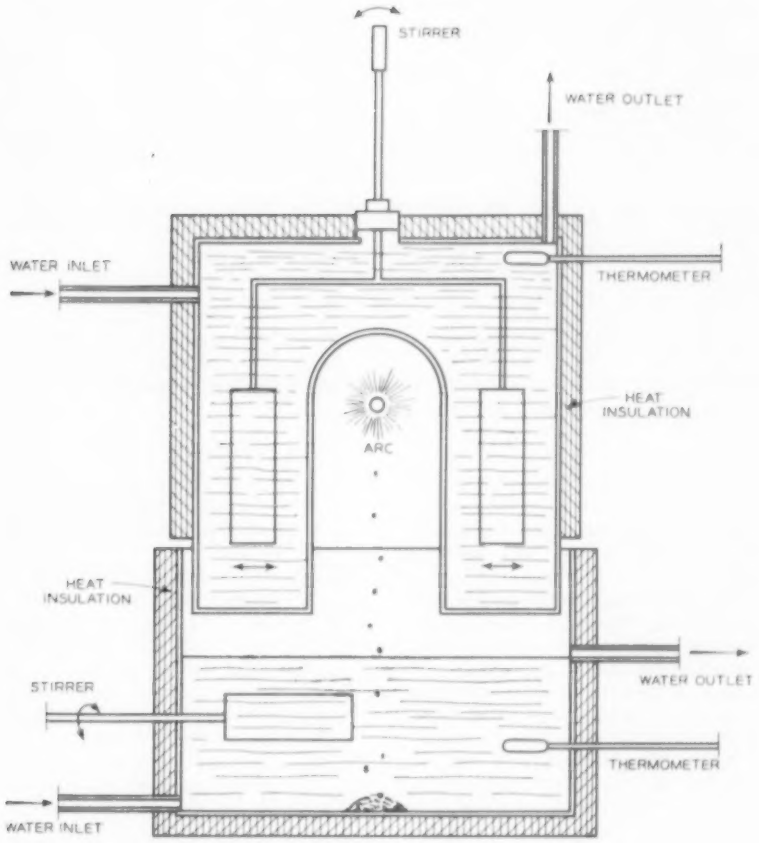

Fig. 1 Cross section of calorimeter

If we examine the coated electrode, we see that, in addition to the number of calories utilized in the fusion of the metal and the coating; a certain amount of heat is dissipated in the form of radiation, or dispersed into the atmosphere by the effects of convection.

These considerations would be incomplete if one did not take into account the number of calories which may be attributable to the endothermic and exothermic reactions which may be produced under the actions of high temperatures in the arc. This quantity of energy being distinct from that coming from the current source, a difference may be established between the energy supplied and the total of the energy accounted for.

From the above we may see that the following energies will arise:

(1) Fusion of the metal
(2) Fusion of the coating
(3) Loss through convection and radiation
(4) Heat of the reactions produced during welding

The aim of this investigation will be the determination of these different items. The evaluation of the heat of reaction will, in addition, allow us to know if this energy can possibly contribute to the improvement of thermal efficiency.

Experimental Apparatus

In order to be able to measure the different items of this thermal balance-sheet, we have constructed a calorimeter, a diagram of which is given in Fig. 1.

The lower part is a trough containing a constant volume of water, into which may fall the droplets of metal melted by the arc, which are covered with a layer of slag.

The upper part, which will collect warm gases and absorb the radiation energy of the arc, consists of a double-walled bell. This bell, filled with a certain quantity of water, surrounds the arc which is formed between two horizontal electrodes. The arrangement already described[2] moves these electrodes, thus ensuring a length of arc, which is constant and determinable in advance.

The two containers are carefully heat-insulated, and provided with agitators which will rapidly equalize its temperature after a test. The rise in temperature of these two containers is measured with thermometers graduated in tenths of degrees centigrade. The thermal insulation is such that the rate of cooling for a temperature 10° C above room temperature is not as much as 0.1° C per minute.

The calorific capacity of the upper bell is 3000 calories, and that of the lower trough is 2000 calories.

The energy supplied during a test is measured with a watthour meter, while the voltseconds and ampèreseconds over the same period are measured with O'Keenan counters.

The calibration of the counters is done by comparison with a voltmeter and ampère meter, the arc in this case being replaced with a resistance of an appropriate value.

Measuring the Different Items of the Thermal Balance Sheet

With the special calorimeter described above, it is possible to separate the different calorific quantities which interest us.

Latent Heat of the Metal-Slag Drops

The rise in temperature of the lower trough can lead to an estimation of this value if we consider the following reasoning:

"The energy received by the lower container measures not only the latent heat of the products of fusion of the electrodes, but also the sum of this value and of a fraction of the energy dissipated by the arc, in the form of convection and radiation."

The greater part of this energy is absorbed by the upper bell by reason of its shape and the upward movement of the warm gases liberated.

Since in our tests the position of the arc does not vary, the distribution of losses, due to convection and radiation, between the upper and lower containers is practically constant and may thus be quite easily measured.

To do this, one sets up, in conditions as identical as possible, an arc of the same power as the welding arcs used in the tests, but using for this measurement electrodes which will not melt, e.g. carbon-lamp arcs. We find in this case that the lower trough will receive only about $^1/_{20}$ of the calories received by the bell.

We should then, in order to find the latent heat of the melted drops, subtract from the figures given for the lower trough, 5% of the calories received by the upper container.

As we know exactly for each electrode the weight of metal and the weight of the coating composition and, in addition, values of specific heat for the steel and the slag, it is possible to calculate the number of calories transferred from one to the other, supposing their temperature to be equal. We may thus determine the first two items on our balance sheet.

Table 1—Summary of Results

	Endothermic			Neutral	Exothermic		
Specification	*A*	*B*	*C*	*D*	*E*	*F*	*G*
Composition of coating	Kaolin, 10 Mg CO3, 90	Oxidizing type	Basic type	Calcinated Kaolin, 90 CaCO3, 10	Acid type	Organic type	Mg, 15 FE3O4, 35 Kaolin, 50
Diameter of coating	5.0 6.0	6.5	6.5	4.7	6.3	5.7	6.0
Weight per cm of coating	0.05 0.12	0.58	0.43	0.06	0.55	0.40	0.26
Heat absorbed by the metal	40 42	39	36	49	44	49	35
Heat absorbed by the coating	2 6	23	16	3	20	20	13
Lost by convection	23 17	18	18	17	19	12	32
Lost by radiation	30 26	16	25	30	24	23	28
Heat of reaction	−5 −9	−4	−5	−1	+7	+4	+8

Note—All these quantities are expressed as a percentage of the energy supplied by the current source. The wire used is of soft steel, 4 mm in diam.

Losses Through Convection and Radiation

As we have explained above, the sum of this energy may be found by increasing the number of calories received by the upper bell by 5%, representing the convection and radiation energy collected by the lower trough.

As may be easily understood, the total of these losses increases with the length of arc. It is for this reason that we have always tried, in our experiments, to use with each type of electrode an arc voltage comparable to that used in normal welding, whereby the arc is struck between the coated electrode and the work to be welded. In any case, the thermal efficiency referring to the melting of a single electrode, the results would be about half of those obtained by the aforesaid method.

Finally, to separate the losses due to radiation from those which result from convection, the total radiated energy was measured in each case by means of the following arrangement:

A thermo-electric couple Pt-Te, specially prepared with a view to measurement of total radiation, i.e., whose useful surface was made uniformly absorbent for the wave lengths of which the calorific emission of such arcs is composed, and placed in an insulating container, receives the radiation to be measured through a fluorine window, which is in practice sufficiently transparent for radiations of this order.

This couple has been calibrated in such a way as to determine the relationship between the energy falling upon it and the electromotive force which is produced by the heating of the warm junction. A special support allows this apparatus to be moved around the fixed point of the arc, enabling the measurement of radiation in different directions. Curves are thus obtained, in polar coordinates, the integration of which will give us the value of the radiation losses of the arc under consideration.

Heat of Reactions

After each test, a difference is noted between the energy collected by the two sections of the calorimeter, and that supplied to the arc by the source of supply, measured by the watthour meter.

This difference represents the heat given off or absorbed by the different reactions in the course of fusion; these reactions may be, among others, the dissociation of carbonates, the evaporation of water or the oxidation of certain constituents of the coating.

If the difference indicated above is positive, we speak of an exothermic electrode, that is to say an electrode which releases energy as a consequence of the different reactions. If, on the other hand, the difference is negative we have an endothermic electrode.

When the difference is almost nil, that is to say when the heat of reaction is small, we may speak of it as a neutral electrode.

Discussion of Results

In Table 1 we have collected all the results obtained with series-production electrodes, or with electrodes made specially for this investigation.

It is obvious that a division between the exothermic, neutral and endothermic types is possible, and that the heat of reaction in all cases represents only a small fraction of the total energy, not exceeding 10%.

In addition we may notice:

(1) If the thickness of the coating is increased without changing its composition, the crater becomes deeper, thus reducing the losses through convection and radiation. The data given in column *A* make this clear.

(2) That coatings containing a high percentage of iron oxide or alkaline-earthy carbonates have a negative heat of reaction, due to the decomposition of these compounds (columns *B* and *C*).

(3) That coatings containing a major proportion of ferro-alloys or organic matter are exothermic, by reason of the oxidation of these components (columns *E* and *F*).

(4) That in all cases almost half of the energy supplied is used only to melt the metal; in other words, the calorific efficiency of the process of electric arc welding remains below 50%. It is not possible to exceed this amount even by incorporating in the coating a strongly exothermic mixture such as magnesium and iron oxide, to increase this efficiency.

As pointed out in the introduction, the only means of raising this efficiency above 50% is the incorporation of a large quantity of iron powder in the coating. This increased efficiency is a supplementary advantage, very rarely utilized for contact electrodes.

Summary

Using a special calorimeter, we determine separately the different energies which play a role during arc welding.

We note that the energy supplied or absorbed by reactions produced under welding is very small, and does not exceed approximately 10%.

We also note that the calorific efficiency for heating and fusion of metal always remains below 50%, even when incorporating constituents giving strongly exothermic reactions.

However, by adding large quantities of iron powder to the coating on "contact" electrodes, we can obtain a calorific efficiency higher than 50%.

Bibliography

1. Doan, G. E., *Trans. A.I.E.E.*, **49**, 723 (1930).
2. Compton and Van Voorhis, *Phys. Rev.*, **35**, 1438 (1930).
3. Myer, J. L., *Z. f. Phys.*, **87**, 1 (1933).
4. Naka, T., and Nakajima, S., *J. Jap. Wdg. Soc.*, **20**, 16 (1952).
5. van der Willigen, P. C. *Philips Techn. Rev.*, 161, 304 (1946).
6. Lancaster, J. F., *British Wdg. J.*, **1**, 412 (1954).
7. ter Berg, J., and Larigaldie, A., The Welding Journal, **31** (5), Research Suppl. 268-s (1952); *Soud. et Tech. Conn.*, 285 (1953).

SIGNIFICANCE OF FATIGUE DATA IN DESIGN OF PRESSURE VESSELS

Elimination of severe stress raisers by improvement of design details is advocated as being more effective than selecting metals of higher tensile strength to insure against progressive fracture

BY THOMAS J. DOLAN

SYNOPSIS. In general, the types of surface defects, notches and abruptness of changes in contour, determine the localized stresses from which progressive fractures initiate if loading is repeated many times. Vessels intended for long life (thousands of load cycles) and which are subjected to large variations in stress (due to pressure variations or thermal fluctuations) should be designed for adequate fatigue resistance by eliminating excessive stress raisers and careful control of fabrication methods and operating procedures. Recent data obtained from fatigue studies are reviewed from the viewpoint of their inferences in use of high-strength steels and increased design stresses. Difficulties of interpretation of laboratory fatigue data for quantitative design of full-sized structures are discussed and related to the statistical nature of fatigue life and the many factors affecting fatigue strength. Elimination of severe stress raisers by improvement of design details is advocated as more effective than selecting metals of higher tensile strength to insure against progressive fracture.

General Considerations

The construction rules and nominal design stresses for pressure vessels have been established primarily by the ASME Boiler and Pressure Vessel Code and the Joint API-ASME Code for Unfired Pressure Vessels. These codes were evolved to cope with static load conditions of operation and represent a collection of specific requirements based upon experience gained in practice over a period of years. They require the exercise of discretion in executing safe details of design and fabrication for static load conditions.

There exist today many varieties of pressure vessels each of which involves a unique set of operating conditions; thus it becomes difficult to cover all possible circumstances in any single code. One of the major factors not covered by codes and specifications is the determination of a rational procedure for design and fabrication in those cases where repeated loading may cause failure by the development of a progressive fracture (commonly referred to as "fatigue"). So many different variables are encountered in boiler drums, gas cylinders, chemical processing vessels, oil refinery equipment, etc., that it is impossible to make a general statement as to whether fatigue is an important factor in the design of a pressure vessel subjected to frequently repeated loading. However, no simple rational process has been evolved for design of vessels that are subjected to large numbers of cycles of repeated loading. The major purpose of the present article is to point out some of the difficulties inherent in the interpretation of fatigue data for inclusion in design procedures and to indicate some of the reasons why careful consideration must be given to the possibilities of fatigue failure in vessels subjected to repeated loading.

The demands of the power industry and of the multitude of different types of vessels required in industrial processing have forced designers to use many new higher strength metals and to strive for more effectively balanced design; that is, by using improved methods of calculating the localized stresses, by better fabrication and higher levels of quality in their construction. Along with these changes and improvements there has been a strong movement to reappraise the codes and ask for modifications to allow increased design stresses where justified by more efficient design and materials. Some engineers have felt that an increase in *actual* "safety factor" may be attained by these improvements in contrast to placing reliance on nominal stresses in the shell calculated only from crude formulas and utilizing a "factor of safety" of, say, 4 based on the static tensile strength of the metal.

It is recognized that the currently used empirical code formulas for design of details such as heads result in yielding in localized regions during the hydrostatic test.[5] Thus localized stresses exceeding the yield point may be encountered with present "low" design stresses, but these have proved safe for ductile metal and relatively static conditions of loading. High localized and secondary bending stresses of this magnitude, however, would develop progressive fracture after a large number of repetitions of loading.

There has been considerable speculation as to whether pressure vessels actually fail from repeated stressing, but resistance to fatigue is perhaps the major uncertainty in the performance of many types of vessels that operate at room temperature or slightly elevated temperatures. With the code requirement of a pressure test at $1^1/_4$ to $1^1/_2$ times the design pressure most vessels when put into service have already demonstrated an ability to withstand the design static load without failure. If precaution is taken to eliminate severe corrosive conditions there should be little doubt about the safety of the vessel for static load during the normal life, but failure might still be possible by creep, brittle fracture at low temperatures, or fatigue. If we confine our attention to the intermediate temperature range (say, 20 to 600° F) the major remaining uncertainty is the possibility of progressive cracks developing from the repetitions of loading in service.

Fatigue failures frequently occur in all classes of machines and structures if enough cycles of loads are applied during their normal life.[1-4] Bridges, marine vessels, railroad rails, aircraft wings, etc., all have been known to experience catastrophic fatigue fail-

Thomas J. Dolan is Head, Department of Theoretical and Applied Mechanics, University of Illinois, Urbana, Ill.

Paper presented at the ASME Metals Engineering Division Conference held in conjunction with the 1956 AWS National Spring Meeting, May 7–11, Buffalo, N. Y.

ures. It seems obvious that for those pressure vessels that are subjected to many* repetitions of loading the possibilities of progressive fracture must be given careful consideration in the *design* and *fabrication*. This is particularly true where increased life, frequent large variations in operating pressure or temperature, and a trend toward greater working stresses are expected. For many vessels the problems of stress determination frequently become more complex because of the existence of thermal gradients and cyclic temperature variations. A steady temperature gradient will superimpose a steady thermal stress that must be considered as a portion of the mean stress in the shell. Furthermore, frequent cyclic variations of temperature may occur in localized zones (for example, White[16] discussed fatigue failures in a boiler drum attributable to cyclic stresses due to temperature variations in the shell at the feed-water inlet). In instances of this nature, local design details are of extreme importance in limiting the service performance of the vessel.

Design Details

Calculated stresses are only crude approximations of the real stresses existing in the crystalline structure of commercial metals. For fatigue conditions the behavior departs significantly from the idealized conditions (of homogeneous, elastic, isotropic metal) assumed for purposes of calculating stress. Damage accumulates during each cycle of loading and develops at localized regions of high stress within poorly oriented or weaker crystals until subsequent repetitions of loading finally cause visible cracks to grow, join and spread.[17] The progressive fracture is invariably nucleated by the presence of a stress raiser. Any abrupt step or recess in the surface (such as at a drum head, bracket, pipe connection, etc.) constitutes a stress raiser that may serve as the nucleus for a fatigue failure. The drastic reduction in fatigue strength due to minor discontinuities such as a small hole or fillet is illustrated by a comparison of the solid curves in Fig. 1; it is not uncommon to have the fatigue strength cut *in half* by poor design details.

Stress raisers cannot be avoided entirely since localized stresses of high magnitude occur at: (*a*) metallurgical notches due to segregation, inclusions, laminations, etc., in the metal; (*b*) mechanical notches caused by the changes of contour necessary in a member for its functional use; or (*c*) notches or other defects developed by corrosion pits, nicks, galling, etc., in fabrication or service. Progressive fractures develop from these discontinuities even though the nominal stresses calculated by the usual formulas may be well below the static elastic strength of the metal. A crack (such as a quench crack or that due to lack of root penetration in a weld) is a severe stress raiser and tends to be self-propagating during each repetition of loading.

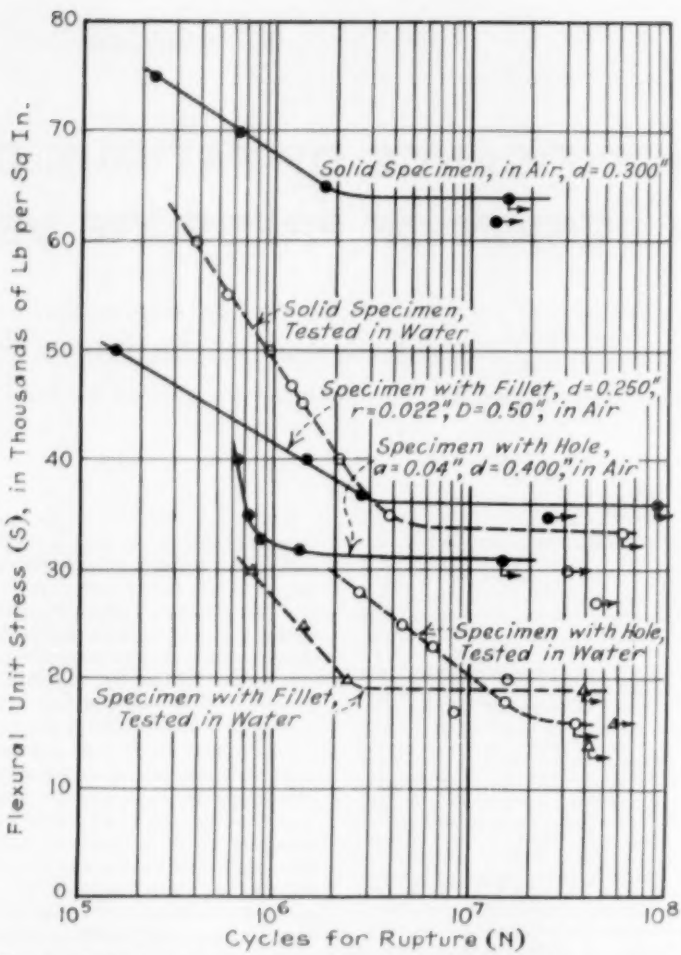
Flexural Unit Stress (S), in Thousands of Lb per Sq In.
Cycles for Rupture (N)
Solid Specimen, in Air, d=0.300"
Solid Specimen, Tested in Water
Specimen with Fillet, d=0.250", r=0.022", D=0.50", in Air
Specimen with Hole, a=0.04", d=0.400", in Air
Specimen with Hole, Tested in Water
Specimen with Fillet, Tested in Water

Fig. 1 Reduction in fatigue strength due to discontinuities or from corrosive effects of tap water. For hot-rolled SAE 3140 steel tested in reversed bending at 1450 cpm[22]

In general, a vessel that is safe from the viewpoint of static load design criteria (and which is not to be subjected to an excessively large number of cycles of loading) would have adequate resistance to fatigue fracture if *all severe stress raisers were eliminated*. Code values for allowable design stresses refer to the nominal calculated membrane stresses in the shell and generally disregard the peak stresses in regions of local or gross discontinuities. For fatigue conditions these localized stresses at abrupt changes in section, such as a head junction or a reinforced opening, or due to misalignment, defects in construction, thermal gradients, etc., *are the significant stresses* that cannot readily be computed from the membrane stress.

In general, the fatigue strength of a steel for a short cyclic life of about 1000 cycles may be as high as 90% of the tensile strength. For larger numbers of cycles the strength falls off somewhat as indicated in Fig. 2 until the endurance limit is reached at about one million cycles of stress. For a rough design criterion one could estimate the relative values of allowable stress for different numbers of stress cycles from curves of this type. As pointed out above, the significant stress considered in the design should be the peak value occurring in the most severely stressed zone in the vessel. By proper attention to design details it is frequently possible to lower the range of peak

* No sharp dividing line can be set as to what should be considered a large number of cycles of load. At high stresses (though localized) this may be counted in the thousands but for low stresses may be millions of cycles. As an arbitrary number, one might say that any figure exceeding 10,000 should be considered "many cycles" and possibilities of fatigue should be appraised.

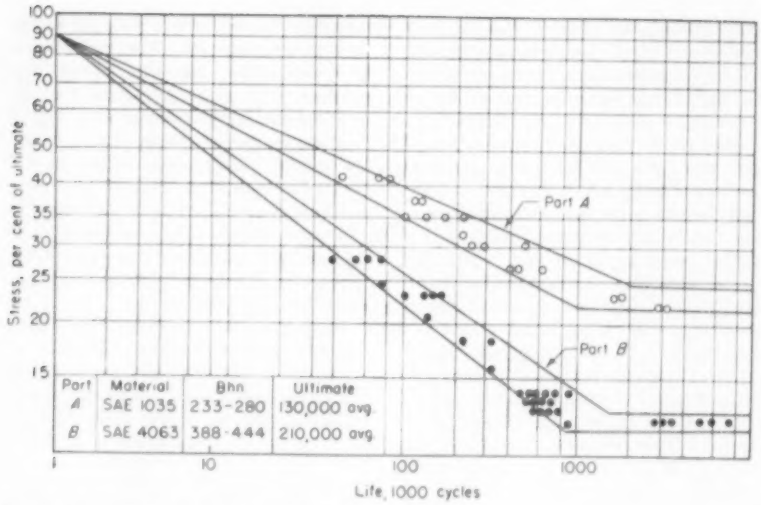
Stress, per cent of ultimate
Life, 1000 cycles
Part A
Part B
Part | Material | Bhn | Ultimate
A | SAE 1035 | 233-280 | 130,000 avg.
B | SAE 4063 | 388-444 | 210,000 avg.

Fig. 2 S–N curves of two as-forged parts[21]

stress developed, and a small decrease is accompanied by a large increase in fatigue life. Thus, if the maximum stresses are controlled by eliminating all *severe* stress raisers, the problem becomes less discouraging and adequate fatigue life is readily obtained.

Interpreting Laboratory Data

The numerical values obtained for fatigue life at a given stress amplitude are influenced by differences in testing technique and type of machine used in performing the test. The method of processing the test sample, (particularly the heat treatment and method used in finishing its surface) the type of loading employed, and the accuracy and stability of the testing machine all seem to have important effects in controlling fatigue life.

It seems important to point out that all data (such as those shown in this paper) that are reported in the literature for fatigue properties of any given metal should be regarded as *qualitative* only and careful consideration should be given to studying all details of the testing technique before appropriate interpretation of the numerical values can be made. For example, a large proportion of the available fatigue data have been obtained from rotating beam tests of small polished specimens to determine a "par" value for the fatigue limit (for say 10 million cycles of stress). At higher stresses (corresponding to a fatigue life of 10^4 or 10^5 cycles) the strains frequently exceed the proportional limit, and hence the flexure formula from which the stresses are calculated is *not* applicable. Thus the nominal *calculated* stresses for the test data are not valid for purposes of estimating the life of a pressure vessel for a given stress cycle. Furthermore, there is ample evidence from data such as those in Fig. 3 that the fatigue strength of forged or hot rolled members is only a small proportion of the strength of ground or polished specimens. Figure 3 also illustrates the fact that a large increase in static tensile strength of the steel may not significantly improve the fatigue limit if the parts are hot rolled or forged; only for polished steels without severe stress raisers does the fatigue strength increase in rough proportion to the tensile strength.

In general, one must expect a lower fatigue strength for a fabricated vessel than the values obtained from laboratory tests of small specimens of the metal from which the vessel is constructed. Some of the many reasons for lower fatigue strength in vessels may be listed briefly as due to differences in: (*a*) size, (*b*) cycle frequency, (*c*) temperature, (*d*) fabrication and (*e*) corrosion or environmental conditions of operation. These differences will be discussed briefly in the following paragraphs.

One must be skeptical about transferring quantitatively the results of fatigue tests of laboratory specimens to full-sized structures such as pressure vessels. Numerous studies have shown that the fatigue limit of bars 2 in. in diameter may be 15 to 20% lower than those of small laboratory specimens. Data of Horger[15] on axles 6 to 9 in. in diameter indicate a possible further reduction in strength as the size is increased. Of course plates and bars of large diameter have a poorer metallurgical condition and hence are inherently weaker than products that have received a great deal of reduction in the rolling operations. The "size effect" in fatigue, however, is in addition to any strength reduction due to poorer quality of metal; that is, small specimens cut from a large member exhibit higher fatigue strength than the full-sized bar.

Limited life fatigue testing can be highly misleading. The same metal tested in two different machines may exhibit different life to failure at the same general stress level. In some instances, two different metals have exhibited a crossing of their S-N curves; this means that entirely different conclusions would be drawn regarding the relative fatigue life of two steels when compared at high strain and again at low strain. Thus a comparison of two members made by testing at high overloads in order to shorten the duration of the test may not always be reliable in predicting their relative performance at the lower stresses expected in service. This only emphasizes the

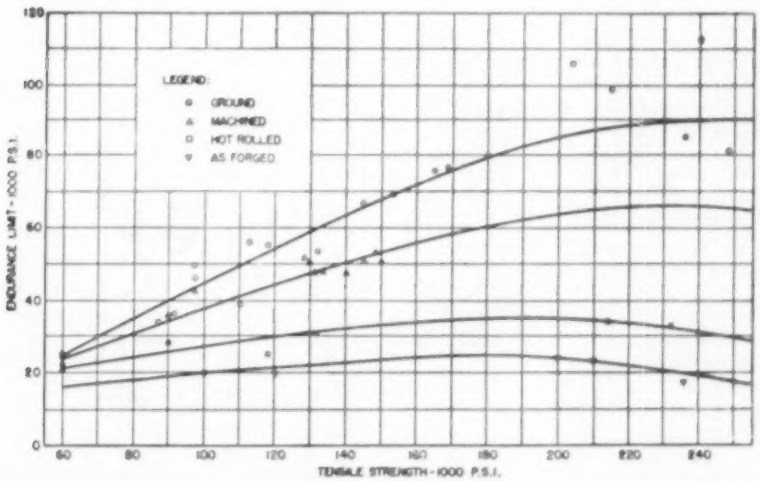

Fig. 3 Relation between endurance limit and tensile strength for unnotched specimens in reversed bending. (Showing reduction in fatigue strength due to method of surface preparation)[21]

need for careful and conservative interpretation of data from random experiments on metals at arbitrarily selected stress levels.

Influence of Fabrication and Operation Conditions

At *high* stress levels the number of cycles of loading for failure may be reduced by testing at a low-cyclic frequency or by imposing long sustained loadings. Gross and Stout[13] have shown that the reduction in plastic fatigue strength may be a significant amount; however, for normal conditions of operation in which plastic deformation, high temperatures, or corrosive conditions are not encountered, the frequency of loading has little influence on the number of cycles required to fracture (even up to thousands of cycles per minute). Periodic rest periods during the repeated stressing have little influence on the fatigue strength of welded plate and perhaps any effects of rest periods on steels may be beneficial rather than harmful.

It is fortunate that the fatigue strength of all steels is increased by depressing the temperature below room temperature.[18] Hence, as far as fatigue is concerned a vessel that is safe for operation at room temperature is safe for operation at any lower temperatures encountered. At moderately elevated temperatures (below the range for which creep becomes predominant) the fatigue properties of most steels are not appreciably lower than at room temperature.[15, 16] At higher temperatures (above about 700° F) the fatigue strength of steels becomes drastically reduced; however, in most instances at the higher temperatures the problem of design for *creep* becomes the primary consideration. The presence of appreciable amounts of alternating loading may have but little influence on the total *time* to cause failure of the vessel particularly in those instances where the loading frequency is not high. That is, considerable time is available for damage by creep, and failure occurs under fewer cycles of stress than might be observed with a high-frequency alternating load. The failure usually is primarily that of excessive deformation and fracture caused by creep rather than a typical progressive fracture by fatigue. However, it is important to note that the reduction in fatigue strength caused by a stress raiser at high temperature is comparable to that obtained at room temperature. Creep under a high mean stress may redistribute the localized stresses at the notch, but is not helpful in reducing the range of stress superimposed by the fluctuation of loading.

Vessels in service are often subjected to mild forms of erosion, corrosion, or chemical attack. It is well known[22, 14] that the fatigue strengths of metals are reduced very drastically (the values ranging from about $^2/_3$ to as low as $^1/_8$ of their fatigue strengths in air) when they are repeatedly stressed in the presence of as mild a corrosive medium as ordinary tap water. The dotted curves of Fig. 1 show vividly the fatigue strength reduction caused by tap water in short-time laboratory tests. For longer times or more active corrosive agent, the strength reductions are even greater. It is interesting to note also in Fig. 1 that the damaging effects of stress raisers and of simultaneous corrosion are somewhat additive. Thus the possibilities of even mild forms of corrosion or erosion should be given serious consideration if many thousands of loading cycles are to be satisfactorily endured over a period of years.

Fabrication of a pressure vessel may involve relatively crude operations of shearing or burning, and may permit the use of rolled plate containing many injurious defects in the form of contaminants, pitted surface or actual surface laminations. All of these factors should be retarded as exceedingly harmful from the viewpoint of fatigue. For example, in recent studies[7] the surface pitting produced by prior corrosion or of small laminations rolled into the surface was as serious as a severe stress raiser in reducing the fatigue strength of $^3/_4$-in. plate. Similarly, arc strikes, underbead cracking and the presence of recesses or abrupt changes of section at weld beads, form very efficient notches from which fatigue failures may be initiated. It is hard to estimate with any assurance the strength reduction due to these defects but they must cut the effectiveness of the design by at least 30% in fatigue strength. Any surface decarburization is of itself a weakening effect that lowers the fatigue strength of the whole plate to the value

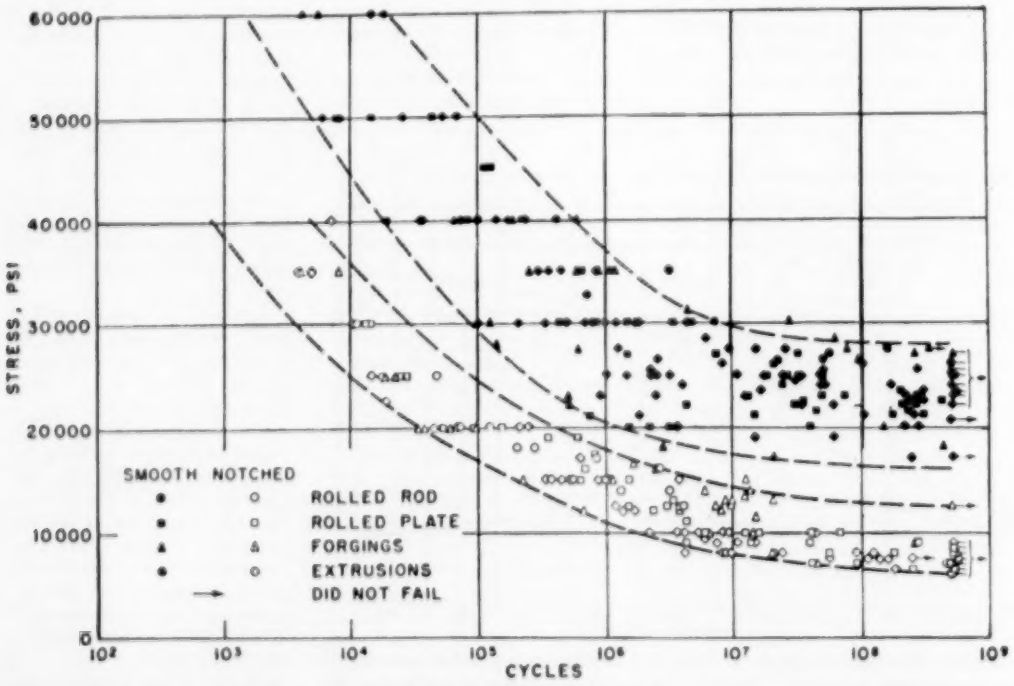

Fig. 4 Rotating beam fatigue data for 75S-T6, aluminum products[19]

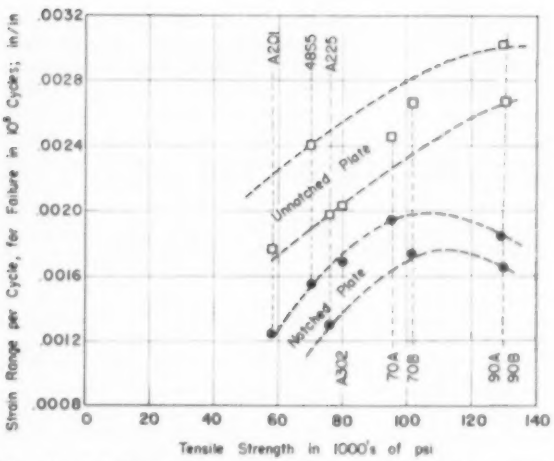

Fig. 5 Relative fatigue resistance of $^3/_4$-in. plates compared with their tensile strengths. Plates tested in biaxial bending to simulate membrane stresses in shell of a pressure vessel. Ordinates represent circumferential strains in vessel. Data from reference No. 7. Code numbers on chart designate the type of steel tested

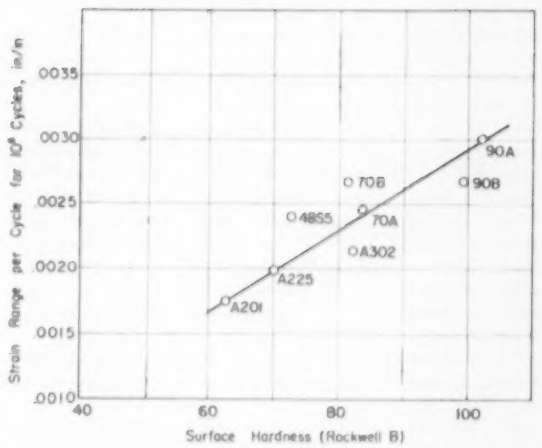

Fig. 6 Relation between fatigue strength (at 10^6 cycles of strain) and surface hardness. For $^3/_4$-in. plates tested in biaxial fatigue; data from reference No. 7. Numbers next to points designate the type of steel tested

corresponding to that of the thin surface layer of low-strength material.

In tests of small vessels subjected to repeated internal pressure, Moore[11] found that the presence of a local defect in the material of the shell (consisting of a depression about $^1/_{16}$ in. wide, $^1/_{32}$ in. deep, and some 2 ft. long in the surface of the plate) was sufficient to develop a premature fatigue failure in the vessel under stress cycles varying from 0 to 16,500 psi in the shell. In general, Moore found that several vessels failed prematurely in fatigue from localized conditions such as: (*a*) slag inclusions in a weld, (*b*) a small tapped hole for a gage connection, or (*c*) surface defects in the plate. Thus the fatigue strength of a vessel is *not* determined by the nominal design stress in the shell. It apparently is limited entirely by the severity of the stress raisers; that is, by the adequacy of design details for openings, intersections of surfaces of revolution, the degree of bending action around knuckles, stiffeners, etc., the adequacy of fabrication details, and the presence of injurious defects or excessive contaminants in the plate.

Statistical Nature of Fatigue Data

The fatigue life of a specimen under a prescribed set of conditions must be regarded as statistical in nature and subject to the same chance variations as any similar "mortality" data.[12] Test data are susceptible to rather wide variations depending upon chance effects in preparing or selecting the test specimen and upon heterogeneity or variability of material.

A typical indication of the "scatter" or statistical spread that may be expected in the fatigue life of carefully prepared laboratory specimens is illustrated in Fig. 4. Data for steels show similar scatter[12] and can only be rationally interpreted in terms of the probability of failure for given conditions of stress amplitude and life. It is not unusual to observe that the fatigue lives of two supposedly similar specimens vary by factors of 10 to 1. The larger the number of samples tested under the same conditions the more complete will be the information regarding the mean life of the group and the statistical spread in values of life from the weakest to the strongest specimen; thus it becomes evident that it is impossible to select one sample and predict its fatigue life. One can only obtain data from which to predict the *probability* that a certain percentage of similar samples would have a life greater than a specified value. Furthermore, the larger the volume of the zones of higher stress in the sample the more likely will be the probability of finding weak spots in the crystalline structure that would exhibit minimum fatigue strength. This is one aspect of the problem that indicates a rational reason for a "size effect" in fatigue. In general, therefore, one must realize that the fatigue strength of individual pressure vessels may be lower than that predicted on the basis of *small scale* laboratory tests of carefully prepared models. Furthermore, a design based on *mean* fatigue life of a group of specimens would predict a life that is not safe for the weaker individuals of the group. If we are to avoid all failures (probability of failure equal zero) the safe number of fatigue cycles in service must be limited to a small percentage of the average or mean fatigue life predicted from tests.

Qualitative Evaluation

This means, of course, that for design purposes one cannot expect to use laboratory test data on a *quantitative* basis. In order to obtain quantitative data for design, it would be necessary to test large numbers of finished parts and to analyze the data in terms of the probability of a member exceeding a given life for a predicted loading history. This is not economically feasible for full-sized members such as pressure vessels.

It appears obvious that one cannot predict with any assurance the fatigue performance of a large structure in a quantitative manner. The art is not sufficiently developed to allow a true deductive analysis to be made in which one could infer or derive from general principles the particular behavior of a given vessel or machine.

Does this mean then that all design for resistance to fatigue loading must be pure guess work or cut and try with redesign based on past mistakes? Fortunately, the problem is not as impossible as it may at first appear. All of engineering design and professional practice are based upon qualitative ideas that have been formulated into crude quantitative relationships over limited ranges of the variables involved. Many of these "laws" or relationships are not based on rational analysis but rely upon past experience in particular fields of application. Any design for fatigue resistance must also rely upon knowledge of what is "good" or "bad" from past experience supplemented by better or more complete analysis of the peak stresses at discontinuities. For example, the basic design formulas are limited in scope to idealized cases such as simple cylindrical shells. In an actual

vessel, large stresses of unpredictable magnitude will occur in localized regions at comparatively rigid reaction points. The significant localized stresses from differential expansions, temperature gradients, etc., around the supports, piping, and reinforced openings cannot be rationally analyzed at the present time. Thus the design stresses must take into account the known theoretical values of stress concentration for holes, fillets, knuckles, etc., and include a margin of safety to take care of the unknown higher stresses in many localized regions of the vessel.

For vessels with a stainless steel clad surface, a study of the fatigue strength and crack propagation in clad metals would be necessary before one could anticipate the probability of a crack initiating in a clad surface and continuing into a stronger backing steel. Furthermore, the strength of welds joining dissimilar metals in a clad vessel is as yet unknown. The effects of lack of root penetration, contamination of the weld metal, and diffusion at the interface between the three dissimilar metals involved, makes it difficult to predict the efficiency and fatigue strengths in the weld and heat-affected zones.

The resistance of $^3/_4$-in. plate specimens of a variety of steels to repeated biaxial bending was studied recently[6, 7] under a stress cycle simulating that developed in the shell of a cylindrical vessel subjected to (zero to maximum) internal pressure. Some of these data are replotted in Fig. 5 for plates tested with the "as-rolled" but pickled surface (designated as "unnotched plate") and for "notched plates" having a $^3/_8$ in. long machined depression of 0.01 in. depth and radius. Unnotched plates of all the steels exhibited great resistance to plastic fatigue; they withstood cyclic strains greater than 0.6 of the yield point strains for 10^5 cycles before failure. Some of the scatter within the zones shaded in Fig. 5 was undoubtedly due to the obvious variations in surface condition produced by processing (corrosion pits, rolling marks, decarburization, etc.); the fatigue resistance of the plates was also less than that exhibited by small *machined* specimens cut from the plates,[13] and considerably less than that expected for small *polished* specimens. The fatigue resistance of the plate tends to increase with the static strength of the steel, but the relationship is not linear; in fact the shaded zone for notched specimens tends to level off (indicating no improvement in fatigue resistance for the highest strength steels). In this respect the data are entirely consistent with the trends shown by Fig. 3 and other similar data in the literature for small notched specimens. Thus there is a limit to the increase in fatigue strength that may be expected by changing to steels of higher static tensile strength. In general, the fatigue strength reduction caused by the notch (Fig. 5) was roughly half that predicted by a theoretical stress concentration factor of 2.8 for the notch. It is important to note, however, that plates with welds of good quality (ground flush with the plate surface) did not reduce the fatigue strength in these experiments.

The data for unnotched plate in Fig. 5 have been replotted in Fig. 6 in terms of the Rockwell B hardness of the test surface of the plates. It is apparent that the relative surface hardness gives a fairly accurate indication of the relative fatigue strength of the plate for the wide variety of steels tested. In fact, the surface hardness appears to be a slightly better index of the fatigue strength than any correlation based on static tensile or yield strength values for the plate. Through intelligent use of fatigue data from studies that closely simulate the service conditions, by eliminating bad design details, and by employing better methods of stress analysis, it should be possible to avoid fatigue failures of most classes of pressure vessels even though significant increases in nominal design stresses are allowed.

If only a few thousand loading cycles are anticipated during the life, static design criteria are probably sufficient under present codes to eliminate possibilities of fatigue failure. However, if many thousands (or millions) of loading cycles are expected, the designer must pay careful attention to every detail of design, fabrication, and operation to assure freedom from fatigue cracks. Elimination of severe stress raisers in the design, adequate inspection to insure against improper or defective material or workmanship, and prevention of corrosive conditions or improper alterations while in service must all be primary considerations for satisfactory fatigue life.

Bibliography

1. Staff of Battelle Memorial Institute, *Prevention of the Failure of Metals Under Repeated Stress*, John Wiley & Sons, New York (1941).
2. Gough, H. J., "Engineering Steels Under Combined Cyclic and Static Stresses," *Inst. Mech. Engrs., Proc.*, **160** (4), 417–440 (1949).
3. Dolan, T. J., "Fatigue as a Factor in Pressure Vessel Design," THE WELDING JOURNAL, **33** (6), Research Suppl., 265-s (1954).
4. Peterson, R. E., "Review of the Fatigue of Materials Field," *Appl. Mech. Revs.*, **5** 1–3 (January, 1952).
5. Gross, J. H., Tsang, S., and Stout, R. D., "Factors Affecting the Resistance of Pressure Vessel Steels to Repeated Overloading," THE WELDING JOURNAL, Research Suppl., **32** (1), 23-s to 29-s (1953).
6. Bowman, C. E., and Dolan, T. J., "Biaxial Fatigue Properties of Pressure Vessel Steels," *Ibid.*, **32** (11), 529-s (1953).
7. Bowman, C. E., and Dolan, T. J., "Resistance of Low-Alloy Steel Plates to Biaxial Fatigue," *Ibid.* **35** (2) 1025 (1956).
8. Boardman, H. C., "Report on the Design of Pressure Vessel Heads," *Ibid.*, **32** (1) (1953).
9. Wilson, W. M., and Burke, J. L., "Rate of Propagation of Fatigue Cracks in 12 by $^1/_2$-in. Steel Plates with Severe Geometrical Stress Raisers," *Ibid.*, XIII (8), 405-s to 408-s (1948).
10. White, A. E., "Changes in a High Pressure Drum to Eliminate Recurrence of Cracks Due to Corrosion Fatigue," *Trans. Amer. Soc. Mech. Engrs.*, **61**, 507 (1939).
11. Moore, H. F., "Tests of the Resistance to Repeated Pressure of Forged, Riveted, and Welded Boiler Steels," *Ibid.*, (Fuels and Steam Power Section) (January-April, 1931).
12. "Fatigue with Emphasis on Statistical Approach II," *Spec. Tech. Publ.* **137**, *ASTM*, (January, 1953).
13. Gross, J. H., and Stout, R. D., "Plastic Fatigue Properties of High-Strength Pressure Vessel Steels," THE WELDING JOURNAL, Research Suppl., **34** (4), 161-s to 166-s (1955). See also: Reports of Progress, Welding Research Council, January, p. 3, 1946.
14. Copson, H. R., "The Influence of Corrosion on the Cracking of Pressure Vessels," *Ibid.*, **32** (2), Research Suppl., 75-s, (1953).
15. Horger, O. J., "Fatigue Characteristics of Large Sections," *Fatigue*, American Society of Metals, p. 77 (1953).
16. Levy, J. C., and Sinclair, G. M., "An Investigation of Strain Aging in Fatigue," *Amer. Soc. Testing. Mats.*, Preprint No. 70 (1955).
17. Dolan, T. J., "Basic Concepts of Fatigue Damage in Metals," *Fatigue*, Amer. Soc. Metals, p. 1 (1953).
18. Zambrow, J. L., and Fontana, M. G., "Mechanical Properties Including Fatigue of Aircraft Alloys at Very Low Temperatures," *Trans. Amer. Soc. Metals*, **41**, 480 (1949). See also: Spretnak, J. W., Fontana, M. G., and Brooks, H. E., "Notched and Unnotched Tensile and Fatigue Properties of Ten Engineering Alloys at 25° C and −196° C," *Ibid.*, **43**, 547–570 (1951).
19. Templin, R. L., and Howell, F. M., "Grain Flow," *Metals Engineering-Design, ASME*, p. 112, (1953).
20. Peterson, R. E., "Stress-Concentration Phenomena in Fatigue of Metals," *Trans. ASME*, Applied Mech. Sect., pp. 157–171, (October-December, 1953).
21. Lipson, C. and Noll, G. C., "Design Practice," *Metals Engineering-Design, ASME*, p. 297 (1953).
22. Dolan, T. J., "Simultaneous Effects of Corrosion and Abrupt Changes in Section on Fatigue Strength of Steels," *Journal of Applied Mechanics*, (*ASME*) **5** (4) A141 (December 1938).

Correction:

"*Stresses in Welded Pressure Vessels*"

by W. P. Kerkhof

•

In the January 1956 issue of THE WELDING JOURNAL RESEARCH SUPPLEMENT, *page 58-s, section 25, paragraph (g), first line reads: The value of allowable stress is independent. This should read: The value of allowable stress is dependent.*

The Editor

EFFECT OF ANNEALING (650° C) ON BENDING FATIGUE OF LARGE WELDED TEST PIECES

Annealing of heavy engine parts after welding found to be justified because of the resultant increase in bending fatigue strength

BY P. E. WIENE

The main object of the present series of experiments was to decide on the often discussed problem of the justification of annealing heavy engine parts after welding; and as the experiment shows an increase in bending fatigue strength of 20% by annealing at 650° C, the inference is that such annealing is profitable for large components of steel with 0.17 C—and most likely for all steels with more than about 0.14 C—exposed to heavy varying stresses, the most important of which are situated at the surface of the material—at least when operating temperatures are not so great that annealing may be expected to take place during service.

Testpieces and Welding Technique

The experimental arrangement is shown in Fig. 1. The welding was carried out by Burmeister & Wain's shop for Diesel engine weldments.

In the *main experiment*, a plate with thickness t = 28 mm (1 1/8 in.) was welded in T for a length of 1 m (40 in.) to an 80-mm (3 1/8 in.) plate. The material, A, was semikilled Siemens Martin steel from the Danish Rolling Mills (Frederiksvaerk) with Lloyd's certificate (see Table 1). Eight testpieces of this type were made, four of which were tested in the as-welded condition, and the other four after 4 hours' annealing at 650° C followed by slow cooling in furnace for 20 hr.

In a *second experiment*, a 22-mm (7/8 in.) plate of similar material, B, was welded to an 80-mm plate for 1 m length, the welding technique being altered.

A *third experiment* was made with 28-mm aluminum-killed Austrian steel, C, Table 1 (probably oxygen-blast converter steel), only, however, after annealing at 650° C.

In the two cases first mentioned, the weld seams were parallel to the direction of rolling for the 28- and 22-mm plates, respectively; in the last case, the weld seams were perpendicular to the direction of rolling. No preheating, no hammering, and no machining after welding was used. The welding was carried out with alternating current and in the best position possible as in production a positioner is always used for important welding operations. After welding, about two months were

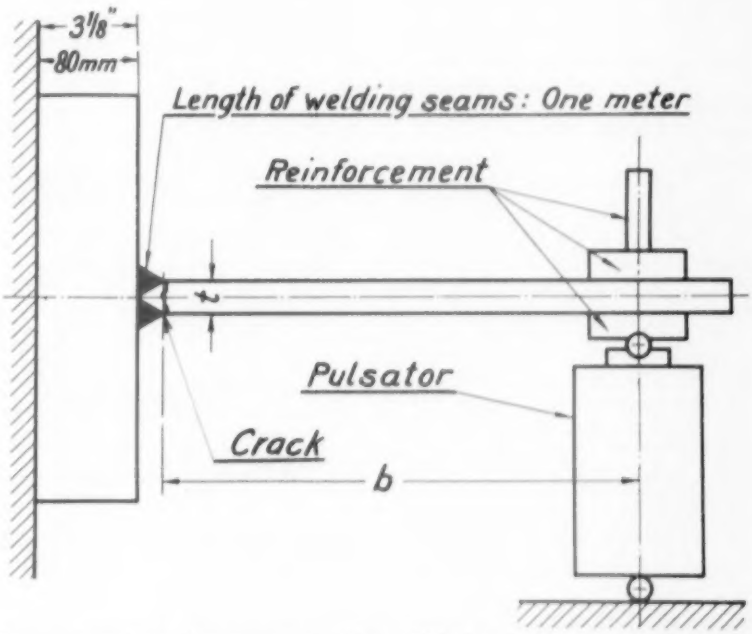

Fig. 1 Experimental arrangement. The weld is 1 m long, perpendicular to the plane of the paper. The pulsator exclusively presses upward so that the lower weld receives stresses varying from zero to pull, the upper from zero to push

P. E. Wiene is Mechanical Engineer, Burmeister & Wain, Copenhagen, Denmark.

Table 1—Plate Material

Material	Thickness, t mm	Thickness, t in	Analysis C, %	Si, %	Mn, %	P, %	S, %	N, %	Ultimate tensile strength kg/mm²	Ultimate tensile strength lb/sq in.	Elongation 200 mm (8 in.) %
A	28	1 1/8	0.17	0.14	0.77	0.023	0.042	0.005	46	66,000	28
B	22	7/8	0.18	0.14	0.71	0.015	0.035	0.005	44	63,000	24
C	28	1 1/8	0.12	0.25	0.50	0.010	0.016	0.008	43	62,000	25.5

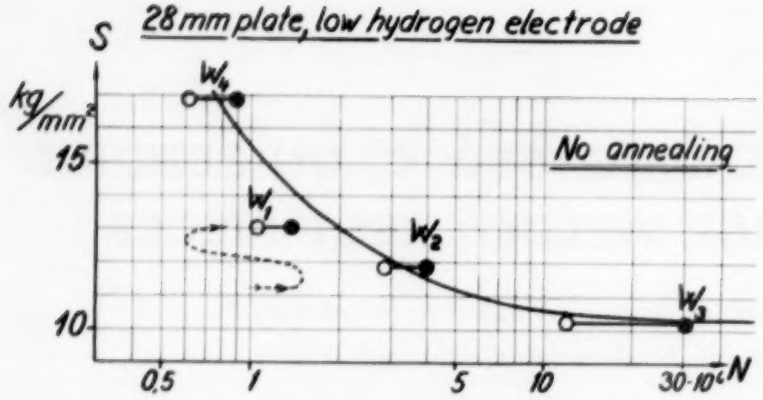

Fig. 2 S-N-curve (S = nominal stress), main experiment without annealing. Clear point: first fissure starts; black point: final crack; arrow: no crack, test continued at higher level

allowed to elapse before fatigue tests were started, whereby natural aging, similar to that in practice, was obtained.

In the main and the third experiment (28-mm plates, A and C), low-hydrogen electrodes were used. After tack welding, two runs were made from the tensile side (lower side, Fig. 1) with 5- and 6-mm electrodes respectively, then three runs from the opposite side (6, 7, 7 mm), five from first (7, 6 mm) and three from second side (6 mm); chiselling after second run; the last runs thus are on the compression side. The altered welding technique of the second experiment is described later.

Testing

The fatigue test was carried out by the Structural Research Laboratory at the Technical University of Copenhagen, by means of an Amsler pulsator (250 ~/min), for one-sided bending stresses, the force acting in one point on the middle of the length and immediately below the reinforcement (Fig. 1), the load thus being distributed fairly even throughout the length of the welding. However, the stress calculated at the center was about 3% higher, and at the ends about 4% lower, than the nominal stress. The calculation of this was checked by strain gage measurements, both statically and dynamically. A check was also made to ensure that no vibrations of significance occurred (natural frequency 250-Hz, frequency of pulsator 4.17 Hz). The stress was measured by means of manometers on the pulsator, and was checked by dial gage and partly also by strain gage.

Effect of Annealing

The results of the main experiment are shown in Figs. 2 and 3 and in Table 2. Three causes may be imagined for the improvement in the fatigue strength by annealing: (1) the welding stresses are relieved, (2) the hardened areas in the transition zone are tempered; and (3) the disengaged hydrogen gets an opportunity to diffuse away.

(1) A closer study of the *welding stresses* has not been made; but there is no doubt that in a structure which has not been annealed these are of the order of the yield point.

At the first outside load, the greater part of the highest stressed areas at the bottom of the notch between weld and plate, will yield further; and as appears from Fig. 4 such material is able to yield well 1% before the stress rises above the yield stress. When the load again is zero, the elastic stresses in the underlying layers will bring the plate back to nearly the starting position, leaving a low tensile or even a compression stress in the surface. In a nonannealed structure the stress in the greater part of the layer which originally was highest stressed, will therefore not (as could immediately be expected) vary from the yield limit upwards (A-B, Fig. 5), but from a compression stress up to the yield point (almost at C-D). In the corresponding annealed structure most of the yielding has taken place during the heat treatment, but the first outside load will make

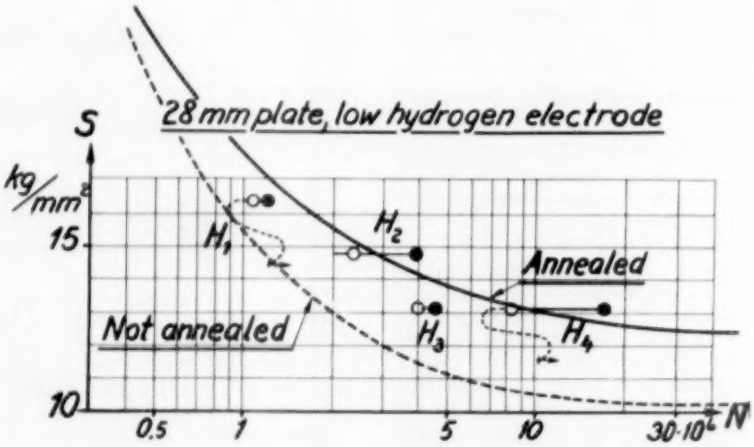

Fig. 3 Same as Fig. 2, but annealed at 650° C. In dotted line, the S-N-curve from Fig. 2

Table 2—Fatigue Tests

Material (see Table 1)	*t, mm*	*Electrodes*	*Penetration*	*Welding seam in relation to rolling direction*	*Anneal*	*Mean endurance limit,* 30 × 10⁶* kg/mm²	*Mean endurance limit,* 30 × 10⁶* psi	*Hardness in Transition zone, max, HV_{10}*	*Plate, min, HV_{10}*	*Fig.*	*Test-piece*
A	28	Low hydrogen	Good	Parallel	No	10.3	14,500	225	159	2	W1-4
					Yes	12.4	17,500	179	112	3	H1-4
B	22	Neutral	Bad	Parallel	No	(10)	(14,000)	203	166	6	W 5
					Yes	(12)	(17,000)	181	125	6	H 5
C	28	Low hydrogen	Good	Perpendicular	Yes	(11)	(16,000)	178	109	7	A H 1-3

* One-sided bending, nominal stresses varying from zero to value appointed.

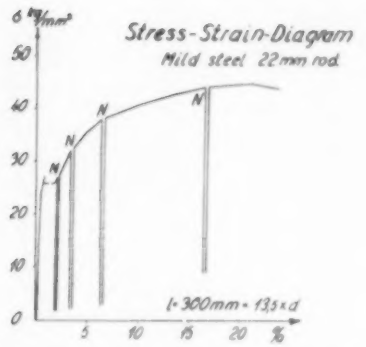

Fig. 4 Stress strain curve for forged steel, analysis approximately as plate material A and B (Table 1); tensile strength: 47 kg/mm² (30 ts/sq in.); lower yield point: 25 kg/cm² (16 ts/sq in.); elongation: 23% on 13, 5d. At N were made 3 to 15 reliefs with subsequent restressings

the stress increase from zero to the yield point and also will produce some further yielding in total as much as for the as-welded test piece. So, for the following load cycles the stress variation will be C-D for the annealed as for the as-welded structure.

(2) All fractures occurred close to the *hardest area* of the transition zone in the plate material, where the geometric and metallurgical notch effects are added, and went on perpendicular to the plate surface.

The hardness measured in the transition zone before annealing, max 225 Vickers (Table 2), corresponds to an ultimate strength of nearly 80 kg/mm² (50 ts/sq. in), and steel of this strength ought in itself to have greater fatigue strength than after annealing where the ultimate strength is about 62 kg/mm² (40 ts/sq in.). The disadvantage of the local hardening zone probably is that a comparatively small area with the great hardness partly prevents the constriction of adjacent softer material, thereby at this very spot resisting the yield which is advantageous in causing the rest of the soft material to slide from the stress level A-B, Fig. 5, down to C-D at the same time locally producing a tri-axial stress distribution. This purely metallurgical effect (plus possibly the disengagement of hydrogen) thus seems to account for the total gain through the annealing of 20%.

(3) The number of tests under the second experiment is too low and other factors vary at same time, so that the effect of *disengagement of hydrogen* cannot clearly be distinguished from the effect of softening the hardened zone.

The Cracks

As indicated by Figs. 2 and 3, a long time often elapsed from the moment that the first crack could be ascertained until the final fracture took place. For instance, on the as-welded testpiece W_2, a crack started at 11 million stress cycles; a couple of other cracks started after a total of 21 million cycles, one of them on the pressure side; but the final fracture did not take place until after 30 million stress cycles. This is probably due to the fact that, even though part of the material is stressed up to fatigue strength, by far the greater part is stressed below this limit; and even though the initial crack increases the notch effect, still a great many stress cycles are required to make it propagate into such undamaged material.[1]

On the push side of the unannealed test bars, the tensile stresses in the surface—due to the welding—will be reduced merely from the yield stress along D-C (Fig. 5) so that the fatigue strength, in fact, is entirely as on the pull side; but as soon as the crack propagates through the layer that originally had tensile stresses, it will stop, because in material without tensile stress the 30% greater variation H-G may be tolerated.

The annealed test bars should immediately be able to stand H-G on the push side; for similar effect of compression mean stress, see[1]; a small yield from compression in the surface may, however, displace the level in the direction of the line E-F.

Cracks on compression side long time before final rupture only appeared at one testpiece which was tested as-welded (W_3, Fig. 2); at the final rupture most of the pieces—as-welded and annealed—showed fatigue cracks starting from the compression side. A closer description of the crack propagation is given in reference No. 2.

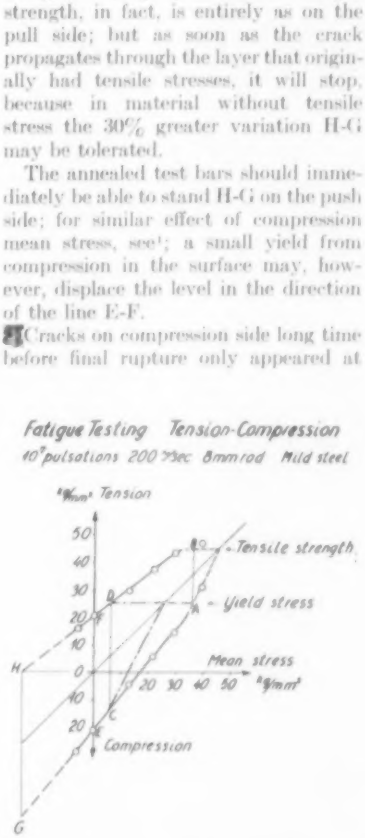

Fig. 5 Smith diagram for the same material as under Fig. 4. With increasing mean stress, the varying stress decreases; however, at a mean stress of 30 kg/mm², and consequently far above the yield point, stress variations of ±15 kg/mm² were still recorded; and at the mean stress of 40 kg/mm², in fact, varying stresses of ±9 kg/mm² were found, accordingly the maximum stress momentarily (but in one case for more than 50 X 10⁶ pulsations) exceeded the tensile strength

Scatter

The maximum deviation from the fatigue curves, Figs. 2 and 3, is about 6%, which is surprisingly small considering the uncertainty to be expected with welding as compared to fatigue tests with small specimens which give a rather great scatter even for very pure steel because the probability of finding a flaw in a small specimen is rather low, but a flaw has a great effect.

Most likely, if a larger number of testpieces were employed in these experiment, some would be found to give a greater deviation. On the other hand, it must be borne in mind that each of these testpieces has a cross-section area equivalent to 650 of the ordinary 7.5-mm rotating beam testpieces. Thus it is highly probable that a large number of "chance" flaws are present in all the big testpieces. In other words, in these few testpieces we have the lower limit of the scatter-band, which ought to be determined for practical purpose.

Thinner Plates and Altered Welding Technique

Included for comparison is a *second experiment* with a couple of similar tests employing 22-mm (⅞ in.) plates instead of the 28 mm (1 ⅛ in.) in the main tests. Further, the welding technique was somewhat altered so as deliberately to produce a lack of penetration, a 2- x 1-mm hole being left in the centerline of the welding seam; 10 runs were made all with 6-mm electrodes, again starting at the tensile side, but in this case with the last run at tensile side; the poor penetration was verified by ultrasonic tests. At the same time neutral electrodes were used instead of low-hydrogen electrodes. By microscopic control, some more slag inclusions were found in the weld material in these testpieces than by the main experiment.

The result thus obtained with one plate welded and one annealed are given in Fig. 6, which—as far as can be concluded from two specimens—indicates that the altered welding technique had no great influence, whereas annealing still gives an improvement.

It is reasonable to suppose that lack of penetration has no appreciable influence on the fatigue strength for bending; and as bending tensions will occur at most points of welded machine constructions, the inference is that in controlling fillet welds in T joints stressed in bending less emphasis should be placed on the relatively gross faults,

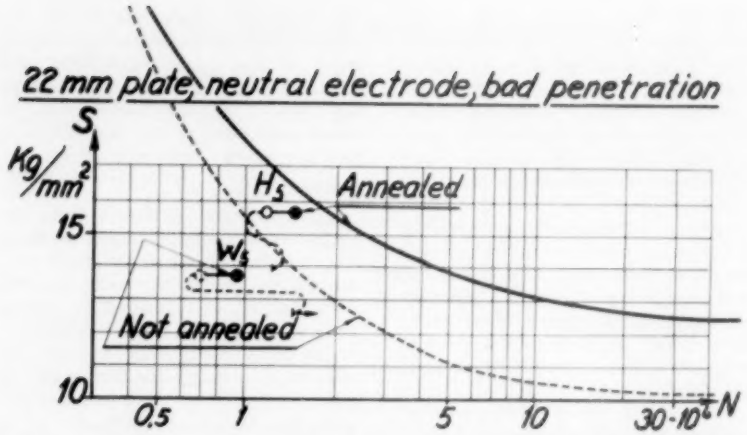

Fig. 6 Second experiment, material B. For comparison, the two curves from Figs. 2 and 3 are drawn in

which an X-ray or isotope examination will reveal, than on superficial faults which will give an increased notch effect and which are most easily revealed by magnetic test. (Also, it is far easier to carry out current control by magnetic test apparatus which can be operated by the foreman, or the welder himself, any faults thus being immediately detected.) Radiation tests are suitable for assemblies subject to pure tensile stresses.

It is more striking that low-hydrogen electrodes failed to give more visible improvement in the main experiment (with 28-mm plate, A) as compared with the neutral electrodes in the second experiment (with 22-mm plate, B). It is possible that the size factor had a bad effect by the 28-mm plate which cancelled out part of the improvement expected from the low-hydrogen electrode; furthermore a crack passing in the plate material and not in the weld itself may be rather independent on the electrode material.

Aluminum-Killed Steel

The *third experiment*, with material C, was carried out in the annealed condition only. The weld seams were parallel to the rolling direction of the 28-mm plate, the welding was done with low-hydrogen electrode, and the technique was the same as in the main experiment.

As appears from Fig. 7 and Table 2, this material at any rate shows no better fatigue strength than the normal Siemens Martin steel, which is appreciably cheaper, despite the fact that the aluminum-killed steel was strained in the rolling direction whereas the normal steel was strained perpendicular to the rolling direction. The transition temperatures as obtained in impact tests are appreciably more favorable for the aluminum-killed steel C than for the normal steels A and B, especially after aging; as often seen, this is not reflected in a corresponding improvement in the fatigue strength of the welded and annealed construction.

Discussion of the Results

The measured fatigue strengths are somewhat lower than some of the results known from the literature.[4–6]

There are several reasons for this; most other experiments have been made as push-pull tests with butt welds whereby the flux becomes essentially smoother than by the present bend tests where the weld forms a comparatively small angle with the adjacent plate surface. Many tests are carried on to 2 x 10^6 pulsations only or to a still lower number.[5] Most test results stated in the literature, have been achieved from welds perpendicular to the rolling direction and from test bars of essentially smaller dimensions,[6] whereby the welding stresses as well as the hardening effect becomes considerably smaller, to which comes the size effect itself. Further the welds referred to are often carried out under laboratory conditions by especially skilled workmen, or the best testpieces have been selected after X-ray examination;[4] the present welds have been made under practical workshop conditions by ordinary welders (holding certificate from the classification societies), and the welds have been controlled by ultrasonic and magnetic particle testing, but not by X-rays, and the whole weldment has been tested in fatigue including the terminations from which cracks often originate.

From reports about fatigue tests it is often difficult to gather the information about all these conditions, and also many designers are not able to judge the importance of such details and thus overrate the fatigue strength of practical weldments especially in heavy constructions loaded by bending.

On the other hand in several cases lower values are reported in literature.[2–3]

A real comparison between tests made under different circumstances is seldom possible due to the variation not only in material, design, size, and nature of load, but also in indefinable details of the execution of the weld.

As experiments with full scale specimens are rather expensive, the number of testpieces in this experiment has been limited; but it seems fully justified from the experiments to draw a conclusion about the advantage of annealing on large welded constructions from similar analysis and exposed to bending fatigue.

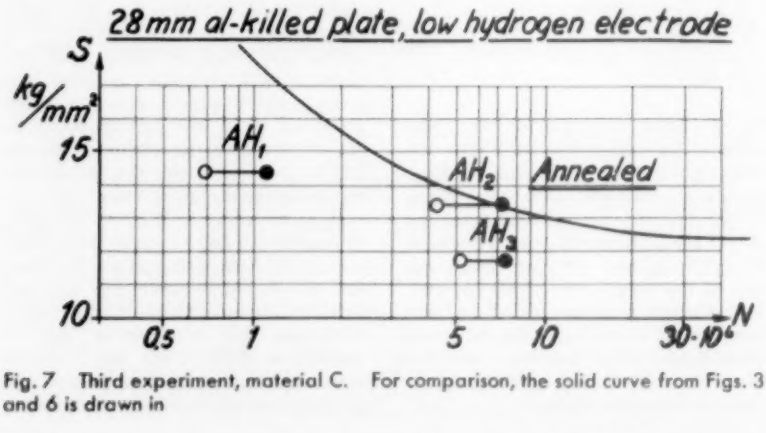

Fig. 7 Third experiment, material C. For comparison, the solid curve from Figs. 3 and 6 is drawn in

Bibliography

1. P. E. Wiene: "Full Scale Fatigue Tests of Diesel Engine Elements," Transact. of the Inst. of Marine Engineers (read in London 22/11/55), and Essais de fatigue sur des pièces de moteur Diesel de grandeur nature, Rev. Gen. de Mécanique, fevr. 1955).

2. P. E. Wiene: "Bending Fatigue of Large Welded Test Pieces with Regard to Velocity of Crack Propagation." International Union of Theoretical and Applied Mechanics, Colloquium on Fatigue, Stockholm, May 25–27, 1955, Springer Verlag.

3. F. Hebrant, H. Louis, W. Soete: "Étude de la relaxation mécanique des tension résiduelles de soudage en sollicitation statique et en fatigue," Revue de la Soudure, no. 3, 1955.

4. M. Hempel u. H. Møller: Die Auswirkung von Schweissfehlern im Proben aus Stahl 37 auf deren Zugschwellfestigkeit. Arch. f. Eisenhüttenwesen 20 (1949, heft. 11–12) s. 375–383.

5. Illinois Engineering Experimental Station, Bull. 384, vol. 47, No. 50, Residual Stresses in Welded Structures, Urbana, March 1950.

6. Newman R. P.: "The Influence of Weld Faults on Fatigue Strength with Reference to Butt Joints in Pipe Lines." *Transact. of the Inst. of Marine Engineers* (read in London 10/1/56).